Universidad Autónoma de Madrid

Facultad de Ciencias

Departamento de Biología Molecular

Histone H3 function and dynamics during Arabidopsis development

Sofía Otero Pérez

Licenciada en Biotecnología

Dirigida por:

Crisanto Gutiérrez Armenta

Bénédicte Desvoyes

Madrid, 2015

Crisanto Gutiérrez Armenta, Profesor de Investigación CSIC en el Centro de Biología Molecular Severo Ochoa

CERTIFICA

Que la Tesis Doctoral titulada “H3 function and dynamics during Arabidopsis development” ha sido realizada en el Centro de Biología Molecular Severo Ochoa y tutelada en el Departamento de Biología Molecular de la Universidad Autónoma de Madrid.

El trabajo realizado por Sofía Otero Pérez reúne todas las condiciones requeridas por la legislación vigente, así como la originalidad y calidad científica para poder ser presentada y defendida con el fin de optar al grado de Doctor.

Y para que conste donde proceda, firmo el presente certificado.

Madrid a 12 de Febrero de 2015

Dr. Crisanto Gutierrez
Director de la tesis

Bénédicte Desvoyes, investigadora postdoctoral en el Centro de Biología Molecular Severo Ochoa

CERTIFICA

Que la Tesis Doctoral titulada “H3 function and dynamics during Arabidopsis development” ha sido realizada en el Centro de Biología Molecular Severo Ochoa y tutelada en el Departamento de Biología Molecular de la Universidad Autónoma de Madrid.

El trabajo realizado por Sofía Otero Pérez reúne todas las condiciones requeridas por la legislación vigente, así como la originalidad y calidad científica para poder ser presentada y defendida con el fin de optar al grado de Doctor.

Y para que conste donde proceda, firmo el presente certificado.

Madrid a 12 de Febrero de 2015

Dr. Bénédicte Desvoyes
Co-directora de la tesis

Agradecimientos

To Alison Smith, for receiving me in her lab as an undergraduate student and take me to dinner. For allowing me to discover the thrill of science, for her positive thinking and inspiration. A Pilar Cubas, por ponerme en el camino.

A Nuria, por rescatar mis brazos del rollo de las plantas, por salvar mi ChIP de la basura, por ser mi amiga a pesar de ser yo la monja enana y ella el colmo de la vanguardia. A Joana, que al principio fue un poco mi hermana mayor, por ser mi guía Michelin, por un montón de tricks and tips y sobre todo por haber saltado aquel día al escenario. A Celina, por poner tanto estilo en el 308, por las series, por su buena cara y por reunirnos cada vez que vuelve a Madrid. To Martina, for such funny moments in Madrid and Salamanca, for her friendship and 2kg of Cola-Cao. A Adriana por su sonrisa y cercanía. A Victoria por todas las semillas que me ha recogido y por saber siempre algo del país al que vas de vacaciones. A Carla, por su generosidad y por sus tartas. A Sofi, por ser tan buena y por esas caras que pone. A Marta y Maribel por el apoyo en los principios. A Elena Ramírez, por empezar con las histonas y también a Irene y Elena.

A Gloria, Charo y Rosa por ser tan majas, porque las mejores comidas han sido en vuestra compañía. A Jorge por Callejeros Villaverde. A Iluminada, por ser cada tarde un torbellino de alegría y cariño. A Isa maquillajes, por las charlas en Winky.

A las chicas de microscopía, a todas gracias por vuestra paciencia. En especial a Mari Ángeles por ser la master del Image J, a Vero por su entusiasmo y a Maite. A Berta y Silvia, por las horas de sorting, por su cariño, empeño y profesionalidad. A Ramón y David por los análisis bioinformáticos. A Diego y a Ángel, por cuidar mi ordenador y buscarme programas. A María Gómez, por creer que puedo. A Carlos Alonso-Blanco por los consejos de jardinería y su buena disposición con el invernadero.

I would also like to thank Philip Benfey, for giving me the opportunity to visit his lab and enjoy an American Summer. To Ross, for taking me to my first baseball match and for the orientation. To Colleen, for driving me everywhere and convince her friends to do it, for taking me to the swimming pool, to a campus party and to have drinks and our beloved Ben and Jerry's! For helping me cutting so many roots and inviting me to the meeting in the mountains: you really made the difference! A Manuel, por los ánimos y la ayuda y junto con Orlando, por tantas risas en conversaciones "prohibidas" en español, a los dos muchas gracias. To Asia and Guy for giving me so many rides, for showing me how to extract embryos and for the European style. To Polly and Hsinyen, for your friendliness. To Heather, for inviting me apple picking and for so

many early mornings. To Erin and John, for inviting me to your place and driving me to the orchard with interesting conversations. To Olivia because even if we only met twice I understood why you were so special for everybody. To Sarah, for taking me out and showing me the good stores. To Eric and Mandy, for allowing me to join you in the baby shower, I'm sure Cooper is now a big boy! To Jeremy, for offering me so many rides y por querer aprender piropos en español. To Sophie and Adam, to Ayal and Joe, to Jamie and all those who joined me in my birthday. To all the lab members: thank you!

Y gracias Marisabel por prestarme tu casa y por compartir conmigo las últimas semanas. A ti y a Blake, gracias.

A Isa, por las conversaciones sobre ciencia y por compartir opiniones, visiones y experiencias en estos años paralelos, siempre es un placer. A mis chicas master, Nuria, Marta y Patri, por ese soplo de aire fresco que pusisteis en mi vida y por haber compartido conmigo esta etapa. A María, por ser mi cómplice en el laboratorio y mi amiga más allá del CBM, por todo el apoyo en los buenos y en los malos momentos y por apuntarte a un bombardeo… ¡muchas gracias!

A mi Patri, por ser mi muy mejor amiga, la que siempre está ahí, incluso a altas horas de la madrugada, la que mejor me conoce, la que más me consiente y la que más me aguanta: ¡tengo muchísima suerte de tenerte en mi vida!

A Bénédicte: siento decepcionarte por no haber cumplido los objetivos que me propusiste: ni bebo cerveza, ni soy atea ni voy a votar a Izquierda Unida ;)… pero tengo que darte las gracias por poner en el buen camino las H3, por dejarme perseguirte hasta el -80, por proponerle a Crisanto que fuera yo a Estrasburgo, por estar siempre dispuesta a contestar mis dudas y hacerlo bien, por todo lo que me has enseñado (¡que es mucho!) y por dejarme crecer. Nos hemos enfadado mil veces y desenfadado otras mil, porque en el fondo, ¡no somos tan diferentes! A mi codirectora, muchas gracias por todo.

A Crisanto, tengo que darte las gracias por tu trabajo constante, por no perder el entusiasmo y por no darte nunca por vencido, por estar siempre disponible, por tener la puerta abierta y por haberme apoyado en todos los proyectos y locurillas que se me han ocurrido a lo largo de estos 5 años. Muchas gracias por confiar en mí desde el principio, más incluso que yo misma, por mandarme a todos los congresos, por dejarme hablar con libertad y no haberte enfadado nunca, por valorar mis opiniones, por tirar de mí cuando me volvía zero risk y pedirme siempre un poco más. Por enseñarnos Cádiz y el Tío de la Tiza, por ayudarme a encontrar nuevos horizontes y, por hacer ciencia de altura… ¡sin taburete!

A mi abuela Pura y a mi tía Victorina, por tanto cariño y entender que siempre tenga que estudiar. Por su sencillez y vitalidad y por las timbas de brisca. A mi abuelo Alfredo, que

aunque se tuvo que ir pronto, fue el mejor abuelo del mundo. También, un poquito solo, a mi hermana.

A mis padres, Puri e Isidoro: por haber sido siempre tan generosos y sacrificados, por haber apostado tan fuerte por mí, por haberme enseñado a esforzarme y que las cosas bien hechas, bien parecen. Por todo el cariño y aguante, por apoyarme siempre y por valorarme tanto. Dijera lo que dijera, me quedaría corta pero creo que en lo bueno soy un reflejo de vosotros y espero que siempre os podáis sentir orgullosos. Aunque no os lo digo mucho, os quiero.

A Kike, por haber sido mi pilar estos años, por ponerme tantos nombres y sacarme todos los días una sonrisa. Por apoyarme y recordarme lo que valgo cuando se me olvida, por cruzar el océano para verme. Por ver conmigo pelis de científicos y animarme siempre con el postdoc. Por todo el amor de estos años y por el que vendrá, te quiero.

Y como los agradecimientos los lee mucha gente, aprovecho para recordaros que podéis estar al día de las noticias científicas más curiosas en “Por ciencia infusa”

http://porcienciainfusa.blogspot.com.es/

Tiene Facebook y Twitter!

“At the end, you can’t connect the dots looking forward; you can only connect them looking backwards (…). Believing that the dots will connect down the road will give you the confidence to follow your heart even when it leads you off the well-worn path and that will make all the difference.”
Steve Jobs

“El azar afortunado suele ser casi siempre el premio del esfuerzo perseverante.”
Santiago Ramón y Cajal

- “Dra Badimon, ¿cuál ha sido el descubrimiento científico más emocionante que ha realizado hasta ahora?
- El del año que viene.”

Entrevista de Julia Otero a la Dra Badimon en los Premios Jaime I de Investigación (2014).

“Have a healthy disregard for the impossible.”
A slogan of a summer camp Larry Page, Google’s CEO, attended when he was a kid.

“It’s all about constitutive talking…”
Sydney Brenner

Index

Abbreviations

A

AIL: **AI**NTEGUMENTA-**L**IKE

ANT: **AINT**EGUMENTA

AP-2: **AP**ETALA-**2**

APC/C: **A**NAPHASE **P**ROMOTING **C**OMPLEX/**C**YCLOSOME

ASF1: **A**NTI-**S**ILENCING **F**UNCTION **1**

ATRX: **α**-**T**HALASSEMIA **X**-LINKED MENTAL **R**ETARDATION PROCESS

ATXR: **A**RABIDOPSIS **T**RITHORA**X** **R**ELATED

B

BBM: **B**ABY**B**OO**M**

BSA: **B**ovine **S**erum **A**lbumin

C

CABIN 1: **CA**LCINEURIN **BIN**DING PROTEIN **1**

CAF-1: **C**HROMATIN **A**SSEMBLY **F**ACTOR **1**

CCS52: **C**ELL **C**YCLE **S**WITCH **52**

CDK: **C**YCLIN **D**EPENDENT **K**INASE

CEI: **C**ortex **E**ndodermis **I**nitials

CEID: **C**ortex **E**ndodermis **I**nitial **D**aughter

ChIP: **ch**romatin **i**mmuno**p**recipitation

CMT3: CHROMO**M**E**T**HYLASE **3**

Col-0: **Col**umbia-**0**

CTAB: **c**etyl **t**rimethyl**a**mmonium **b**romide

CYCD6;1: **CYC**LIN-**D6-1**

D

DAPI: 4',6-**di**a**m**idino-2-**p**heny**l**indole

Daxx: death domain-associated protein 6

DDM1: **D**ECREASE IN **D**NA **M**ETHYLATION **1**

DMSO: **d**i**m**ethyl **s**ulf**o**xide

DPS: **d**ays **p**ost **s**owing

E

EDTA: **E**thylene**d**iamine**t**etraacetic **a**cid

EDU: 5–**e**thynyl–2′–**d**eoxy**u**ridine

En: **En**kheim

EREBP: **e**thylene-**r**esponse **e**lement **b**inding **p**rotein

ESC: **E**mbryonic **S**tem **C**ell

EZ: **E**longation **Z**one

F

FAS1: **FAS**CIATA **1**

FAS2: **FAS**CIATA **2**

G

GFP: **G**REEN **F**LUORESCENT **P**ROTEIN

GMC: **G**uard **M**other **C**ell

H

HBSS: **H**ank's **B**alanced **S**alt **S**olution

HEPES: 4-(2-**h**ydroxy**e**thyl)-1-**p**iperazine**e**thane**s**ulfonic acid

HIRA: **HI**STONE **R**EGULATOR **A**

HP1: **H**ETEROCHROMATIN **P**ROTEIN**1**

HS: **h**orse **s**erum

HTR: **H**ISTONE **T**HREE **R**ELATED

L

LB: **L**uria-**B**ertani

LRC: **l**ateral **r**oot **c**ap

M

MMC: **M**eristemoid **M**other **C**ell

MOPS: 3-(N-**Mo**rpholino)**p**ropane**s**ulfonic acid

mRFP: **m**onomeric **R**ED **F**LUORESCENT **P**ROTEIN

MSI1: **M**ULTICOPY **S**UPPRESSOR OF **I**RA**1**

MSS: **M**ura**s**hige and **S**koog

N

NaOAc: sodium acetate

NASP: **N**UCLEAR **A**UTOANTIGENIC **S**PERM **P**ROTEIN

NEB: **n**uclei **e**xtraction **b**uffer

NDR: **n**ucleosome **d**epleted **r**egions

NP-40: **n**onyl **p**henoxypolyethoxylethanol

O

ORC: **O**RIGIN **R**ECOGNITION **C**OMPLEX

ORI: DNA replication **ori**gin

P

PcG: **P**oly**c**omb **g**roup

PCNA: **P**ROLIFERATING **C**ELL **N**UCLEAR **A**NTIGEN

PLT: **PL**E**T**HORA

PHD: Plant **H**ome**d**omain

PMSF: **p**henyl**m**ethane**s**ulfonyl**f**luoride

Pol: **Pol**ymerase

PTM: **P**ost**t**ranslational **m**odifications

Q

QC: **Q**uiescent **C**enter

qPCR: **q**uantitative **PCR**

R

RAM: **R**oot **A**pical **M**eristem

RBR: **R**ETINO**B**LASTOMA **R**ELATED

rDNA: **r**ibosomal **DNA**

RT: **R**oom **T**emperature

S

SAM: **S**hoot **A**pical **M**eristem

SCR: **SCA**RECROW

SHR: **SH**ORT**R**OOT

T

TE: **T**ransposable **E**lement

TFBS: **T**ranscription **F**actor **B**inding **S**ite

TSS: **T**ranscription **S**tart **S**ite

TTS: **T**ranscription **T**ermination **S**ite

U

UBN: **UBIN**UCLEIN

W

Wb: **W**estern **b**lot

Wt: **w**ild **t**ype

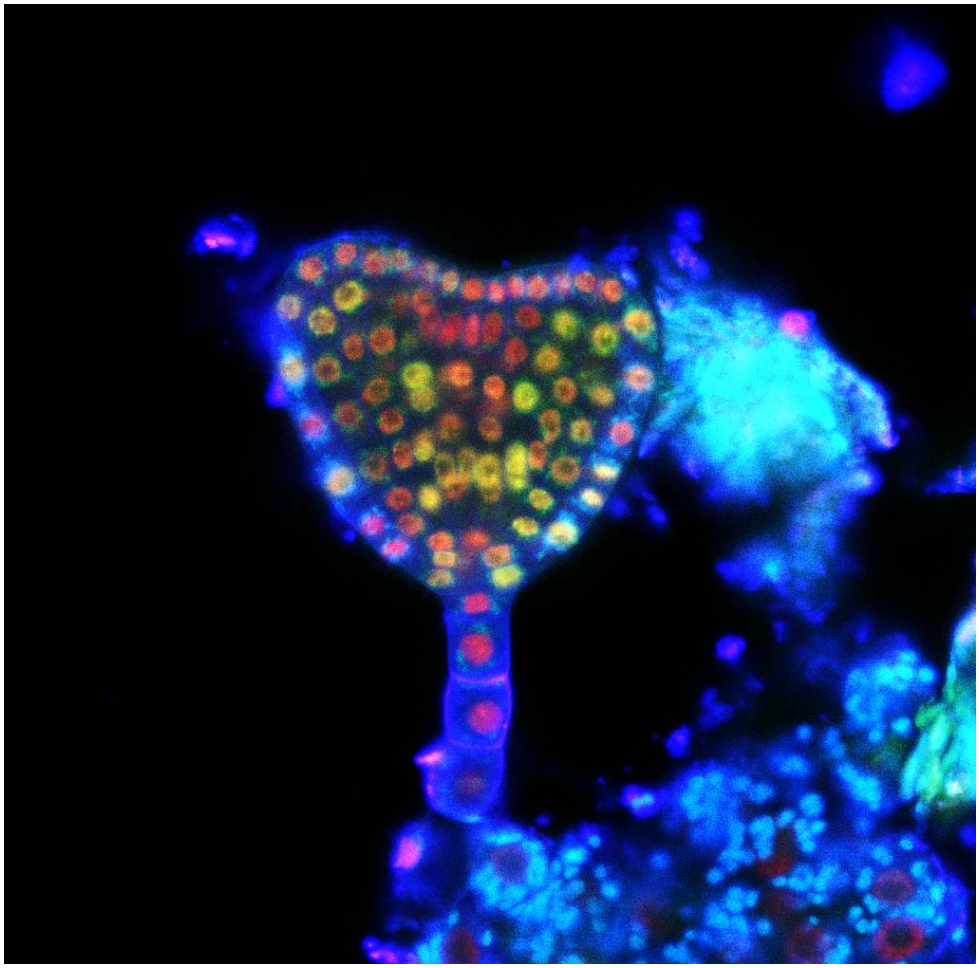

Resumen

La cromatina se regula a través de múltiples mecanismos. Algunos afectan a las histonas, componentes clave que empaquetan el ADN eucariótico en nucleosomas y que influencian todos los procesos que afectan al ADN. En concreto, la introducción de variantes de histonas, isoformas proteicas no alélicas similares en secuencia a las histonas canónicas pero con diferentes cualidades, contribuye a diversificar la cromatina. En este proyecto hemos estudiado las relaciones funcionales entre la histona canónica H3.1 y la variante H3.3. Primero, se identificó la localización de las histonas en el genoma de plántulas de *Arabidopsis thaliana*. Descubrimos que la histona H3.1 se asocia preferentemente con heterocromatina y marcas de silenciamiento, mientras que la cromatina activa está enriquecida en H3.3, que se asocia con marcas de activación y alcanza un máximo en el extremo 3' de los genes. Además, los sitios genómicos mapeados como orígenes de replicación están enriquecidos en ambas histonas.

Intrigados por los defectos de desarrollo observados en los mutantes de chaperonas de H3, decidimos estudiar la relevancia de su dinámica en embriogénesis y organogénesis fusionando histonas H3 a GFP. Durante la embriogénesis hemos determinado que el contenido de H3.1 está directamente relacionado con el potencial proliferante de la célula. Tras la germinación, la coordinación entre proliferación celular y diferenciación es esencial para orquestar la organogénesis de plantas, un proceso reflejado en la cromatina, puesto que hemos detectado que las células que atraviesan el último ciclo celular en el meristemo de la raíz sufren una reprogramación en su contenido de H3 durante G2, con figuras mitóticas de bajo contenido en H3.1. Se analizaron los promotores de genes de H3 y sus chaperonas y se encontraron motivos de unión para varios factores de transcripción, incluyendo la subfamilia APETALA 2, que contiene miembros como PLETHORA. Así, concluimos que estas proteínas son candidatos a regular la reprogramación de H3.

En células en endoreplicación, la H3.1 se incorpora de nuevo en cada fase S del endociclo y se elimina coincidiendo con el último nivel de ploidía, un proceso de reprogramación similar al observado. Además el descenso en el contenido de H3.1 se asocia con el inicio de la diferenciación, en linajes mitóticos y endoreplicantes. Las dinámicas de H3 también se han analizado en mutantes *fas*, determinando que el desequilibrio en H3.1/H3.3 es el responsable del fenotipo de reducción de heterocromatina, pero no afecta a los dominios de desarrollo de la raíz. Finalmente, el estudio de las proteínas H3.1 durante el desarrollo del polen ha mostrado que cada gen de H3.1 se expresa en diferentes células y en distintos estadios.

Estos resultados subrayan el impacto de las dinámicas y función de H3 durante el desarrollo de Arabidopsis.

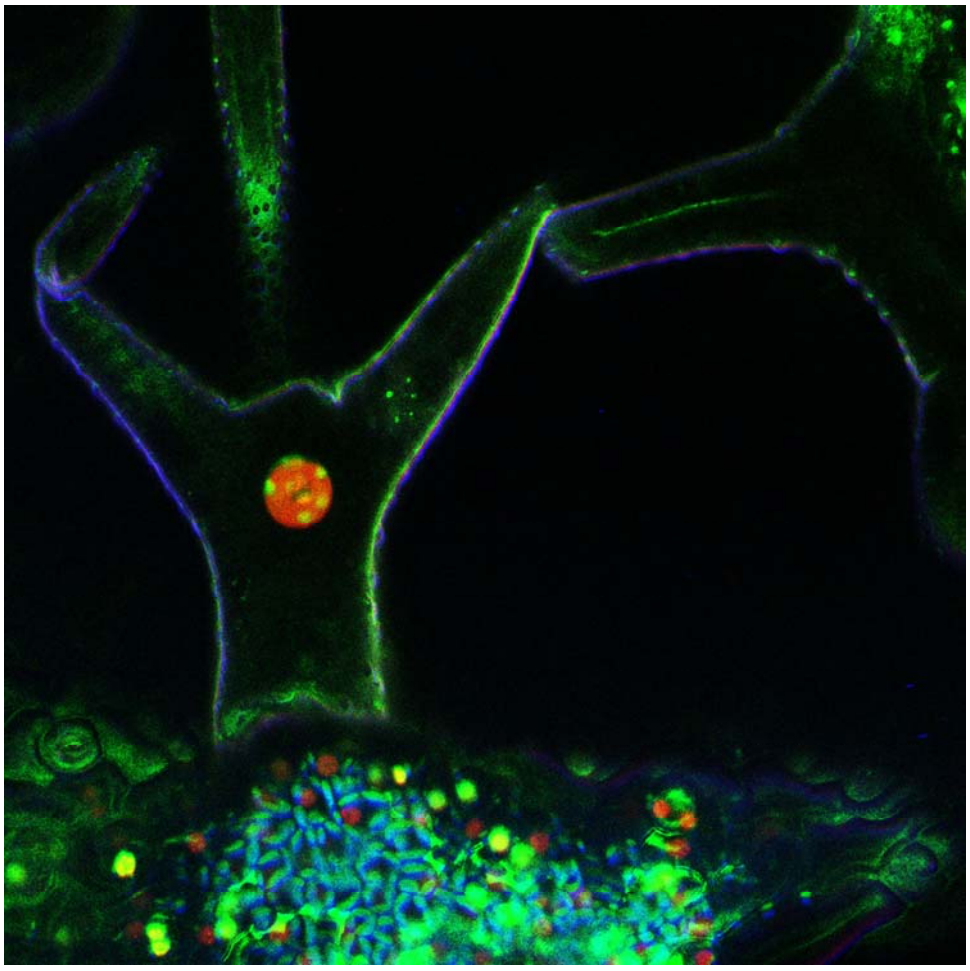

Abstract

Chromatin is regulated through a plethora of mechanisms. Some rely on histones, pivotal components that package eukaryotic DNA to form the nucleosomes and influence all processes that act or depend on DNA. Particularly, the introduction of histone variants, non-allelic protein isoforms similar in sequence to the canonical histones but different in qualities, help diversify chromatin. In this project we have studied the functional relationships between canonical histone H3.1 and the variant H3.3. First, we genome-wide mapped them in seedlings of *Arabidopsis thaliana*. We have found that H3.1 is preferentially associated with heterochromatin and silencing marks while H3.3 is enriched in active chromatin and activation marks, peaking towards the transcription termination site of the genes. Interestingly, genomic sites mapped as replication origins are enriched in both histones.

Intrigued by the developmental defects observed in H3 chaperone mutants, we decided to study the relevance of H3 dynamics along development by tracking GFP-tagged H3 histones in key scenarios of plant growth: embryogenesis and organogenesis. In short, we have determined that the H3.1 content is directly related to the proliferation potential of the cell. Upon germination, coordination between cell proliferation and differentiation is essential to orchestrate plant organogenesis, a process reflected in chromatin, since we have detected that cells undergoing their last cell cycle in the root meristem suffer a reprogramming of their H3 content during G2, mitotic figures displaying a low amount of H3.1. Analyzing the promoters of H3 genes and related chaperones we found binding sites for several transcription factors, including the APETALA 2 subfamily, a group containing members like PLETHORA, root patterning genes that control the longitudinal zonation pattern. This indicates a role of these transcription factors in regulating the H3 reprogramming.

When switching to endoreplication, H3.1 is again incorporated in every S-phase of the endocycle and evicted coinciding with the last endocycle round, a reprogramming process similar to the one observed in mitotic cycle. Since the decrease in H3.1 content has been observed in both endoreplicating and mitotic lineages, H3.1 replacement seems to be a process associated with differentiation independently of the cell dynamics leading to it. H3 dynamics has also been analyzed in *fas* mutants, determining that the H3.1/H3.3 misbalance is responsible for the reduced heterochromatin phenotype but not for altering root developmental domains or the associated H3 reprogramming. Finally, the study of H3.1 proteins along pollen development has shown that each H3.1 gene is expressed in different cells at different stages of pollen formation.

Together, these results highlight the impact of H3 dynamics during Arabidopsis development.

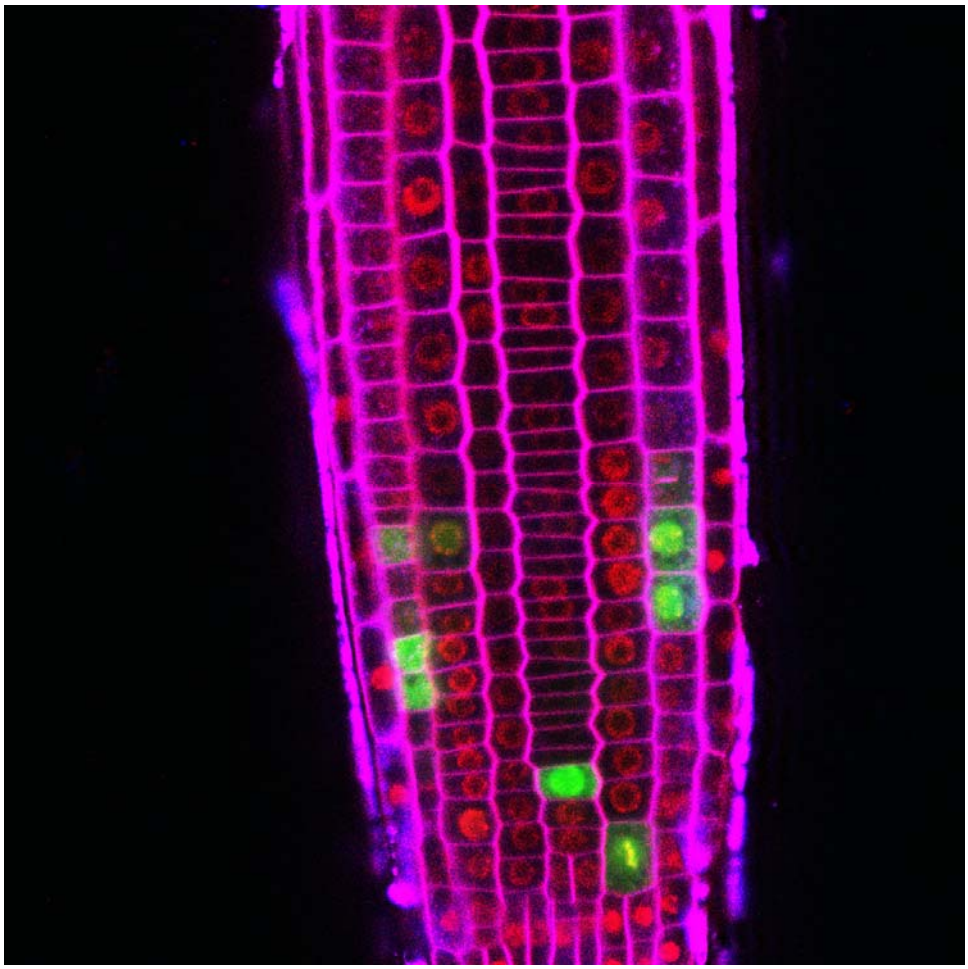

1. Introduction

1.1.1 Histones, the "extraordinary" proteins.

In 1833 Robert Brown determined that the ovoid present in the pollen cells of orchids and plants from the *Asclepiadaceae* family was important for plant reproduction and embryo development and called it "*the nucleus*", suggesting a key role of this compartment for cell function (Brown, 1833). Some years later, Walther Flemming discovered a material in the nucleus that was easily stained and named it *Chromatin* (Flemming, 1882). In this context, at the beginning of cytology, Albretch Kossel was studying the cell chemistry of the "nuclear substance" in bird erythrocytes when he was able to isolate what he coined "histones", basic proteins in a salt-like conformation with nucleic acids that "stand between protamines and *ordinary* proteins" (Kossel, Nobel Lecture 1910). Therefore, since their discovery, which was worth a Nobel Prize in Physiology or Medicine in 1910, histones have been considered *"extraordinary"* for their location and properties, so much that in the forties they were even proposed to be the genetic material (Stedman E., 1947). Although this fundamental function is reserved for DNA, histones are not simple scaffolding proteins but they modulate all processes affecting DNA, such as transcription, replication, repair or recombination.

1.1.2 The nucleosome.

Histones control DNA accessibility because eukaryotic DNA, except in dinoflagellates (Gornik et al., 2012), is wrapped around an octamer of histones forming the nucleosome, the basic unit of the 11-nm chromatin fiber. The octamer, which is the nucleosomal core, is formed by 4 different kinds of histones (a tetramer of two histone H3-H4 dimers together with two more H2A-H2B dimers) that fold 147 bp of DNA in left-handed superhelical turns (Fig 1.1). The fifth histone class, histone H1, additionally condenses chromatin into the 30 nm fiber by binding to linker (internucleosomal) DNA (Campos and Reinberg, 2009). Regarding chromatin compaction, even if the fiber is heterogeneous, two domains are generally distinguished: the highly condensed heterochromatin and the more accessible, relatively decondensed euchromatin, corresponding to areas where active transcription occurs.

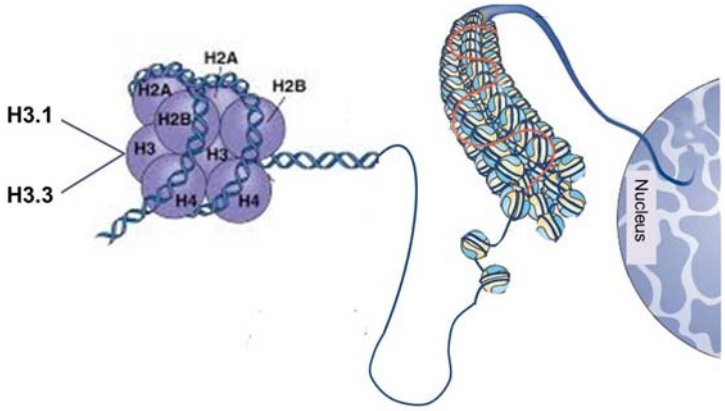

Fig 1.1. The nucleosome. DNA is wrapped around an octamer of histones (H3, H4, H2A and H2B, 2 copies of each) in the eukaryotic nucleus, forming the nucleosome, the basic unit of the chromatin fiber. Adapted from (Probst et al., 2009) and Addison Wesley Longman Inc.

Structurally, histones have a globular domain organized in a helix-turn-helix-turn-helix conformation, that is, the histone fold domain responsible for the interaction with the other core histones in the nucleosome. The rest of the polypeptide chain, the tails, are in a disordered state and protrude from the nucleosome (Das et al., 2010), making contacts with adjacent histones and other proteins. These fragments are rich in basic (positively charged) amino acids that can often be posttranslationally modified.

1.1.3 Histone posttranslational modifications.

Posttranslational Modifications can help open or package chromatin. For instance, acetylation of lysines neutralizes the positive charge of the amino acid and phosphorylation of serines, threonines or tyrosines adds a negative charge to the chain, weakening the electrostatic interactions between histones and DNA, facilitating access of protein machineries and favoring transcription. In turn, ubiquitylation, which consists on the addition of a long polypeptide (76 aa) to the histone lysines, will also affect nucleosome conformation. On the contrary small neutral modifications like methylation will not likely directly perturb chromatin structure (Bannister and Kouzarides, 2011). However, PTMs also impact chromatin through a second mechanism: the recruitment or rejection of proteins in charge of downstream processes. This way, some modifications attract chromatin remodelers that reposition nucleosomes; others prevent the binding of transcriptional repressors and some marks bind proteins that allow repressive states. It is well known that HETEROCHROMATIN PROTEIN 1, HP1, a key protein for heterochromatin structure, binds H3K9me3 in animals. On the other hand, in plants H3K9me3 is found in euchromatin while the typical mark of heterochromatin is H3K9me2. In *Arabidopsis thaliana*, this mark is bound by CHROMOMETHYLASE 3, an enzyme that methylates DNA at CHG sites and thus creates repressive states (Feng and Jacobsen, 2011). Notably, PTMs are regulated by enzymes that erase them or read and write them in neighbor histones, creating chromatin microenvironments. This would be the case of H3K27me3, a repressive mark recognized and spread to newly synthesized histones by the Polycomb group (PcG) complexes in developmentally important loci (Gurard-Levin and Almouzni, 2014).

In short, histone PTMs greatly influence chromatin structure and activity not only in transcription but in all processes affecting DNA transactions. Nevertheless, there exists another strategy to increase complexity in chromatin: the introduction of histone variants.

1.1.4 Histone variants.

Histone variants are non-allelic protein isoforms that help diversify chromatin (Talbert et al., 2012). The variants differ from their canonical counterparts in multiple aspects. While the

canonical histones are coded by multiple intronless genes and are cell cycle regulated, that is, expressed only during the S-phase of the cell cycle in a replication dependent manner, the variants differ in the amino acid sequence and are usually coded by fewer genes that contain introns (March-Diaz and Reyes, 2009). Importantly, the variants are incorporated throughout the whole cell cycle, in a replication independent manner, allowing a rapid chromatin response to different environmental stimuli (Talbert and Henikoff, 2014).

All histone families contain variants, except histone H4 for which variants are rare. H1 family is the most diverse while H2A variants are those showing more sequence variability compared to the canonical proteins (Maze et al., 2014).

1.1.5 The H3 family

Regarding the histone H3 family, the canonical protein is named H3.1 and the paradigmatic variant is H3.3, differing from the replication-dependent H3.1 in only a few amino acids. In vertebrates 10 genes out of 20 code H3.1 identical proteins (with an additional 3 genes for H3.2, a replication-dependent histone identical to H3.1 except for 1 amino acid) and 2 code for the replacement H3.3. In Arabidopsis the family is smaller, with 5 genes out of 15 coding for H3.1 and 3 for H3.3. Surprisingly, some organisms, like Ascomycetes (for instance the budding yeast *S. cerevisiae*), have retained only H3.3 proteins and do not contain genes for H3.1. However, there is no eukaryote with only H3.1 genes, probably because H3.3 can be incorporated in any cell cycle phase (Malik and Henikoff, 2003).

The H3 group also includes one gene for the centromeric variant (CENH3 or CENP-A in mammals), the H3 histone incorporated in the centromeres which is essential for centromere function and kinetochore formation and has a divergent, poorly conserved N-terminal tail (Dunleavy et al., 2011; Otero et al., 2014). Finally, some other genes with heterogeneous characteristics belong to the family, sharing features of H3.1 and H3.3. Interestingly, some are specific of certain tissues or cell types (like H3.5 in human testis (Schenk et al., 2011) or HTR10 in plants, specific of sperm cells (Okada et al., 2005) whereas others respond to environmental stimuli (H3.Y in primates, (Wiedemann et al., 2010)) or have an unknown function.

As mentioned above, the universal replacement variant H3.3 only differs from H3.1 in four amino acids at different positions. Even if histones are highly conserved proteins, these substitutions are not conserved, as the differences in H3.3 genes are thought to have emerged several times in evolution (Malik and Henikoff, 2003). While in animals the residues distinguishing both proteins are A_{31}-S_{87}-V_{89}-M_{90} in H3.2 (with an additional C_{96} in H3.1) and S_{31}-A_{87}-I_{89}-G_{90} in H3.3 (S_{96}), in plants, both monocots and dicots, the key substitutions are

located at different positions and involve different amino acids (A_{31}-F_{41}-S_{87}-A_{90} in H3.1, and T_{31}-Y_{41}-H_{87}-L_{90} in H3.3) (Table 1; Fig 1.2) (Ingouff and Berger, 2010; Otero et al., 2014).

	H3.1	H3.3
Animals	A_{31}-S_{87}-V_{89}-M_{90} (C_{96})	S_{31}-A_{87}-I_{89}-G_{90}(S_{96})
Plants	A_{31}-F_{41}-S_{87}-A_{90}	T_{31}-Y_{41}-H_{87}-L_{90}

Table 1. Amino acids differentiating H3.1 and H3.3 in animals and plants. 4 amino acids distinguish H3.1 from H3.3 in plants. In animals this is the case for H3.2 while there is a 5 aa difference between H3.1 and H3.3.

Even if the difference is small, these four amino acids have proved to be fundamental for the different properties of both histones for several reasons.

1) First, these four substitutions are sufficient to allow the binding to specific histone chaperones. CAF-1 is found in complex with H3.1 while HIRA chaperones H3.3. Both proteins guide histone deposition in a replication dependent or independent manner respectively (Tagami et al., 2004).
2) Second, in some cases the unique amino acids help to specifically modify the histones. In Arabidopsis one of the positions of H3.1, A31, specifically fits in ATXR5, an enzyme that incorporates a methyl group into lysine 27, H3K27me1, a heterochromatin mark. This way, a single amino acid difference between both histones enables different chromatin outcomes, as it protects H3.3 from heterochromatinization due to the presence of T_{31}, that doesn't fit in the binding pocket of ATXR5 (Jacob et al., 2014).

   In the same direction, a modification specific of H3.3 was observed in animal cell lines. It was reported that part of total H3 is phosphorylated at serine 31 in late prometaphase and metaphase and that these histones are exclusively located at pericentromeric heterochromatin in metaphase chromosomes, contrary to H3S10/28 phosphorylation (Hake et al., 2005).
3) Finally, the specific substitutions guide the genomic location of each histone, as mutations at these positions alter their genome-wide distribution (Goldberg et al., 2010; Shi et al., 2011).

In *Drosophila melanogaster*, it was first shown that H3.3 was incorporated into active loci, including rDNA, independently of DNA replication (Ahmad and Henikoff, 2002). Mapping of both histones in flies revealed that H3.3 is enriched in the coding sequence of active genes and

highlighted its correlation with RNA Polymerase II and H3K4me2, a modification typical of active transcription in flies (Mito et al., 2005; Wirbelauer et al., 2005).

Genome-wide maps of H3.3 in mammalian embryonic stem cells (ESC) showed that H3.3 is enriched around the transcriptional start site (TSS) of both active and repressed genes but only in the bodies of active genes, H3.3 content correlating with gene expression. H3.3 is also enriched at transcription factor binding sites (TFBS) and telomeres (Goldberg et al., 2010) and it is necessary for the establishment of H3K27me3 at the promoters of key developmental genes regulated by Polycomb complexes (Fig 1.2). These last two observations indicate that in ESCs, H3.3 is not always related to transcriptionally active sites (Banaszynski et al., 2013).

Upon differentiation to neuronal precursors, the pattern of H3.3 changes in cell-type specific genes: the content of H3.3 decreases if the genes will no longer be expressed or it is maintained or increased if the genes will be transcribed. With differentiation, the H3.3 content is also modified at the TFBS of cell-type specific genes (Goldberg et al., 2010)

In plants, GFP-tagged versions of genes belonging to the H3.1 or H3.3 groups have shown that H3.1 colocalizes with DAPI-dense chromocenters whereas H3.3 is found in rDNA nucleolar foci (Ingouff et al., 2010; Shi et al., 2011). However, no genome-wide map of both histones existed at the beginning of this project. In root dividing cells it was observed that H3.3 is constitutively expressed while H3.1 spots the organ with the patchy pattern typical of cell cycle regulated proteins (Ingouff et al., 2010), but the dynamics of each protein during organogenesis and development in somatic tissue remained unexplored.

1.1.6 H3 function along development.

One of the main challenges to study the function of H3.1 and H3.3 during development by using genetic approaches is the numerous genes coding each histone. Nevertheless, as the variant is usually coded by fewer genes, several mutants have been developed (Table 2).

In Drosophila the knockout of the two genes coding H3.3 (*H3.3A* and *H3.3B*) causes partial lethality, upregulation of H3 genes and sterility of the surviving individuals, both males and females. However, as the semi-lethality and the transcriptional misregulation are solved when either H3.1 or H3.3 is expressed, these phenotypes are thought to be caused by decrease nucleosome replacement. Thus, in Drosophila H3.1 can substitute for H3.3 provided that it is expressed also out of S-phase, something allowed in the survivors thanks to the upregulation and polyA stabilization of H3.1 transcripts. Despite the interchangeability in somatic tissue, H3.3 is however essential to reorganize chromatin in male meiosis (Sakai et al., 2009).

In *Xenopus laevis*, depletion of H3.2 (H3.1 in frogs) and H3.3 using morpholinos causes defects at early gastrulation. In turn, depletion of only H3.3 genes delays the defects till late gastrulation, indicating the need of H3.3 in chromatin dynamics during this phase of embryonic development (Szenker et al., 2012). Contrary to the observations in flies, the phenotype cannot be rescued providing exogenous H3.2, suggesting that at least in Xenopus gastrulation the two histones do not seem to be interchangeable.

In *Mus musculus* several strategies have been developed to knock out H3.3 genes. In 1999 a gene trap mutated *H3f3a*, one of the two H3.3 genes in mice. As a result of the mutation, 50% of the newborns die within the first 24 hours. The gene was expressed constitutively until 13.5 days post-coitum during embryonic development and in several key organs of adults. Survivors displayed reduced growth rate and a neuromuscular deficit, males also showing reduced copulatory activity and getting few pregnancies when copulations occurred, pointing to a role of this gene in male fertility (Couldrey et al., 1999).

In another study the *H3f3b* was knocked out and again partial lethality and infertility was observed in almost all the survivors of both sexes. Interestingly, in mouse embryonic fibroblasts derived from these mice, chromosomal bridges were observed in mitosis and the karyotype exhibits abnormalities: chromosomes with fragmented ends, rearrangements and endoreplication. Another remarkable characteristic in these mutants is the presence of ectopic CENP-A foci and an increase in pericentromeric heterochromatin.

Importantly, mutations in H3 genes have been found in a variety of tumors: pediatric gliomas, adult glioblastomas, chondroblastomas, insulinomas and giant cell tumors of bone. For instance H3.3A and canonical H3.1B are mutated in a variety of ways (K27M, G34R and G34V for H3.3A and K27M for H3.1B) in adult glioblastomas and diffuse intrinsic pontine gliomas, the last one among the leading causes of terminal cancer in children, pointing to a role of H3 proteins in the maintenance of cell proliferation and cancer progression (Maze et al., 2014).

1.1.7 H3 dynamics along development

The most common strategy to follow H3 dynamics along development has been the tagging of histones with fluorescent proteins. This approach is also useful due to the lack of antibodies that distinguish H3.1 and H3.3 (although recently an anti-H3.3 was released).

Most studies differentiating H3.1 from H3.3 are conducted in cell cultures and usually control the expression of H3 histones under constitutive or inducible promoters, not following the endogenous dynamics of the proteins (see for instance (Ahmad and Henikoff, 2002; Ray-Gallet et al., 2011)). Only a few cases of histone dynamics have been reported along development,

usually focusing on germline, fertilization processes or the first stages of embryonic development but, to our knowledge, never in adult organisms.

In Drosophila the asymmetric delivery of H3.1 has been detected in the stem cells of the male germline (Tran et al., 2012). Also in this organism the replacement of protamines by maternal H3.3 was observed in the male pronucleus at fertilization (Loppin et al., 2005). In mouse embryos, the mobility of all the H3 proteins has been analyzed at different stages, linking the mobility of the canonicals with increased cell plasticity (Boskovic et al., 2014). In Arabidopsis, the dynamic of several histone H3 proteins has been tracked in mature gametes and at fertilization. In the first case, H3.3 proteins and some unusuals are present while H3.1 is strikingly absent. Upon fertilization, *de novo* synthesis of the different histones starts and the somatic balance is already restored at the 2-cell embryo (Ingouff et al., 2007; Ingouff and Berger, 2010).

As already mentioned, histones do not passively bind DNA: they are escorted by several histone chaperones specific of each variant.

1.1.8 Histone chaperones.

Under physiological conditions, the basic positively-charged histones bind non-specifically to negatively-charged DNA and produce insoluble aggregates (Tyler, 2002). To solve this problem, a plethora of histone chaperones, negatively-charged proteins, bind histones and assemble nucleosomes in a stepwise manner (Das et al., 2010).

Regarding H3 chaperones, ASF1, CAF-1 and HIRA are highly conserved in animals, plants and fungi and will be analyzed in detail later on. In addition, some other chaperones have been described lately. Indeed, histone chaperones guide histones in a variety of situations. For instance, the histone chaperone NASP (nuclear autoantigenic sperm protein), protects the pool of soluble H3-H4 histones in mammalian cells, controlling the amounts of available histones depending on changes in demand (Cook et al., 2011). Other chaperones, like Daxx (death domain-associated protein 6) - ATRX (α-thalassemia X-linked mental retardation process) mediate replication-independent deposition of H3.3 at telomeres in murine ESCs (Goldberg et al., 2010; Lewis et al., 2010) (Fig 1.2). Loss of these two chaperones results in aneuploidy and telomere dysfunction and embryos do not eventually differentiate and die (Michaelson et al., 1999). Mutations in ATRX and Daxx have been detected in pancreatic neuroendocrine tumours, myelodysplastic syndromes, relapsed acute myeloid leukaemia, neuroblastomas and glioblastomas (Maze et al., 2014). Contrary to ATRX, no homologue of Daxx has been found in Arabidopsis (Otero et al., 2014). Another H3.3 chaperone, DEK (Sawatsubashi et al., 2010), is

upregulated in several cancers (Wise-Draper et al., 2005) and has four homologues in Arabidopsis (Fig 1.2), one of which, DEK3, colocalizes with protein-coding genes and modifies nucleosome occupancy and chromatin accessibility (Waidmann et al., 2014).

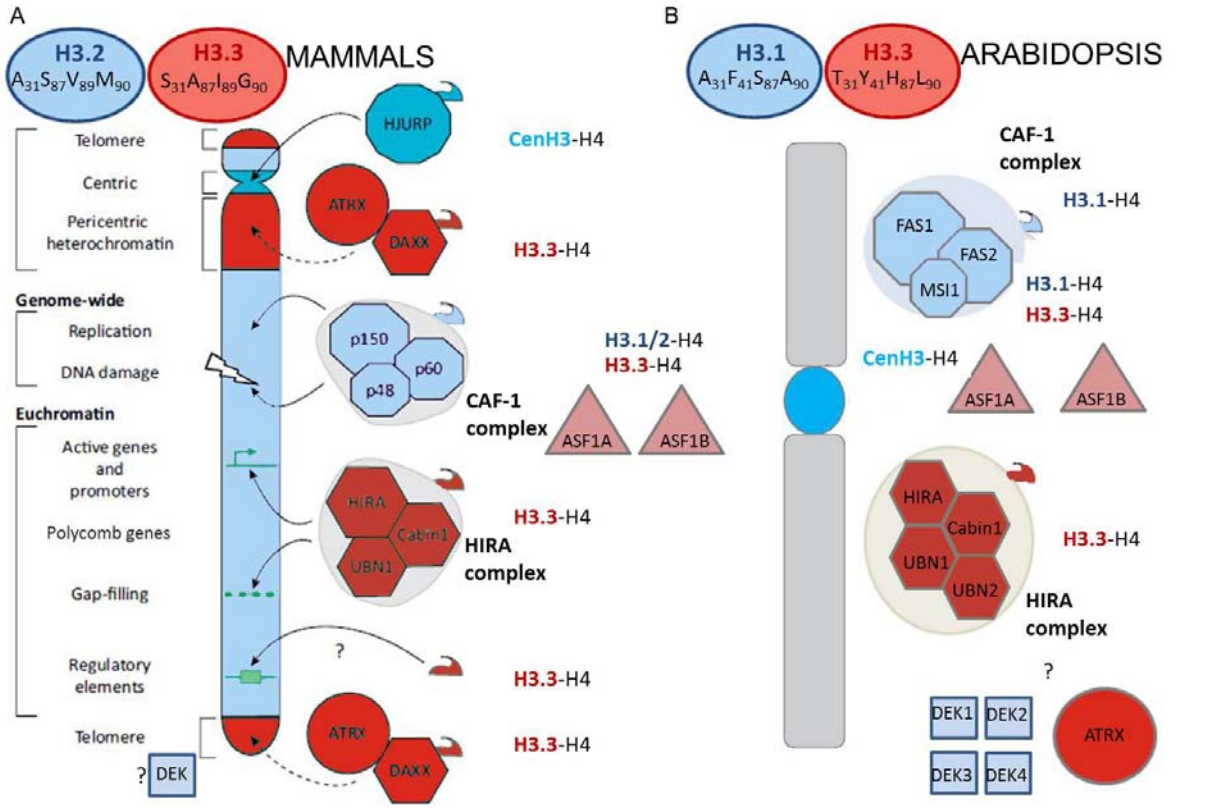

Fig 1.2. State of the art of H3 dynamics and histone chaperones in mammals (A) and Arabidopsis (B) before this study. The genome-wide distribution of H3.1 and H3.3 in Arabidopsis was unknown. The interactions among members of the HIRA complex had not been studied in Arabidopsis. ATRX and DEK have homologs in the model plant whose functions have yet to be explored. Adapted from (Filipescu et al., 2013)

1.1.8.1 ASF1

Anti-silencing function 1 (ASF1) chaperones H3-H4 dimers, containing either H3.1 or H3.3, and delivers them to CAF-1 and HIRA (Tagami et al. 2004) (Fig 1.2). It was first discovered in *S. cerevisiae* by its ability to derepress transcriptional gene silencing (Le et al. 1997). Nevertheless, ASF1 is conserved in all eukaryotes studied, specially its N-terminal domain. Even if some species only have one *ASF1* gene, two isoforms are found in mammals and also in plants (Sillje and Nigg, 2001; Zhu et al., 2011).

The importance of ASF1 is demonstrated by the mutant phenotypes observed (Table 2). In chicken cells, lack of Asf1 is translated in an increase of cells in S phase, chromosomal aberrations and cell death, the domain that interacts with histones being crucial for cell viability (Sanematsu et al., 2006). Interestingly, Asf1 is not only a histone donor but also an acceptor, as

Asf1 buffers excess histones upon replication arrest and keeps them protected to quickly deliver them again as soon as replication restarts (Groth et al., 2005). Regarding the task distribution between the two Asf1 isoforms in human cells, even if they share common roles as histone chaperones and during replication regulation (Groth et al., 2007), their expression is differentially regulated. While Asf1a expression is constant, Asf1b disappears as soon as the cell exits the cell cycle. Remarkably, Asf1b presence is a direct readout of the proliferation capacity of the cell. In fact, Asf1b expression correlates with a higher risk of metastasis and disease progression and can be used as a prognosis marker (Corpet et al., 2011).

In Arabidopsis, single T-DNA mutants do not exhibit any obvious phenotype, indicating redundant functions between the two isoforms, ASF1A and ASF1B, that do not necessary correspond to the Asf1a and Asf1b described in mammals. However, the double mutant is a smaller plant with defects in vegetative and reproductive development that displays cell number reduction, S phase arrest, increased DNA damage, S and DNA damage checkpoints activation and upregulation of DNA repair genes, including some of the homologous recombination pathway (Table 2) (Zhu et al., 2011; Lario et al., 2013).

Loss of…	H3.1	H3.3	ASF1	CAF-1	HIRA
Mus musculus	Unknown	*H3f3a or H3f3b:* partial lethality. Few pregnancies.	Unknown. Lethal in vertebrate cells.	P150: 16-cell arrest.	Embryonically lethal: 1-cell stage
Drosophila melanogaster	Unknown	Partial lethality. Sterility of the survivors.	Unknown.	Embryonically lethal	Embryonically lethal
Arabidopsis thaliana	Unknown	Unknown	Smaller plants with defects in vegetative and reproductive development	MSI1: embryonically lethal. FAS1 and FAS2: pleiotropic developmental defects	Slight developmental phenotypes.

Table 2. Developmental phenotypes observed upon loss of H3.1, H3.3, ASF1, CAF-1 and HIRA in mice, flies and Arabidopsis.

Altogether, these studies highlight the importance of ASF1 in replication, cell proliferation and genome integrity.

1.1.8.2 CAF-1

Histone chaperone CAF-1 assembles and deposits $(H3.1\text{-}H4)_2$ tetramers (Winkler et al., 2012) in a replication-dependent manner and during DNA repair (Burgess and Zhang, 2013). Highly conserved in eukaryotes, it consists of three subunits that receive different names

depending on the species (p150, p60 and p48 in mammals and FAS1, FAS2 and MSI1, respectively, in plants) (Fig 1.2). It directly interacts with PCNA (proliferating cell nuclear antigen) through the p150 subunit (Shibahara and Stillman, 1999), linking CAF-1 to the replication fork. Regarding ASF1, the connection is made through p60 (Tyler et al., 2001).

CAF-1 loss also results in strong and pleiotropic phenotypes (Table 2). While none of the three subunits is essential in yeasts, p150 loss in Drosophila is lethal (Loyola and Almouzni, 2004) and causes embryonic developmental arrest at 16-cell stage in mice due to defects in heterochromatin maturation (Houlard et al., 2006). Like in yeasts, mutants of the three subunits are available in plants, with the advantage of studying CAF-1 function in an adult multicellular organism. FAS1 and FAS2 subunits are not essential and mutants are viable and fertile. On the contrary, *msi1* null mutants are embryonically lethal (Kohler et al., 2003; Guitton et al., 2004). Indeed, cosuppresor lines for *MSI1* show phenotypes not observed with the loss of the other subunits (Hennig et al., 2003), something expected as MSI1 is part of several other complexes with different cellular functions such as RBR-E2F (Ach, 1997; Ausin et al., 2004), histone methyltransferases from the Polycomb group (Kuzmichev et al., 2002; Kohler et al., 2003; Hennig and Derkacheva, 2009) and flowering regulators (Bouveret et al., 2006).

Regarding the two largest subunits of the complex, they will be both referred to as *fasciata* (Kaya et al., 2001), the name coming from the fasciation observed in the leaves, since only minor differences are observed between single *fas1* and *fas2* mutants (Exner et al., 2006) and the double mutant is undistinguishable from the parental single mutants. *De visu*, the plants are smaller, have altered phyllotaxis (pattern of organ initiation at the shoot apical meristem, SAM) and shorter roots (Reinholz, 1966; Leyser, 1992). The cellular organization of both the shoot and the root apical meristems (SAM and RAM, zones of cell proliferation in charge of development of the aerial or subterranean parts of the plant, respectively) is disrupted, including anatomical variations, disorganization of the stem cell niche and stochastic misexpression of meristem regulator genes, like *WUSCHEL* in the SAM and *SCARECROW* in the RAM, among others (Kaya et al., 2001). *fasciata* mutants also display defects in seedling development, including a shorter elongation zone and reduced cell number in hypocotyls and leave epidermal cells. Also, CAF-1 mutants show more trichome branches without an increase in their cell ploidy, indicating CAF-1 could be important for trichome differentiation (Exner et al., 2006). Altogether these phenotypes point to a role of CAF-1 in multiple developmental processes that require a correct balance between proliferation and differentiation.

Interestingly, *FAS1* is an E2F target, indicating a regulation of the expression of this subunit by the cell cycle machinery. Moreover, in *fasciata* mutants the G2 DNA damage checkpoint is activated, mitotic progression is inhibited and an early entry in endoreplication is observed (Ramirez-Parra and Gutierrez, 2007), with increased ploidy levels detected in various ecotypes (Columbia (Col) and Enkheim (En))(Exner et al., 2006). This way, the switch to the endocycle program could be a mechanism to bypass the DNA damage that causes cell cycle arrest. In some aspects, the *fasciata* mutant phenotype becomes more severe along generations: telomeres are shortened, the rDNA copy number is reduced and anaphase bridges are accumulated, together with reduced viability and decreased fertility (Mozgova et al., 2010).

Transcriptional gene silencing is stochastically disrupted in *fasciata* mutants (Ono et al., 2006). However, CAF-1 is needed for heterochromatin compaction but not for heterochromatin repression, as *fasciata* mutants have reduced heterochromatin, with normal methylation, but silent heterochromatin genes (Schonrock et al., 2006). Intriguingly, CAF-1 has been found to be important to prevent hypermethylation of TEs (Stroud et al., 2013).

Altogether, these data underscore the multiple roles of CAF-1, including coordination between cell proliferation and differentiation, genome stability, telomere length and rDNA copy number maintenance, heterochromatin compaction and stable inheritance of epigenetic states.

1.1.8.3 HIRA

HIRA (histone regulator A) is the chaperone that incorporates H3.3 in a replication independent manner (Tagami et al., 2004). It was first discovered as a regulator of histone gene transcription in yeasts, where contrary to most species two genes perform this function, *HIR1* and *HIR2* (Sherwood et al., 1993). In addition to HIRA, two more proteins are part of the complex: UBINUCLEIN (UBN) and CABIN1, both proteins with conserved domains in eukaryotes (Balaji et al., 2009).

In mouse cells, HIRA is necessary for H3.3 deposition at genes but not at TFBS or telomeres (Goldberg et al., 2010; Lewis et al., 2010). This correlates with RNA PolII distribution, pointing to H3.3 being deposited by HIRA during transcription (Ray-Gallet et al., 2011) (Fig 1.2). However, in ESC, HIRA also interacts with PRC2 through H3.3K27me3, reinforcing the role of HIRA for H3.3 deposition at genes independently of their transcriptional state (Banaszynski et al., 2013). Moreover, HIRA deposits H3.3 at any transiently naked (non-nucleosomal) DNA in a gap filling protective mechanism, distributing H3.3 broadly (Ray-Gallet et al., 2011) (Fig 1.2).

Interestingly, HIRA accumulates in damaged chromatin regions before repair and introduces H3.3 to prime chromatin for transcription after DNA repair (Adam et al., 2013). This way, HIRA and H3.3 are important not only for transcription and correct maintenance of epigenetic landscapes, but also to restore normal transcriptional activities after genotoxic stress. Another important characteristic of mammalian HIRA is that it can incorporate H3.3 during replication when CAF-1 is depleted and H3.1 deposition is impaired, a process that does not work for CAF-1 to deposit H3.3 (Ray-Gallet et al., 2011).

In animals, HIRA loss has lethal consequences (Table 2). In Drosophila and mice, HIRA is essential for H3.3 deposition and chromatin decondensation of the male pronucleus before the first round of replication in the zygote (Loppin et al., 2005; Lin et al., 2014) In mouse zygotes derived from mutant females, which arrest at the one-cell stage, it has also been observed that replication and transcription are highly reduced or absent in both the female and male genomes, demonstrating a role of HIRA also in the maternal genome. In addition HIRA is necessary for rDNA transcription and ribosome biogenesis in the zygote (Lin et al., 2014).

Taken together, these results imply that lack of H3.3 may be bypassed, like in Drosophila mutants, but HIRA is essential for embryonic development in mice and flies, even if some strategies have allowed the development of viable adult *hira* flies (Bonnefoy et al. 2007). Strikingly, in Arabidopsis, *hira* mutants only show slight pleiotropic defects during vegetative development, including shorter roots, a higher degree of leaf serration and cotyledons bending. Crossing these *hira* lines with mutants for other members of the complex (UBN1, UBN2 and CABIN1) does not increase the developmental defects observed (Nie et al., 2014), indicating that HIRA is not essential for plant fertilization or embryonic development. However, as expected, *hira* mutants have alterations in their transcriptome. In particular, genes that respond to biotic or abiotic stresses are downregulated. Interestingly, these genes, that usually contain H2A.Z in wild type plants, are also upregulated in plants deprived of H2A.Z, suggesting a connection between H3.3 and H2A.Z. Finally, HIRA and H3.3 histones are found to be upregulated in protoplasts, suggesting HIRA could play a role in dedifferentiation (Nie et al., 2014). Taken together all these data underscore the versatility of HIRA, a key chaperone in many cellular processes.

1.2.1 Arabidopsis as a model organism in epigenetics

Arabidopsis thaliana is an attractive organism to study epigenetics for several reasons. First of all the plant genome is relatively small (around 125Mb), full sequenced and well-annotated (Arabidopsis Genome, 2000); Arabidopsis.org), facilitating functional studies. Second, the Arabidopsis life cycle is short (around two months), undergoing two stages: the diploid sporophyte, the life-form that represents most of the Arabidopsis life cycle, and the haploid gametophytic stage, in charge of producing the gametes (Berger and Twell, 2011), which after fertilization will generate a large number of descendants. In addition, Arabidopsis is easily transformed and many knockouts are available. Interestingly, plants tolerate mutations in key chromatin genes that are lethal in other organisms (Kaya et al., 2001; Roberts et al., 2002; Houlard et al., 2006; Szenker et al., 2012; Nie et al., 2014), allowing the study of defective phenotypes in adult plants and along development. Arabidopsis is also appealing because in plants, organogenesis is a post-embryonic process: the plant has to develop leaves, flowers, fruits and main and lateral roots once it has germinated (Perianez-Rodriguez et al., 2014), fine-tuning cell proliferation and differentiation and usually combining cell cycle and endoreplication. These circumstances create an ideal scenario to study epigenetic changes during growth and morphogenesis in response to developmental and environmental cues.

In this project we have studied histone H3.1 and the variant H3.3 in different organs of Arabidopsis, taking advantage of the specific cell characteristics and dynamics in each system at various developmental stages. The different organs and processes used in this study are described.

1.2.2 The Root Apical Meristem.

The Arabidopsis root is an appropriate system that has been the focus of intense research over the last years. The Arabidopsis root is a thin, low auto-fluorescent and highly organized organ that is easily imaged by confocal microscopy (Geldner and Salt, 2014), characteristics that have propelled the use of the root as a tool to understand plant organogenesis.

Physiologically, the root provides the plant with water and nutrients and performs a structural function, as it anchors the aerial part of the plant (Petricka et al., 2012). Even if the primary root meristem, the promeristem (Scheres, 1994), is already established in the embryo, it gets activated during germination becoming the Root Apical Meristem (RAM), a group of actively proliferating cells that allows continuous growth of the organ.

Maintenance of the RAM depends on the stem cell niche, a microenvironment containing active stem cells located around the quiescent center (QC) in a striking coexistence

of adjacent stem cell subpopulations with different cycling activities, a situation also common in stem cell niches found in animals (Li and Clevers, 2010). The stem cells around the QC will produce different cell types (Figure 1.3): in the rootward part of the QC, columella stem cells will produce distal columella cells. Epidermis and lateral root cap, the most external cell layers of the root cylinder, originate from the epidermis/lateral root cap (LRC) initial cells while cortex and endodermis will result from an asymmetric division of cortex/endodermis initial daughter cells (Petricka et al., 2012). Regarding the vascular tissue, the vascular initials in the shootward part of the QC will generate xylem and pluripotent procambial cells that will later generate the phloem through periclinal divisions (Mahonen et al., 2006). Transcriptional and proteomic data of the different cell types are available thanks to the identification of markers specific of each cell layer that allowed cell type separation by cell sorting (Brady et al., 2007; Petricka et al., 2012).

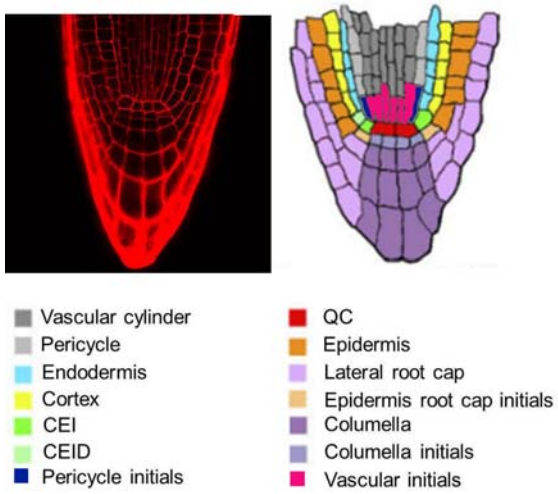

Fig 1.3. Root tip. The different cell types and the stem cell initials are marked in different colors. QC: quiescent center. CEI: Cortex endodermis initials. CEID: cortex endodermis initial daughter cells. Adapted from (Levesque et al., 2006)

The QC cells are characterized by a low proliferation rate, restrained by the proteasomal degradation of the transcription factor ERF115 (Heyman et al., 2013) and by the exclusion of CYCD activity in these cells, mediated by WOX5 (Forzani et al., 2014). Nevertheless, QC cells are a stem cell subpopulation that act as the reservoir of stem cells in the RAM and divide to substitute damaged stem cells (Heyman et al., 2013). Another fundamental function of the QC cells is preventing differentiation of the adjacent stem cells (van den Berg et al., 1997), a pathway where WOX5 also plays a pivotal role (Sarkar et al., 2007). Together, the outlined functions point out the QC cells as the organizers of the stem cell niche, an essential task that requires QC identity specification early in embryogenesis.

Two independent pathways are in charge of the QC fate: the PLETHORA (PLT) route (Aida et al., 2004; Galinha et al., 2007) and the SCARECROW (SCR)/SHORTROOT (SHR)

pathway (Helariutta et al., 2000; Nakajima et al., 2001; Sabatini et al., 2003). PLT an SHR are mobile transcription factors that participate in various key processes in the root. SHR is expressed in the stele and moves to adjacent cell layers to activate SCR expression, both proteins being members of the GRAS family of transcription factors. In addition to QC identity, SHR and SCR are responsible of protoxylem formation (Carlsbecker et al., 2010; Miyashima et al., 2011) and activation of CYCD6;1 in cortex/endodermis initial daughter (CEID) cells to regulate the asymmetric division that generates the two cell layers of the ground tissue: cortex and endodermis (Sozzani et al., 2010).

On the other hand, the PLETHORA family is formed by several proteins that belong to AINTEGUMENTA-like (Roudier et al., 2011) subclass of the AP2/EREBP family of transcription factors. As mentioned above, PLT1 and PLT2 specify QC identity and maintain stem cell activity (Aida et al., 2004). In addition, two other members of the family are expressed in the RAM (PLT3 and PLT4) and the four of them display gradient distributions with maxima in the stem cell area. This gradient was shown to be fundamental for root development, as the dosage of PLT proteins controls meristem size by regulating stem cell maintenance, cell proliferation and cell cycle exit to differentiation (Aida et al., 2004; Galinha et al., 2007). Remarkably, the gradient that is formed by cell-to-cell movement of PLT proteins and by growth dilution, responds to auxin signals slowly, maintaining the longitudinal zonation pattern, that is, the developmental zones along the root, stable despite environmental adaptation. This fact points out PLT proteins as a fundamental factor in the root to coordinate cell division and differentiation (Mahonen et al., 2014).

1.2.3 Developmental domains in the root.

Along the root, cells will divide, elongate and finally differentiate to acquire their specific characteristics and functions. A new cell produced by the initials will undergo cell cycle for an undetermined number of times (but normally 3-4) while staying in the RAM, cell division stopping at different distances from the QC depending on the cell type. As the proliferation capacity of the cells decreases as they become located away from the QC, two different domains are distinguished in the RAM: the proliferation domain, next to the stem cell niche where cell division is very likely, and the transition domain, in the more shootward part of the RAM, where cell division is rare and cell growth is still slow (Ivanov and Dubrovsky, 2013) (Figure 1.4A). After passing through the RAM, cells lose their ability to divide and greatly increase their growth rate, multiplying their length several times their width: they are now part of the elongation zone (EZ) (Figure 1.4A).

Once the cells have reached their final size, they acquire maturity characteristics and specialize (Petricka et al., 2012). Three examples are well known: epidermal, phloem and endodermal cell differentiation. In the first case, cells become hair or nonhair cells depending on their position relative to cortex cells, a process regulated by a complex network of transcription factors (Tominaga-Wada et al., 2011). In the second example, sieve elements in the phloem are in charge of transporting photoassimilates. In the differentiation process these cells lose their nucleus and most of their organelles, a process controlled by the NAC family of transcription factors (Furuta et al., 2014b). Finally, endodermal cells engross their cell walls with suberin and lignin to form the casparian strip. The casparian strips are impermeable barriers that avoid water and solutes seeping through the space between the endodermal cells, forcing the absorbed substances to pass through the endodermal cytoplasm, a selective filter, before reaching the vascular tissue, the transport highway of the plant. The recently discovered CASP proteins participate in the casparian strip formation and, remarkably, they are already present in the endodermis at the elongation zone (Roppolo et al., 2011), indicating that differentiation begins already in this area of the root. Indeed, another characteristic of differentiation, cell endoreplication, also starts early in root development, precisely at the boundary between meristematic and elongation zone and preceding rapid cell expansion (Hayashi et al., 2013).

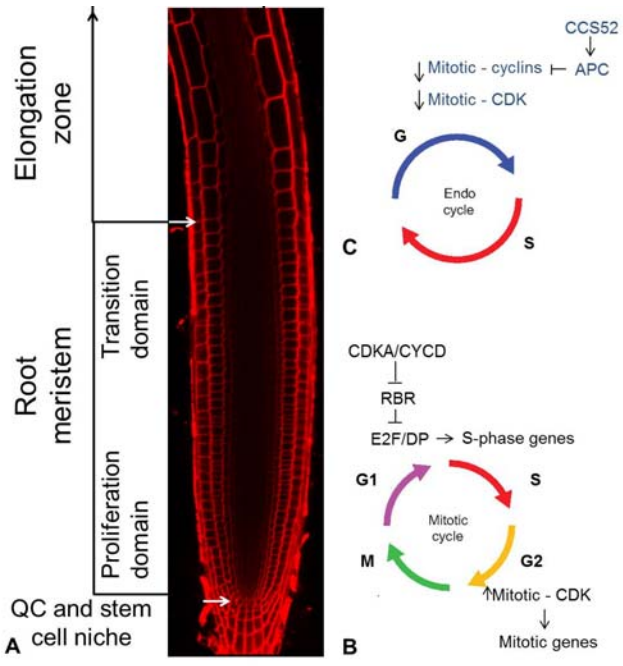

Fig 1.4. Root developmental domains. (A)The root meristem is divided in two different domains, the proliferation domain, where cells actively divide, and the transition domain, where mitosis are less frequent. In the elongation zone cells start rapid elongation and do not divide again. The differentiation zone is not shown. (B) Cells actively cycle in the RAM. The main regulatory mechanisms of cell cycle are shown (C) Cells enter the endocycle program before starting rapid elongation. A decrease in mitotic cyclins and CDK promote endocycle entry. Adapted from (Gutierrez, 2009).

1.2.4 Cell cycle and endoreplication.

The cell cycle is a highly controlled unidirectional process with the objective of producing two daughter cells, that can be identical to the mother (symmetric division) or have

different structural or functional properties (asymmetric division). Several successive phases can be distinguished in every cell cycle (Figure 1.4B). In G1, the gap phase between mitosis and S-phase, the cell grows and duplicates all its components, except the nuclear content. In this period, origins of replication are licensed, loading the pre-replication complexes at replication origins that will fire in S-phase, the DNA synthesis phase of the cell cycle were the genetic material will be doubled (Desvoyes et al., 2014). In addition, in G1, a first transcriptional wave will be held to express genes needed during S-phase, like most members of the ORC (ORIGIN RECOGNITION COMPLEX) family or FAS1, the largest subunit of the histone chaperone CAF-1. These genes are targets of the E2F transcription factors (TFs) which become active once RBR (RETINOBLASTOMA-RELATED) is phosphorylated by CDKA/CYCD complexes (CYCLIN DEPENDENT KINASE A/CYCLIN D), causing RBR inactivation and release of E2F activity. In G2, the gap between DNA replication and mitosis, DNA integrity is monitored (G2 checkpoint) and a new transcriptional wave driven by CDKs acting in the G2-to-M transition (Mitotic-CDK, like again CDKA and CDKB) produces the cell components acting in mitosis. CENH3, the centromeric histone, is also loaded in this phase to mark centromeres (Lermontova et al., 2006). At mitosis, chromatin becomes condensed in prophase after phosphorylation of serine 10 in H3, forming the visible chromosomes that will be aligned in metaphase and distributed to the new-born cells in the subsequent phases (Houben et al., 2007). Cytokinesis, the separation of the daughter cells, will be directed by the phragmoplast, a cell structure that controls vesicle trafficking to form the cell plate that will divide the cell (Gutierrez, 2009).

In turn, endoreplication is a cell cycle variant that skips mitosis after DNA replication. The result is a polyploid cell containing an exponential number of copies of each chromosome (4C, 8C, 16C, 32C etc. instead of 2C). In plants, like in animals, the endoreplication onset is triggered by downregulation of the Mitotic-CDKs while allowing the continuous activity of CDK acting in G1-to-S progression (S-CDKs). Nevertheless, S-CDKs are periodically inactivated to allow a transition to G1-like gap phase, where pre-replicative complexes are loaded (Edgar et al., 2014) (Figure 1.4C).

CDKs need to bind to cyclins to be active and cyclin levels are regulated by the anaphase promoting complex/cyclosome (APC/C). Therefore, APC/C controls endoreplication initiation through the ubiquitination of many mitotic cyclins, tagging them for proteasomal degradation. Remarkably, APC/C is activated by CELL CYCLE SWITCH 52 (CCS52), all three CCS52 genes promoting endoreplication onset in Arabidopsis (Edgar et al., 2014; Polyn et al., 2014). At

the same time, the expression of *CCS52* genes seems to be regulated by E2F proteins that together with their DP partners have also been implicated in the mitosis-to-endocycle transition. For example, E2FA-DPA (De Veylder et al., 2002) and E2FC-DPB overexpression (del Pozo et al., 2006) promote the endocycle onset.

Endoreplication is not a process exclusive of the root; rather it is a common developmental process in many organs of flowering plants: leaves, hypocotyls, fruits, the endosperm of the seeds and the sepals (Roeder et al., 2010; Edgar et al., 2014).

Regarding endoreplication, the hypocotyl is an interesting organ, as it only grows by cell expansion: cell divisions are absent or insignificant (Gendreau et al., 1997). In addition, when the seedlings are grown in the dark they adopt a skotomorphogenic program that consists on hypocotyl elongation at the expense of cotyledon and root formation, a strategy to seek for the light that allows one extra round of endocycle (Josse and Halliday, 2008), ploidy levels reaching up to 32C (Ramirez-Parra et al., 2004).

On the contrary, some cell types never endoreplicate, such as the stomatal lineage (Melaragno et al., 1993) that generates the guard cells of the stomata only through mitotic divisions. The stomatal differentiation process is well-known: a protodermal cell in the epidermis is converted into a meristemoid mother cell (MMC). The MMC undergoes an asymmetric division to generate a meristemoid, that will become a guard mother cell (GMC). In turn, the GMC will divide symmetrically only once to produce the two guard cells that will mature to generate the pore and become a functional stomata, in charge of gas exchange (CO_2 intake and water loss through transpiration) (Dow and Bergmann, 2014).

1.2.5 Gametophyte and embryo development.

During the vegetative phase of development, plants increase their photosynthetic capacity and their size and biomass. In the adult vegetative stage plants acquire reproductive competence and eventually switch to the reproductive phase (Huijser and Schmid, 2011). This transition is the result of integrating endogenous and environmental cues with the objective of flowering, a decision that is of utmost importance as flowering in the right time will be fundamental to obtain reproductive success (Jarillo and Pineiro, 2011).

The Arabidopsis flowers produce male and female gametophytes, also known as pollen and embryo sac respectively (Berger and Twell, 2011). During gametophyte development, reprogramming takes place to reset previously established chromatin modifications and restore pluripotency in the zygote. However, in flowering plants some epigenetic modifications are inherited, the so called epialleles (Calarco et al., 2012), and some can have dramatic

developmental consequences (Cubas et al., 1999). Gametophyte development is therefore an interesting scenario, as in addition both male and female gametophytes are multicellular, resulting from several divisions of the diploid mother cell. The female gametophyte is produced in the ovules. First, the megaspore mother cell (diploid) undergoes meiosis to produce haploid megaspores that after three nuclear divisions will generate the seven-celled gametophyte. It is formed by three antipodal cells, two synergid cells, one central cell and one egg cell. The antipodal cells in Arabidopsis have no known function while the synergid cells receive the pollen tube and degenerate. On the contrary, the central cell is the companion diploid cell that after fertilization will produce the endosperm whereas the egg cell is the female gamete (Drews and Koltunow, 2011; Kawashima and Berger, 2014).

On the other hand, mature pollen is produced in the anthers. The diploid pollen mother cells undergo meiosis to form tetrads of haploid microspores that at first are surrounded by a callose wall. The enzyme callase produced in the tapetum, a cell layer of the anther important for pollen development, releases the individual microspores that enlarge by vacuolation. As the vacuole gets bigger, the nucleus is pushed against the wall, an important event that facilitates the subsequent asymmetric mitotic division that produces one small cell and one big cell, the generative and vegetative cells respectively. The vegetative cell will no longer divide, however, the generative cell, engulfed in the vegetative cell cytoplasm, will divide to generate the two sperm cells (McCormick, 2004).

The sperm cells are identical male gametes that will fertilize the central and egg cells of the female gametophyte in a double fertilization process that will generate the endosperm and the zygote respectively. On the contrary, the vegetative cell will not contribute DNA to any of the fertilization products. Interestingly, the vegetative cell is reprogrammed to activate its TEs (transposable elements), downregulating DDM1 (DECREASE IN DNA METHYLATION 1), a chromatin remodeler that acts as a master regulator of TE activity in Arabidopsis. The objective of the vegetative nucleus reprogramming is TE silencing in the neighbour sperm cells, where an accumulation of 21 nucleotide siRNAs produced after TE activation in the vegetative cell is detected. These siRNA, able to travel from cell to cell, keep DDM1 activity high in the gametes, preventing transposition of TEs and promoting transgenerational TE silenced (Slotkin et al., 2009). However, recently some studies challenge the possibility of siRNA travelling from the vegetative to the sperm cells, pointing that maybe these siRNAs are inherited from microspores (Kawashima and Berger, 2014).

Sperm and vegetative cells also display different DNA methylation levels during development. Asymmetric CHH methylation decreases from the microspores to the sperm cells, while CG methylation remains constant. On the other hand, the vegetative cell loses CG methylation and restores CHH methylation (Calarco et al., 2012; Kawashima and Berger, 2014), something expectable as loss of global DNA methylation induces CHH hypermethylation (Stroud et al., 2013). The biological relevance of these dynamics is not yet well understood, although increasing the CG methylation levels in the vegetative cell has proved to be detrimental for pollen viability (Schoft et al., 2011).

Once the double fertilization takes place, the zygote (2n) elongates and divides multiple times to develop a full organism. During embryogenesis, the embryo adopts globular, triangular, heart and torpedo shapes, becoming finally a mature embryo having a radicle (the embryonic root) and two cotyledons. The root and hypocotyl originate from the lower lower tiers of cells generated at the triangular stage. Also, the hypophyseal cell in the suspensor will contribute to the root meristem by becoming the root cap cells and the quiescent center, the organizer of the root that will be specified at early heart stage (Scheres, 1994; Doerner, 1995) (Figure 1.5).

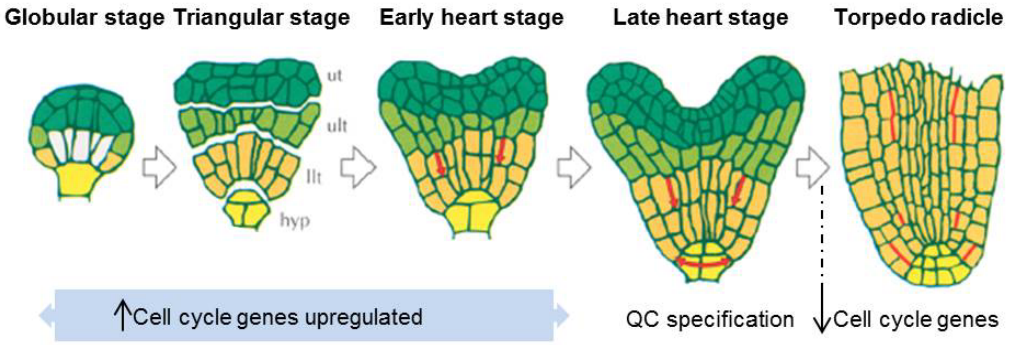

Figure 1.5. Embryonic development. The axes of the future plant are defined early in development. In the transition from globular to heart stage cell cycle genes are upregulated and QC is specified in late heart stage. From heart to torpedo stages, cell cycles genes are downregulated. Ut: upper tier. Ult: upper lower tier. Llt: lower lower tier. Hyp:hypophyseal cells. (Adapted from (Doerner et al. 1995)).

Interestingly, during the first stages of embryonic development, cell cycle genes are upregulated whereas they get repressed in the transition from heart to torpedo stage, where embryos show a high level of functional differentiation in roots and cotyledons (Spencer et al., 2007).

Once the seed germinates, radicle and cotyledons will protrude and the meristems will take command: the vast majority of the plant body is yet to come.

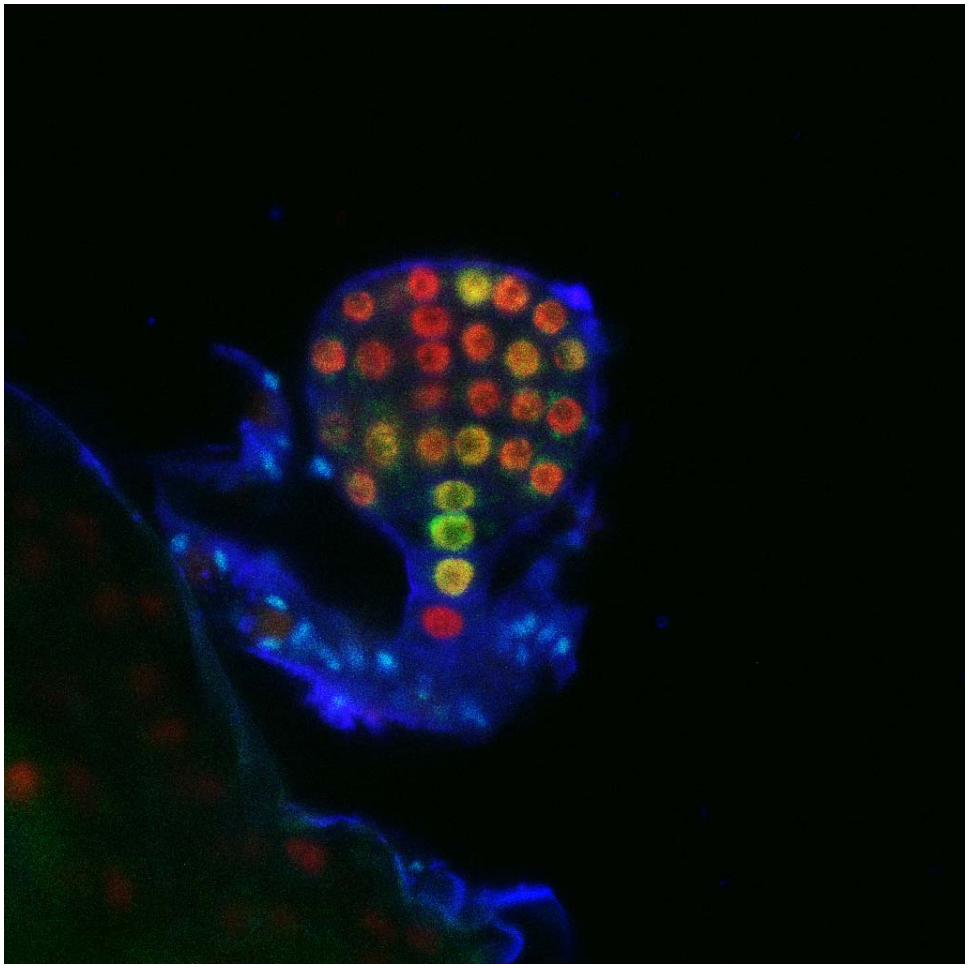

2. Objectives

Objectives of the work

The current study aims at investigating the role of histone H3 proteins, the canonical H3.1 and the variant H3.3, in *Arabidopsis thaliana*. Of special relevance is studying H3 dynamics along development and understanding the crosstalk between chromatin and cell population transitions during organogenesis, a mostly unexplored topic for which the model plant is an excellent system.

The objectives we propose are:

1. Gain insight into the function of H3.1 and H3.3 in Arabidopsis. Genome-wide map of both histones to analyze their distribution in relation to gene expression, chromatin marks and genomic elements.

2. Understand the relevance of the H3.1/H3.3 balance along development, focusing on embryogenesis and root organogenesis.

3. Examine histone H3 dynamics in proliferating and differentiating cells taking advantage of the root anatomy and organogenesis, where cell cycle, endocycle and differentiation are tightly coordinated both temporally and spatially.

4. Analyze the implications of H3 misbalance in the *fas* chaperone mutants.

5. Decipher the implications of H3 histones in specific cell types.

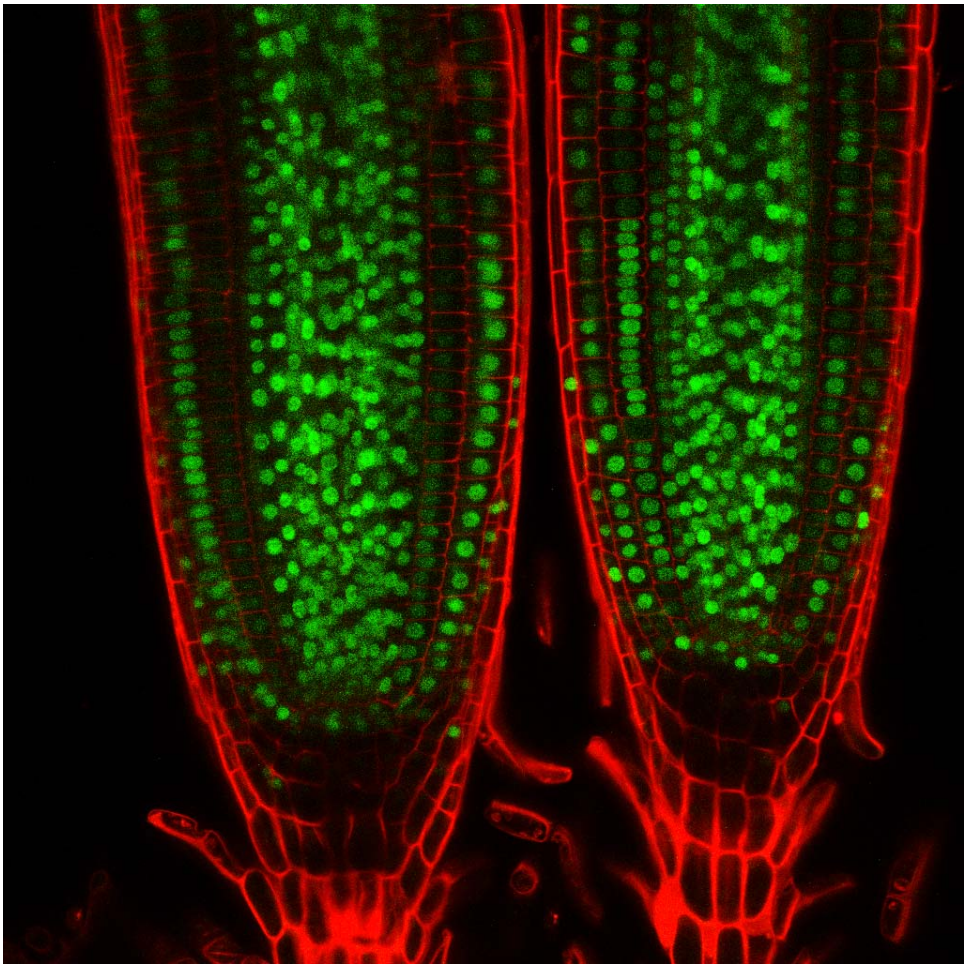

3. Materials and Methods

3.1. Materials

3.1.1 Bacterial strains

Cloning was performed using *Escherichia coli*, either DH5α or Z competent cells (Zymo Research). Gateway vectors were amplified using DB3.1 strain. Plant transformation was carried out with *Agrobacterium tumefaciens*, strain C58C1.

3.1.2 Plant ecotypes and growth conditions.

To generate transgenic plants, Columbia ecotype (Col-0) was used. Plants were grown in an incubator at 22ºC (or 20ºC) and 60% moisture under long day conditions (16-hour light/8-hour darkness) in either 1% or 0.8% agar MSS plates (1% sucrose, 0.5x Murashige and Skoog salt, 2.24g/l Duchefa, and 0,5g/l MES, pH 5.7).

3.1.3 Lines generated through transformation

pHTR3::HTR3-GFP/4xMyc;
pHTR4::HTR4-GFP/4xMyc;
pHTR5::HTR5-GFP/mRFP/4xMyc
pHTR13::HTR13-GFP/mRFP/4xMyc

3.1.4 Other lines used in this study

fas1-4 mutants (Exner et al., 2006).
CYCB1;1:GFP (Colon-Carmona et al., 1999)

3.2. Molecular biology techniques

3.2.1 Genomic DNA extraction from seedlings

Flower buds or small rosette leaves were frozen in liquid nitrogen together with glass beads and ground in Silamat S5 (Ivoclar Vivadent) for ten seconds. 200µl of extraction buffer (0.14M d-Sorbitol, 0.22M Tris-HCl pH8, 0.022M EDTA pH8, 0.8M NaCl, 0.8% CTAB, 1% n-Lauroylsarcosine) were added to the tissue. The samples were spinned and heated at 65ºC for 5 minutes shaking at 600rpm. After incubation, 200µl of chloroform were added and the mixture was shaken and then centrifuged at maximum speed for 7 minutes. The supernatant was then transferred to a new Eppendorf tube and 200µl of isopropanol were put in for precipitation at room temperature for 10 minutes. The DNA was pelleted centrifuging at 14000rpm for 15 minutes and then the pellet was washed with 70% ethanol, air dried for five minutes and resuspended in 100µl of water.

3.2.2 Protein extraction

To evaluate the expression level of tagged histones, 4-5 seedlings were frozen in liquid nitrogen together with glass beads and ground for ten seconds in Silamat S5 (Ivoclar Vivadent). Afterwards, the tissue was resuspended in 150µl of lysis buffer (50mM HEPES, 150mM NaCl, 1mM EDTA, 1% Triton X-100, 0.1% SDS) and sonicated for 10 cycles in Bioruptor® (30 seconds on/30 seconds off) to help homogenization. Samples were incubated in a rotating mixer wheel at 4ºC for 30 minutes and then centrifuged 10 minutes at maximum speed. The proteins were quantified using BCA protein assay (Pierce BCA Protein Assay Kit, Thermo Scientific), compatible with the concentrations of the different detergents present in the buffer and 50µg of proteins were loaded in 15% Tris/Glycine polyachrylamide gels to run SDS-PAGE electrophoresis and subsequent Western Blot. Briefly, proteins in the gel were transferred to a methanol-activated Immobilon- P membrane (0.45µm, Millipore) for 1 hour at 250mA using the wet electroblotting system from Bio-Rad. The membrane was then blocked for 20 minutes with 5% dried milk in PBS 0.1% Tween and then incubated with the primary antibody overnight at 4ºC (1:3000 Anti-Myc tag antibody, clone 4A6 from Millipore or 1:5000 anti-GFP ab290 from Abcam). After three washes of 10 minutes with PBST the membrane was incubated with the secondary antibody for 1 hour (diluted 1:10000, either ECL mouse/rabbit IgG HRP linked, Amersham GE Healthcare Life Sciences), washed again 3 times and proteins were detected by chemiluminescence.

3.2.3 RNA extraction

Seedlings or roots grown for the appropriate time were frozen together with glass beads in liquid nitrogen. 250µl of Trizol (Life Technologies) were added to the tissue and it was ground for 8 seconds in Silamat S5 (Ivoclar Vivadent). Another 250µl of Trizol were added and the materials were thoroughly mixed. 100µl of chloroform were used to extract the total RNA. After spinning the samples for 10 minutes at 4ºC, the upper phase was transferred to another tube. The RNA was precipitated using isopropanol and glycogen for 15 minutes at -20ºC and then centrifuged for 10 minutes at 4ºC. The pellet was washed with 75% ethanol, air dried for 5 minutes and then resuspended in 44µl of nuclease free water. After that, it is treated with DNase (Roche, 10U/µl) for 20 minutes at 37ºC and extracted again using phenol:chloroform:isoamyl alcohol (25:24:1). RNA was then precipitated with 1/10 3M sodium acetate, pH 5.2, 1µl of 20mg/ml glycogen and 2.5 volumes of 100% ethanol. Pellets were then

washed with 75% ethanol, air dried and resuspended in 40 µl of nuclease free water. RNA was quantified using NanoDrop (Thermo Scientific). RNA quality was assessed by fractionating 500ng of RNA in a 1% agarose gel.

3.2.4 RT-PCR

To obtain cDNA, 500ng of total RNA were used. The reverse transcriptase reaction was performed using oligo dT as a primer and the SuperScript III kit from Life Technologies, following kit instructions.

3.2.5 Quantitative PCR (qPCR)

cDNA was diluted 16 times and 2µl were mixed with the desired primers and the reagents of the GoTaq qPCR master mix (Promega). Standards, negative controls and unknown samples were run in ABI Prism 7900HT SDS. The efficiency of amplification for each primer pair was determined setting a standard curve with different dilutions of cDNA. The slope of the line (n) was used to calculate the efficiency with the following formula: $10^{*(-1/n)}$

To measure the expression of the different histones, the absolute copy number of each cDNA was calculated with the help of standards where the copy number is known. For this purpose, amplicons for the different primers were amplified by PCR and purified directly from a low agarose gel following the protocol described in Sambrock and Russell with slight modifications. Briefly, the bands were excised from the gel and weighed. Then, a solution of 20mM Tris-HCl 1mM EDTA was added at a ratio of 1µl of solution per 1mg of agarose slice and the bands were melt at 65ºC. Two successive phenol extractions were performed, the first with hot phenol (37ºC) and the second with phenol:chloroform:isoamyl alcochol. DNA was then precipitated with 1/10 of 3M NaoAc, pH 5.2, and 2.5 volumes of 100% ethanol.

The concentration of each amplicon was measured using NanoDrop and the number of copies of dsDNA was calculated using the algorithm found in the website http://cels.uri.edu/gsc/cndna.html

Several dilutions of these standards were run in the ABI Prism and the crossing points of each dilution and the number of copies were plotted in standard curves where the unknown samples were interpolated to obtain the absolute copy number.

To calculate the relative expression of different genes, the ΔΔCt method was used. First the Cts of the gene of interest and the Cts of the reference gene (a housekeeping gene, normally UBQ10 or GAPDH) were compared ($\Delta Ct = Ct_{target} - Ct_{reference}$). Then, the ΔCt of each sample was normalized to the control sample, in these studies Col-0 or WS ($\Delta\Delta Ct = \Delta Ct_{target} - \Delta Ct_{control}$).

3.2.6 GATEWAY Cloning

A genomic fragment containing the promoter and the coding region, except for the termination codon, of different histone H3 genes was amplified by PCR using Pfx (Life Technologies) and specific primers containing the attB sites. The PCR products were purified using Wizard SV Gel and PCR Clean-Up system and cloned into pDONR221 (Life Technologies) using BP Clonase II (Life Technologies). Colonies were analyzed using restriction enzymes after obtaining plasmid DNA and those that were positive were sent for sequencing. Clones without mutations were transferred to the corresponding Gateway Destination vectors using LR Clonase II (Life Technologies). Recombinant plasmids were assessed by restriction enzymes and the frame was checked by sequencing the plasmids.

Destination vectors used in this study:

pGWB4: plant expression vector allowing C-terminal fusion of the protein to GFP. Plants are resistant to both hygromycin and kanamycin.

pGWB16: plant expression vector allowing C-terminal fusion of the protein to 4xMyc. Plants are resistant to both hygromycin and kanamycin

pGWB453: plant expression vector allowing C-terminal fusion of the protein to mRFP. Plants are resistant to kanamycin.

All these vectors were provided by Tsuyoshi Nakagawa (Research Institute of Molecular Genetics, Matsue, Japan) (Nakagawa et al., 2007a; Nakagawa et al., 2007b).

3.2.7 Chromatin Immunoprecipitation (ChIP)

3.2.7.1 ChIP-seq

ChIP was carried out as in (Villar and Kohler, 2010) with some modifications. Briefly, 1g of 10-day-old seedlings (Col-0, HTR13-Myc 16.4 and HTR5-Myc 8.8) was vacuum-infiltrated with 1% formaldehyde in water for 20 minutes on ice to crosslink histones and DNA. Miracloth mesh was used to keep the plants submerged. Crosslinking was quenched with 135mM Glycine and the material was infiltrated again for 5 minutes. Then the plants were washed 4 times with Milli-Q water, pat dried on towel paper and frozen in liquid nitrogen.

To isolate the nuclei, the material was ground into a fine powder that was transferred to 15 ml of Nuclei Extraction Buffer (NEB1, 0.4M sucrose, 10mM Tris-HCl (pH 8.0), 10mM MgCl2, 1mM PMSF, and 1× protease inhibitors) and homogenized with vortex. Then the solution was filtered through a layer of Miracloth and a 70µm strainer, keeping it always cold. After centrifuging the samples for 20 minutes at 3000x*g* and 4ºC, the pellet was resuspended in 1ml of NEB2 (0.25M sucrose, 10mM Tris-HCl (pH 8.0), 10mM $MgCl_2$, 1% Triton X-100, 1mM PMSF, and 1 x protease inhibitors) pipetting up and down and centrifuged again for 10 minutes at 12000x*g* and 4ºC. This pellet was resuspended in 400µl of NEB3 (1.7M Sucrose, 10mM Tris-HCl (pH 8.0), 0.15% Triton X-100, 1mM PMSF, and 1 x protease inhibitors) using the pipette tip and mild vortex. The solution was placed on top of a cushion of 400µl of NEB3 and centrifuged for 1 hour at 14000rpm speed, at 4ºC.

The supernatant was discarded and the pellet resuspended in 300µl of Nuclei Lysis Buffer (50mM Tris-HCl (pH 8.0), 10mM EDTA, 1% SDS, and 1 x protease inhibitors). The samples were then sonicated using Bioruptor (Diagenode) for 30 cycles (30 seconds on, 30 seconds off) to obtain a DNA smear ranging from 200 to 800bp (sonication time had been optimized previously, sonicating nuclei extracted in the same conditions and taking 10µl aliquots every 10 minutes, reverting the crosslinking afterwards and running the samples in an agarose gel to check DNA sizes) and centrifuged for 5 minutes at 16000x*g* and at 4ºC.

At this point, to immunoprecipitate the same amount of chromatin, the chromatin in each sample was quantified as in Brookes et al. 2012. Arbitrary chromatin concentration was obtained measuring the amount of proteins in the sample after alkaline lysis. For this purpose, the absorbance at 280nm of a 1:50 dilution of the sample in 0.1M NaOH was measured. As it is a mixture of proteins the conversion factor 1mg/ml was used. After multiplying by 50 the amount of chromatin was obtained in mg/ml and 700µg were used for immunoprecipitation.

Before adding the antibody, the 700µg were diluted ten times with ChIP dilution buffer (1.1% Triton X-100, 1.2mM EDTA, 16.7mM Tris-HCl (pH 8.0), 167mM NaCl, and 1 x protease inhibitors) to decrease the SDS concentration to 0.1%. Samples were then precleared for 1 hour with 40µl of protein G PLUS agarose beads (Santa Cruz Biotechnology) to eliminate the unspecific background. After that, 10% of the sample was taken as input and finally the antibody (10µg of anti-Myc, clone 4A6 or 1µg of Rb pAb to rat IgG, ab6703, Abcam) was added and incubated overnight in a rotating mixer wheel at 4ºC. The inputs were kept in the freezer at -20ºC.

The next day, 50µl of protein G PLUS agarose beads were rinsed with ChIP dilution buffer and added to the sample for two hours to recover the immune complexes. The bead pellet was washed with 4 different buffers, twice with 1ml each, first a short wash after vortexing and then a 5-minute wash incubating the samples in a rotating mixer wheel at 4ºC. First the samples were washed with low salt wash buffer (150mM NaCl, 0.1% SDS, 1% Triton X-100, 2mM EDTA, and 20mM Tris-HCl (pH 8.0), then with high salt wash buffer (500mM NaCl, 0.1% SDS, 1% Triton X-100, 2mM EDTA, and 20mM Tris-HCl (pH 8.0)), LiCl wash buffer (0.25M LiCl, 1% Igepal CA-630, 1% sodium deoxycholate, 1mM EDTA, and 10mM Tris-HCl (pH 8.0)) and finally TE (10mM Tris-HCl (pH 8.0) and 1mM EDTA).

To elute the immune complexes, 250µl of elution buffer (1% SDS, 0.1M $NaHCO_3$) were added to the beads and the tubes were incubated for 15 minutes at 65ºC and 600rpm. After a spin, the supernatant was transferred to a new tube and the elution process was repeated again with another 250µl of elution buffer.

The inputs were thawed and their volumes were adjusted to 500µl with elution buffer. 20µl of 5M NaCl were added to all the samples to reverse crosslinking and the tubes were incubated at 65ºC with strong shaking (950rpm) overnight.

The last day of the protocol, the samples were first incubated with 1µl of 10mg/ml RNaseA for 30 minutes at 37ºC. Then, 10µl of 0.5M EDTA and 2µl of 10mg/ml proteinase K were added for 2 hours at 45ºC. After that, the immunoprecipitated DNA was recovered with phenol:chloroform:isoamyl alcohol (25:24:1) using phase lock gel tubes (3 Prime), mixing the samples for 30 seconds and then centrifuging for 15 minutes. The supernatant was recovered and split into 2 different tubes. Then the DNA was precipitated with 1µl of 20mg/ml glycogen, 1/10 of 3M NaOAc, pH 5.2, and 3 volumes of 100% ethanol. After mixing by inversion, the tubes were kept for 1h at -20ºC and were then spinned for 30 minutes at maximum speed, 4ºC. The pellets were washed with 1ml of 75% ethanol twice and then air-dried for 15 minutes. Each pellet was resuspended in 20µl of nuclease-free water and identical samples were combined in a final volume of 40µl. The pellets were kept on ice for 20 minutes to ensure correct rehydration and then ChIP result was analyzed through PCR.

Quantification was performed with Qubit (Life Technologies) using the high sensitivity kit for dsDNA. Finally, samples were again precipitated and washed as previously indicated and the dry pellets were sent to UCLA for sequencing (Steve Jacobsen's lab).

3.2.7.2 Library preparation

For ChIP-seq library preparation, the TruSeq ChIP sample preparation kit was used (Illumina). Briefly, ChIP fragments were repaired to produce blunt products. Then the ends were adenylated with a single "A" and ligated to adaptors with a single "T" overhang. PCR was then used to selectively enrich those DNAs that have an adaptor at both sides and to amplify the amount of DNA in the library. The samples were then sequenced using the HiSEq 2000 sequencing systems.

For RNA library preparation, 0.1g of RNA from 10-day-old seedlings was treated with DNaseI (Roche, 10U/µl), and poly(A) purification was performed using the Dynabeads mRNA Purification Kit (Invitrogen). Then the TruSeq stranded mRNA sample preparation kit was used to generate the library: first RNA is fragmented and copied to cDNA. Single stranded cDNA is then transformed into dsDNA and then adenylated, ligated to adaptors, amplified and sequenced as indicated above.

3.2.7.3 ChIP-seq data analysis

Sequenced reads were aligned to the *Arabidopsis thaliana* genome using Bowtie, allowing up to 2 mismatches. Reads mapping to identical positions in the genome were collapsed into 1 read. Regions of H3.1 and H3.3 enrichment were defined using the SICER software package, with the input genomic DNA as a background control (parameters: Window size scanned (W) =200; Gap size (space between significant windows allowed such that they would be merged, G) = 400; FDR (significant cutoff) <1E-3). Regions of H3K27me1 ChIP-seq enrichment were defined with SICER, using H3 ChIP-seq reads as a background control (parameters: W = 500; G = 1,500; FDR <0.05). Regions of H2A.Z enrichment were defined by tiling the genome into 500-bp bins (250-bp overlap) and then computing the log2 ratios of the scores of H2A.Z to input genomic DNA. These scores were then z-score–transformed, with a cutoff of z >2 cutoff applied. Finally, adjacent H2A.Z-enriched regions were merged. Gene expression levels were determined by calculating reads per kilobase per million mapped reads for each gene. Transcription-binding sites were obtained from AGRIS (http://arabidopsis.med.ohio-state.edu). Plots were normalized for their sequencing depths and smoothed. Smoothing was performed for presentation purposes.

3.2.7.4 ChIP with sorted cells.

Root endodermal cells sorted according to the presence of pEN7::YFPH2B (Heidstra et al., 2004) were collected. 245,000 cells for Col-0, 245,000 cells for HTR13-Myc and 152,160 cells for HTR5-Myc were processed. Due to the low cell number, the True Micro ChIP kit from Diagenode was used with some modifications. Cells were resuspended in 250µl of nuclei lysis buffer. Another 250µl of HBSS were added and samples were sonicated in 15 ml Falcon tubes for 5 cycles in Bioruptor, 30 seconds on, 30 seconds off. The samples were dyalized with Slide-A-lyzers G2 cassettes (Pierce) in ChIP dilution buffer, changing the buffer twice every 2 hours until the end of the day. Thanks to dialysis, the samples were maintained in small volumes with the concentration of SDS diluted. The final volume of each sample was around 600µl, of which 60 (10%) were kept as inputs and the rest split in two, one half to immunoprecipitate with 1.5µg of anti-Myc tag antibody and the other as a negative control with 1µg of anti IgG, both referenced above. The samples were immunoprecipitated overnight in a rotating mixer wheel at 4ºC. The next day, 10µl of pre-washed protein G magnetic beads were added to each sample following kit instructions. After 3 hours incubating at 4ºC the beads with the immune complexes, the samples were centrifuged and washed as indicated in the kit. Elution, decrosslinking and recovery of immunoprecipitated DNA was performed as in the True Micro ChIP kit protocol, resuspending the DNA in 30µl of nuclease free water and analyzing it through qPCR. The inputs were quantified using Qubit and thanks to the standard curve prepared from a known amount of DNA, the ChIP samples were also quantified using qPCR data.

3.3 Cell biology techniques

3.3.1 Transgenic plants generation

Agrobacterium tumefaciens (C58C1 strain) were transformed and grown for 2 days at 30ºC in plates containing two antibiotics (rifampicin and the antibiotic of each construct). A bacterial culture of 5ml was set and 1ml was used to check the colonies through PCR. An inoculum of 200ml was centrifuged at 5000rpm for 15 minutes and resuspended in a solution of 5% sucrose and 0.05% Silvet l-77. Columbia wild type plants were transformed using the floral dip method (Clough and Bent, 1998) and transformants were selected with 50µg/ml kanamycin. In the next generation plants with only one insertion were selected and in the T3 the

homozygous lines, either using antibiotics or looking at the fluorescence in roots of plated seedlings with the Axioscop2 plus microscope (CCD camera).

3.3.2 Confocal microscopy

3.3.2.1 Sample mounting for confocal microscopy

Roots were stained either with propidium iodide (1mg/ml) or 10µM FM4-64 (Life technologies). Leaves and cotyledons were infiltrated with FM4-64. The different tissues were observed using confocal LSM510 (Zeiss).

3.3.2.2 Embryo extraction

Siliques were placed on top of double sided tape and were opened using a syringe. The embryo sacs were transferred to a slide with a 25µl drop of embryo extraction buffer (4% paraformaldehyde, 5% glycerol in PBS) and dissected using two syringes. 25 µl of 10 µM FM4-64 were added and the embryos were infiltrated for a few seconds to allow the staining. Embryos were then observed using confocal LSM710 (Zeiss).

3.3.2.3 Pollen extraction and staining

Flowers and flower buds of different ages were dissected and anthers were extracted in water. Water was then removed and a drop of 1µg/ml DAPI+ 0.1% Triton was added for around 40 minutes in a dark moisture chamber. After this time the solution was discarded and samples were mounted in a drop of Mowiol 4-88 (Sigma). Preparations were sealed with nail polish and observed in the confocal at 63x, zoom 3.

3.3.3 Live imaging

Seedlings were grown for 3 days at the usual conditions and then transferred to glass bottom dishes with a drop of water. A piece of solid media was cut from a template of the same size and placed on top of the root. The dish was closed with parafilm and hung vertically (using two strips of tape) in the plant culture chamber overnight. Once in the inverted LSM510 confocal (Zeiss), 100µl of 10µM FM4-64 were injected under the solid media, the dish was closed again and the roots were observed *in vivo* at 63x. Images were acquired every few minutes (to avoid photobleaching) either manually or with a programmed series. In case mitoses are not observed in a 30 minute period, changing the plate is recommendable. Movies were edited using the Image J Fiji software.

3.3.4 Analysis of confocal images

3.3.4.1 Positioning of mitotic figures in the root meristem

The end of the meristem was determined in each cell file of the epidermis containing a mitotic figure. To do so, cell length was measured from the first cell focused in the epidermis plane near the root tip along the file, considering the end of the meristem the first rapidly elongated cell (Casamitjana-Martinez et al., 2003), that is, a cell which size doubles the average size of the cells in the meristem that will not divide again. In this analysis, the cell marking the end of the meristem will be at position - 1 and the next cell towards the root tip at position -2 and so on. Once the end of the meristem was localized and the position of cells in mitosis was identified, the relative position was calculated according to:

Ratio = cell position/cell determining the end of the meristem

This way, a mitotic figure in the first cell near the root tip would have a ratio of -1 and a hypothetic mitosis in the cell where the meristem ends will have a ratio near 0. Cells were measured using ImageJ Fiji.

3.3.4.2 Measurements of fluorescent intensity in the nuclei along the root

Several images were acquired along the root without changing the acquisition parameters (e.g. pinhole or gain). As the fluorescence of the histones varies several times along the root, two conditions were set, c1 being the best parameter set for the cells in the meristem that renders saturated images in the endoreplication zone, and c2, the best parameter set for endoreplicated cells. The focus was not changed between c1 and c2. Images for the two conditions were acquired in every region of the root and each condition was used for a different graph, being condition c2 the most suitable, since saturated images did not appear. The fluorescent intensity of each nucleus was measured using Fiji.

3.3.5 Flow cytometry of roots and hypocotyls.

Seeds from all the GFP-tagged histone lines and Columbia (Col-0) were grown for 5 days under the usual conditions. As most cells in the root are differentiated, root tips (~5mm) were cut to enrich the sample in apical tissue and avoid the masking of possible differences between cell populations. This resulted in two samples per line, the apical tissue sample (enriched in root tips) and the differentiated tissue sample (depleted of root tips). Regarding the hypocotyls, seedlings were grown in the dark for different days (3-10) and only the aerial part was selected for flow cytometry.

The different tissues were chopped in 250µl of cold nuclei isolation buffer (45mM $MgCl_2$, 30mM Sodium Citrate, 20mM 4-MOPS pH 7.0; 0,1% Triton X-100, Galbraith et al. 1991) using a single edge razor blade (GEM) in petri dishes, on ice. 250µl of Galbraith buffer were added and the released nuclei were collected with a cut-off 1ml tip. To avoid clogging of the flow cytometer, the sample was then filtered through 30µm nylon filters to eliminate cell debris and collected in flow cytometry tubes. Nuclei were then stained with DAPI (2µg/ml) and kept on ice until running the samples in the flow cytometer (FACSCanto II, Becton Dickinson). 10,000 events were measured and each experiment was repeated 3 times.

Using FL7 (DAPI detector, logarithmic scale) and FSC-A (detects light scattered forward), the different populations were detected and gated. With FL8-A vs FL8-W (DAPI detectors in a linear scale, detecting area and width) the singlets (single events) were discriminated from aggregates. FL1 detects GFP signal, an information that was combined with ploidy data. As Col-0 nuclei will have no GFP signal, these nuclei were used to fix the GFP negative gate. All analyses were performed with FlowJo software.

3.3.5 Root protoplasts preparation

Root protoplasts were prepared as in (Brady et al., 2007) with some modifications. Young (6 dps) seedlings were grown under the usual conditions (10 plates per line, 2 rows per plate) over a nylon mesh (SEFAR Nitex 03-100/44) that will facilitate root cutting. Roots were sliced with a surgical blade and transferred to a small petri dish containing a 70µm strainer and 7ml of solution B. Solution B was always prepared fresh, adding 1.5% cellulase (Calbiochem) and 0.1% pectolyase (Sigma #P3026) to solution A (600mM Mannitol, 2mM $MgCl_2$, 2mM MES, 10mM KCl). The mixture was heated at 55 ºC in a bath for 10 minutes to inactivate proteases. When cooled down, 5mM $CaCl_2$ and 0.1% BSA were added. The roots were incubated in the protoplasting solution for 1 hour in an orbital shaker at 100rpm. They were stirred with a transfer pipette at 20 and 50 minutes after incubation start. Once incubation time finished, the strainer with the sliced roots was washed with complete solution A (solution A supplemented with 5mM $CaCl_2$ and 0.1% BSA) and the liquid in the petri dish was collected in a 15ml Falcon tube and centrifuged at 200g for 12 minutes at 4ºC. The supernatant was aspirated and discarded while the pellet was carefully resuspended with a transfer pipette in 250µl of complete solution A and subsequently filtered through a 70µm strainer (431751, Corning) and a 40µm strainer (431750, Corning) and collected in a flow cytometry tube. An additional 250µl of complete solution A were added to the 15ml falcon tube to wash the walls

and the filtering process was repeated, getting a total volume of 500µl. The tubes were kept on ice until processing. Protoplasts were observed under the microscope to check integrity. Viability was assessed with Direct Blue (Sigma) under the microscope.

3.3.7 Sorting of root protoplasts.

Col-0 seedlings and lines carrying a double construct (Myc-tagged histones and marker lines for different root cell types) were protoplasted as previously indicated. Root protoplasts were sorted with FACSCVantage SE (BD Bioscience) previously calibrated with beads. A 130µm nozzle was used and pressure reached 9psi. PBS was used as sheath buffer. Cell populations were detected plotting forward scatter against side scatter. GFP positive populations were identified confronting FL1 (530±30) and FL2 (585±42) and collected in low binding tubes containing 250µl of solution A (no BSA) until collecting 50,000 cells. Then another tube replaced the first one and kept on collecting cells until the sample was finished. An aliquot was taken (50µl) to do a postsort control and check the percentage of cells that appeared in the proper gate after sorting. Sorted cells were kept on ice and fixed by adding 1% formaldehyde for 10 minutes. Crosslinking was stopped with 0.135M Glycine. To allow a better aggregation of the cells, BSA was added at a final concentration of 5mg/ml and then the samples were centrifuged at 200x*g* for 12 minutes at 4ºC. The supernatants and pellets were checked under the microscope to observe the absence or presence of cells, respectively. Subsequent centrifugations were performed until cells were no longer observed in the supernatant. The pellets were frozen in liquid nitrogen and stored at -80ºC.

3.3.8 EdU labeling combined with immunostaining of GFP-tagged proteins.

The protocol is based on (Kotogany et al., 2010) and (Du et al., 2012) with modifications. HTR13-GFP and HTR3-GFP seedlings (4 dps) were transferred to 6-well plates with liquid MS and incubated with 20µM EdU for 30 minutes. From this point on the samples were protected from light. After one wash with liquid MS the seedlings were infiltrated in MTSB buffer (50mM PIPES, pH6.9, 5mM EGTA, 5mM MgSO4) with 4% paraformaldehyde for 20 minutes. After several washes with MTSB, PBS and water the seedlings were placed on Superfrost ± charged slides and were dried overnight at room temperature. The next day, the aerial part of the seedlings was cut and the roots were surrounded with Pap-Pen to create a hydrophobic region, leaving a small space on one side to facilitate subsequent washes. Seedlings were rehydrated in MTSB and then treated with driselase solution (20mg/mL driselase (Sigma)

in 1x MTSB) for 45 minutes at 37ºC in a humid chamber to allow cell wall permeabilization. After several washes with PBS, cell membranes were permeabilized with 1x MTSB, 10% DMSO and 3% NP-40 for 1 hour at RT. Roots were blocked with 3% BSA, 10% Horse Serum (HS) in 1x PBS for 1 hour at 37ºC. Then the roots were incubated with the primary antibody (α-GFP from Life Technologies) diluted 1:2000 in 1% BSA, 10% HS, 0.1% Tween-20, 1x PBS overnight at 4ºC.

The next day the slides were washed in 3% BSA-PBS 3 times and then incubated for 1 hour with the secondary antibody (α-rabbit alexa-488 from Life Technologies) diluted 1:500 in 1% BSA, 10% HS, 0.1% Tween-20, 1x PBS. After repeating the washes, the Click-it cocktail was added as indicated in the kit for 30 minutes. The slides were washed with PBS three times and stained with 10µg/ml DAPI for 15 minutes. After repeating the 3 washes with PBS and wash again with water, the slides were mounted using Mowiol 4-88 (Sigma) and observed under confocal LSM710 (Zeiss).

3.4. Bioinformatic analysis

3.4.1 *In silico* promoter analysis

Position weight matrices (PWMs) for TF-binding sequeces (Franco-Zorrilla et al., 2014; Mathelier et al., 2014; Weirauch et al., 2014) were used to scan Arabidopsis promoter sequences (0.5 kb upstream the translation start site) using RSAT (Turatsinze et al., 2008). The parameters for scanning were pvalue<5e-04 and background sequences inferred from the input with a Markov order 2. Over-representation of particular cis-motifs was scored by comparing their frequencies in the promoters of root patterning genes against their corresponding frequencies in the complete promoters set, following an hypergeometric distribution ($p<0.05$). TF-binding site densities were obtained by scanning the motifs along 3 kb upstream sequences using the same parameters as above, and mapped motifs were converted to frequency histograms (number of binding sites/total number of genes) and represented with GNUPLOT 4.6.

Gene expression data along the root were obtained from (Brady et al., 2007). Series GSE8934 was downloaded from GEO (http://www.ncbi.nlm.nih.gov/geo/) and raw data normalized with RMA. Median normalized gene expression (Log2 intensity) along the root was plotted for the genes containing each of the significantly enriched TF-binding sequence within 0.5 kb upstream the translation start site and for all the probesets represented in the array. Statistical differences between TF-containing and -not containing genes were computed in R using Wilcoxon exact test.

Root expression profiles were obtained from the above data and analyzed in two steps: first, we identified genes showing variable expression patterns along the root by applying one-way ANOVA, selected 5,125 genes ($p<0.01$) and clustered them using the average linkage hierarchical clustering method. In a second step, we focused on genes showing higher expression values at distal root slices (2,794 genes) and classified them into 10 groups with K-means. Clusters were calculated and drawn using MultiExperiment Viewer (http://www.tm4.org). Finally, we scored the representation of TF-binding sites in each of the clusters and compared it with that corresponding to the complete Arabidopsis genome, following an hypergeometric distribution ($p<0.01$).

3.4.2 Microarray data analysis

The objective of the microarray analysis using data from (Brady et al., 2007) was finding genes with very similar expression levels in the first slices of the root that will decrease in slice 4. To do so, transcriptomic data from slices 1 and 2 (or 2 and 3) with a similar expression level (fold change fc = [0.67, 1.50]) were selected. The expression value of these genes was compared to the one in slice 4 using the following formula:

f c=(s1+ s2)* 0.5/s4

being s1, s2 and s4 expression values for slices 1, 2 and 4, respectively. We have selected genes with:

fc > 1.50 – 2.00: subexpression on slice 4.

fc < 0.50 – 0.67: overexpression on slice 4.

Selected genes are detailed in supplementary tables.

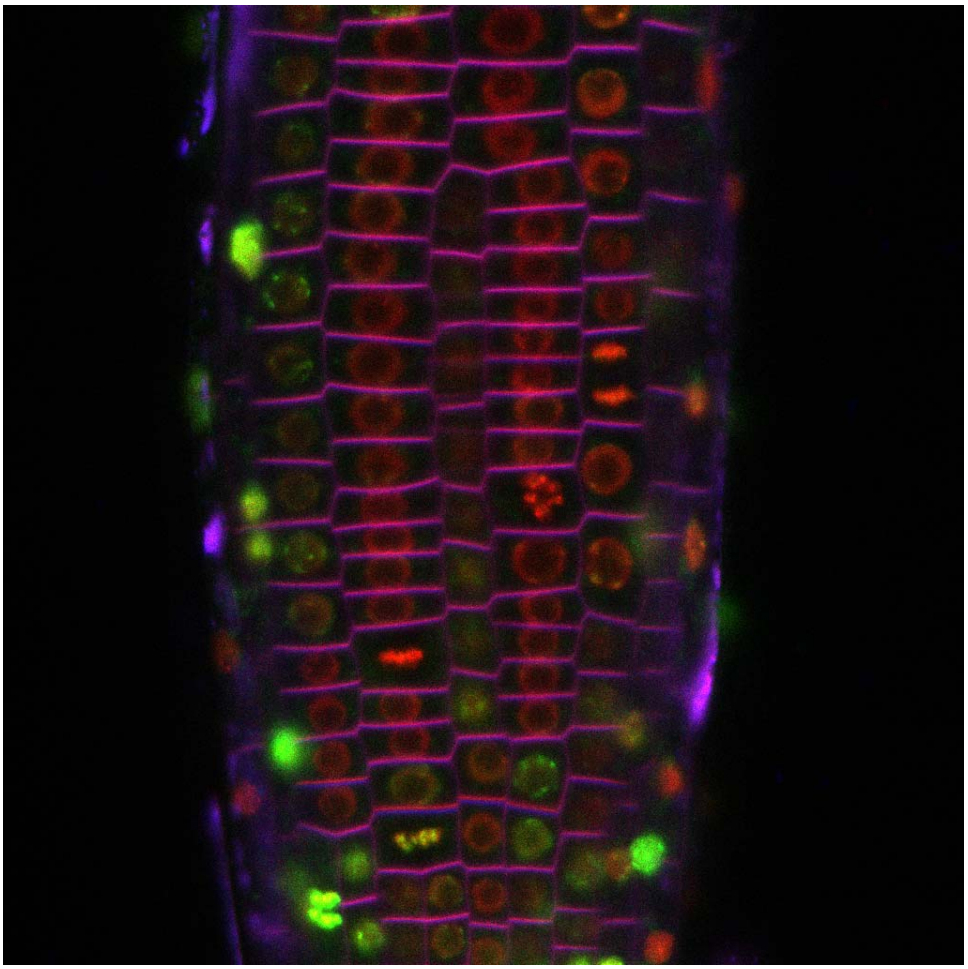

4. Results

4.1. Functional analysis of the genome-wide distribution of histone H3.1 and the variant H3.3 in *Arabidopsis thaliana*

4.1.1. Strategy to profile H3.1 and H3.3 genome-wide

Histone variants and their covalent modifications influence gene expression and the active/inactive state of the chromatin that is inherited along cell generations. Understanding the role of the different H3 proteins in a genome-wide scale is fundamental to interpret the implications of different epigenetic landscapes in a certain organism. H3.1 and the H3.3 variant had been profiled previously in Drosophila (Mito et al., 2005; Wirbelauer et al., 2005) showing that H3.1 was evenly distributed along the genome while H3.3 had a clear preference for actively transcribed genes, in agreement with its replication-independent incorporation. In mouse cells, H3.3 was also preferentially found in genes and was observed to vary with differentiation (Goldberg et al., 2010). However, in plants, the genome-wide location of H3 proteins had not been characterized. In order to know the distribution of H3.1 and H3.3 in the five chromosomes of *Arabidopsis thaliana*, we performed ChIP-seq experiments. As there is no antibody available to distinguish plant canonical H3.1 from the H3.3 variant, we generated Myc-tagged versions of archetypical members of each group under the control of their endogenous promoters (Figure 4.1A).

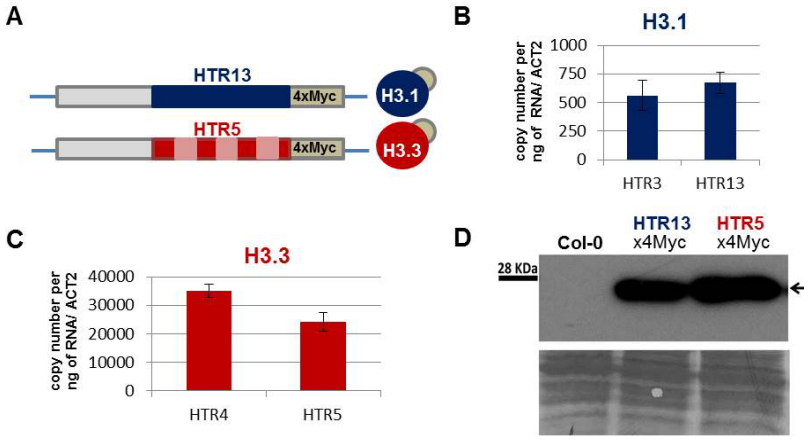

Fig 4.1. Histone-tagged lines. (A) The genomic sequence of HTR13 and HTR5 was fused to the 4xMyc epitope under the control of their endogenous promoters. (B) qPCR detecting the expression of the endogenous H3.1 genes. (C) qPCR detecting the expression of the endogenous H3.3 genes. (D) Western blot analysis of the tagged histones.

The histone H3 family had been previously described in Arabidopsis (Okada et al., 2005; Ingouff and Berger, 2010) informing of a patchy pattern for the H3.1 class and a constitutive expression of H3.3, with similar expression patterns among proteins of the same class. We checked the endogenous expression of two genes of each class in roots, confirming similar expression levels in each group and a higher expression of the constitutive variant

(Figure 4.1B,C). As once synthesized all proteins in each class are identical, we expected a similar behavior of all genes and we chose HTR13 as a representative of the cell-cycle regulated H3.1 histone and HTR5 as a paradigm of the H3.3 variant. Homozygous lines for both histones were selected and transgene expression was checked by Western blot, observing a slightly higher expression of the constitutive variant, as expected by qPCR data of the endogenous genes (Figure 4.1D).

4.1.2 Profile of H3.1 and H3.3 in Arabidopsis thaliana

Chromatin immunoprecipitation was performed on 10-day-old seedlings followed by massively parallel sequencing (ChIP-seq). High coverage maps with 75-90 million reads that uniquely mapped to the Arabidopsis genome were generated.

We first observed that H3.1 and H3.3 were differently distributed in the five chromosomes of Arabidopsis (Fig 4.2A): while H3.1 was enriched in pericentromeric heterochromatin, marked by high transposable elements (TE) density, H3.3 was depleted in these regions. Looking in detail in the genome, we observed that this differential distribution was also the rule for certain genes and elements, including dispersed heterochromatin blocks, enriched in H3.1 (Fig 4.2B).

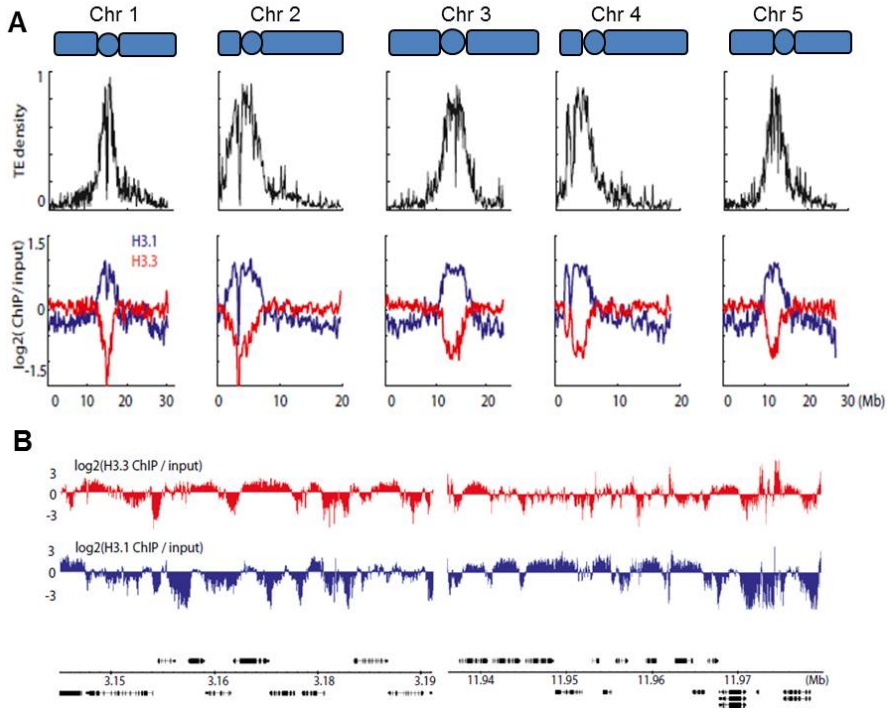

Fig 4.2. Genomic profile of H3.1 and H3.3 in Arabidopsis. (A) Map of both histones in the 5 chromosomes of Arabidopsis, showing ChIP-seq reads normalized to input DNA. TE density marks pericentromeric heterochromatin. (B) An example of different regions in chromosome 1 where anticorrelation of H3.1 and H3.3 can be observed. Genes are shown in black.

4.1.3 Functional analysis of the differential distribution of H3.1 and H3.3

To compare the distribution of the two histones with gene expression data, RNA from 10-day-old seedlings was also extracted and subjected to RNA-seq. Using these reads (33,353,995 that uniquely map to the Arabidopsis nuclear genome), genes were grouped according to different expression levels and H3.1/H3.3 reads were plotted over each cluster. We found out that H3.1 largely correlated with silent regions of the genome (Fig 4.3A) and TE (Fig 4.3C), stressing the relationship of H3.1 and heterochromatin. On the contrary, H3.3 was enriched in active genes, peaking towards the transcriptional termination site (TTS) (Fig 4.3B), independently of gene size (Fig 4.3D), a trend also observed in *Caenorhabditis elegans* (Ooi et al., 2010).

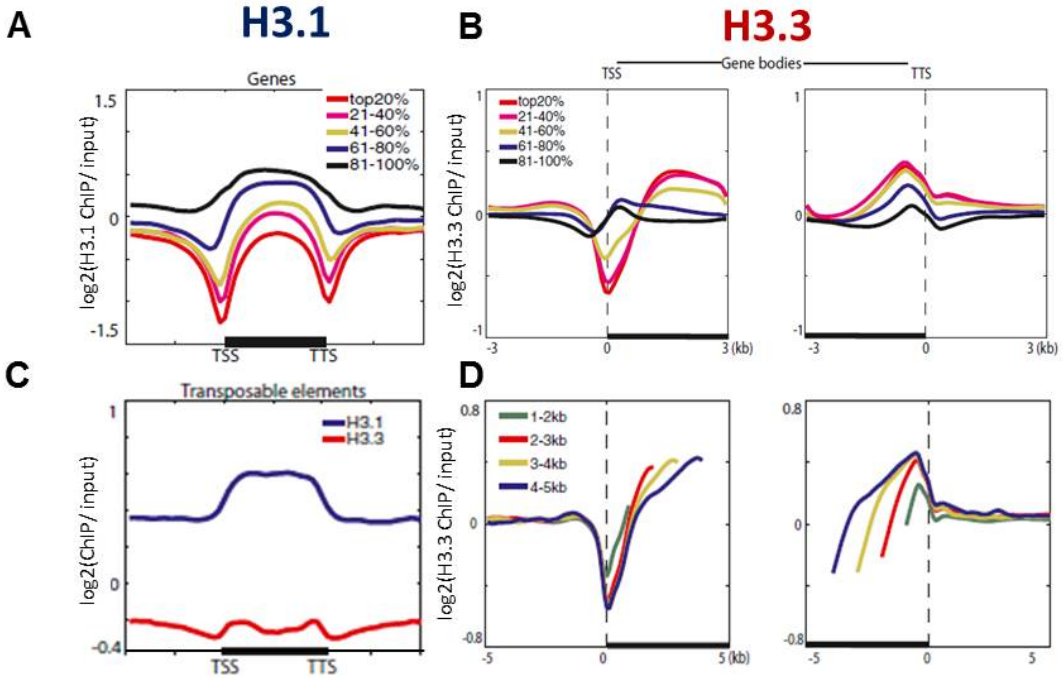

Fig 4.3. Histone H3 and gene expression (A) H3.1 anticorrelates with gene expression. Black bar indicates genes from transcription start site (TSS) to transcription termination site (TTS). Flanking regions are the same length as the gene body (B) H3.3 is enriched in active genes, peaking towards the 3' end. The average distribution of H3.3 reads 3Kbs downstream or upstream the TSS or TTS respectively is shown (C) H3.1 is enriched over transposable elements (TE), black bar representing TEs. (D) H3.3 reads represented over genes of different sizes. X axis is as in B covering 5Kbs.

To gain insight into the relationship of each histone H3 to DNA methylation, regions significantly enriched in H3.1 (20097 regions) or H3.3 (19983 regions) were grouped as described in Materials and Methods. Available data for DNA methylation levels determined by bisulfite sequencing (Jacob et al., 2009) were analyzed over the H3.1 and H3.3 regions. H3.1 regions were rich in all kinds of DNA methylation, no matter the sequence context (CG, CHG and CHH, H meaning A, T or C) (Fig 4.4A), indicating an association between H3.1

and DNA methylation. Methylation was also analyzed in relation to 3 gene categories previously determined: body-methylated genes, unmethylated genes and promoter-methylated genes. The first group is highly expressed and constitutively active, being more expressed than unmethylated genes. Promoter-methylated genes, the third class, have a lower expression level and are usually tissue-specific (Zhang et al., 2006). H3.1 was found to be enriched over promoter-methylated genes, emphasizing the association of H3.1 with silent regions (Fig 4.4B). On the contrary, H3.3 was associated with the highly expressed body-methylated genes (Fig 4.4C), that are typically enriched in CG methylation (Fig 4.4D). Even if the function of methylation in gene bodies is unknown, it is a characteristic conserved across eukaryotes (Feng et al., 2010; Zemach et al., 2010) that, as H3.3, it is skewed towards the 3'end of the genes.

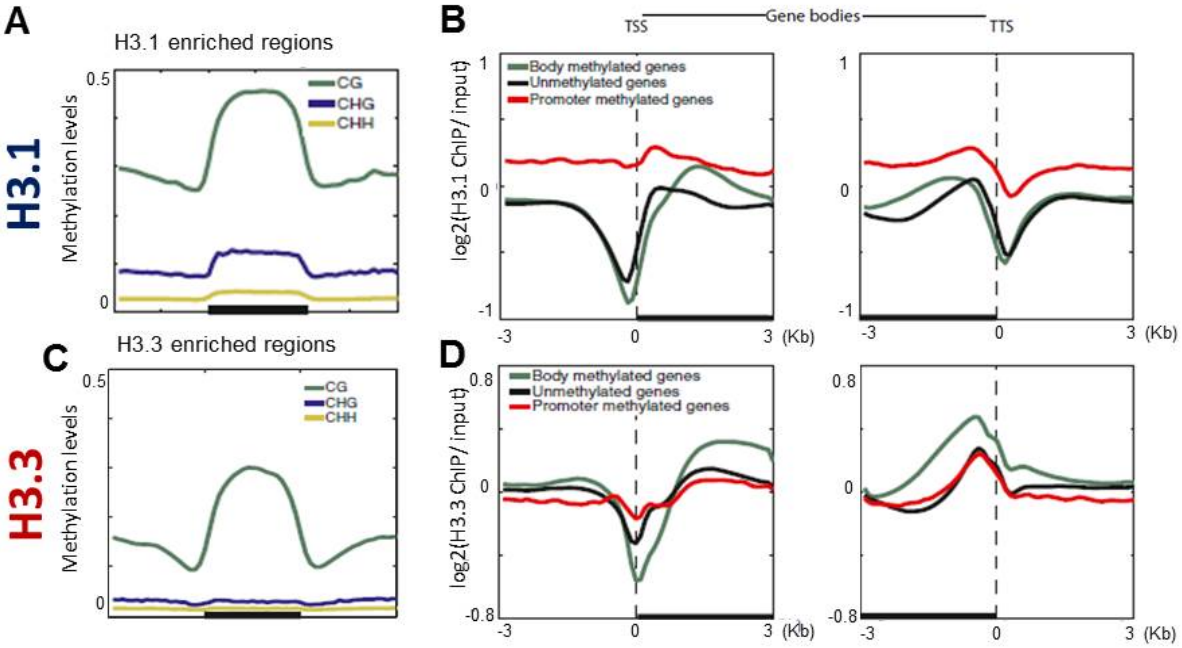

Fig 4.4. Histone H3 and DNA methylation (A) H3.1 enriched regions are associated with all types of DNA methylation. (B) H3.1 reads plotted over body methylated, unmethylated or promoter methylated genes show H3.1 is enriched over promoter methylated genes. X axis is as in figure 4.3B). (C) H3.3 enriched regions correlate with CG methyation. (D) H3.3 is enriched over body methylated genes.

Mass spectrometry studies revealed that Arabidopsis H3.1 had been associated with H3K27me1/me2/me3 whereas H3.3 was enriched in active marks (Johnson et al., 2004). Given the clear association of H3.1 with pericentromeric heterochromatin and DNA methylation and the association of these characteristics with certain chromatin marks, we wanted to explore the relationship of H3.1 with silencing marks of different origins taking also advantage of their position in the genome. H3K9me2 is a typical mark of

heterochromatin, present in pericentromeric and dispersed heterochromatin (Bernatavichute et al., 2008). To know if H3.1 was also enriched in heterochromatic patches of the chromosome arms, H3.1 ChIP-seq reads were plotted over H3K9me2 enriched regions located in the arms. H3.1 was highly enriched over these sites, indicating a global association of H3.1 and heterochromatin (Fig 4.5A). H3.1 was also enriched over H3K27me1 sites (Jacob et al., 2010), a mark associated with gene silencing and now known to be important to avoid heterochromatin overreplication (Jacob et al., 2014) (Fig 4.5B). Another silencing mark, H3K27me3, is the classical mark driven by the polycomb system, present in 17% of coding genes (Zhang et al., 2007), usually transcription factors with a role in development. This mark does not frequently overlap with H3K9me2 or DNA methylation and the enrichment of H3.1 in H3K27me3 regions indicates a strong correlation of H3.1 with gene silencing outside heterochromatic regions, led by DNA methylation or H3K27me3 (Fig 4.5C). Interestingly, H3.1 has been found to be specially enriched in several chromatin states: the two heterochromatin states (8 and 9), state 5, the classical polycomb chromatin and also in states 2 and 4, together with state 5 the ones where gene expression is lower (Sequeira-Mendes et al., 2014), confirming the association of H3.1 with gene silencing in different contexts.

Regarding the H3.3 variant it was not associated with H3K9me2 or H3K27me3. Analyzing H3.3 enriched regions we found H3.3 correlated with H3K4me1, a mark typically found in transcribed regions (Zhang et al., 2009), ubiquitinated H2B (Roudier et al., 2011) and RNA Polymerase II signal (Chodavarapu et al., 2010), consistent with H3.3 association with active chromatin (Fig4.5D). H3.1 did not show any relation with these elements (Fig 4.5E).Another interesting point was the connection of H3.3 with the histone variant H2A.Z, as both histones had been associated in Drosophila and humans (Henikoff et al., 2009; Jin et al., 2009). In Arabidopsis, H2A.Z does not correlate with DNA methylation and is enriched at transcription initiation sites (Zilberman et al., 2008). When H3.3 reads were plotted over H2A.Z regions, grouped as indicated in Materials and Methods, a strong anticorrelation was observed for these two histones (Fig 4.5F), indicating a possible plant specific characteristic. Later, it was determined that H2A.Z and H3.3 are usually characterizing the same chromatin states, even if H2A.Z is also present in state 5, depleted of H3.3 and with low gene expression (Sequeira-Mendes et al., 2014).

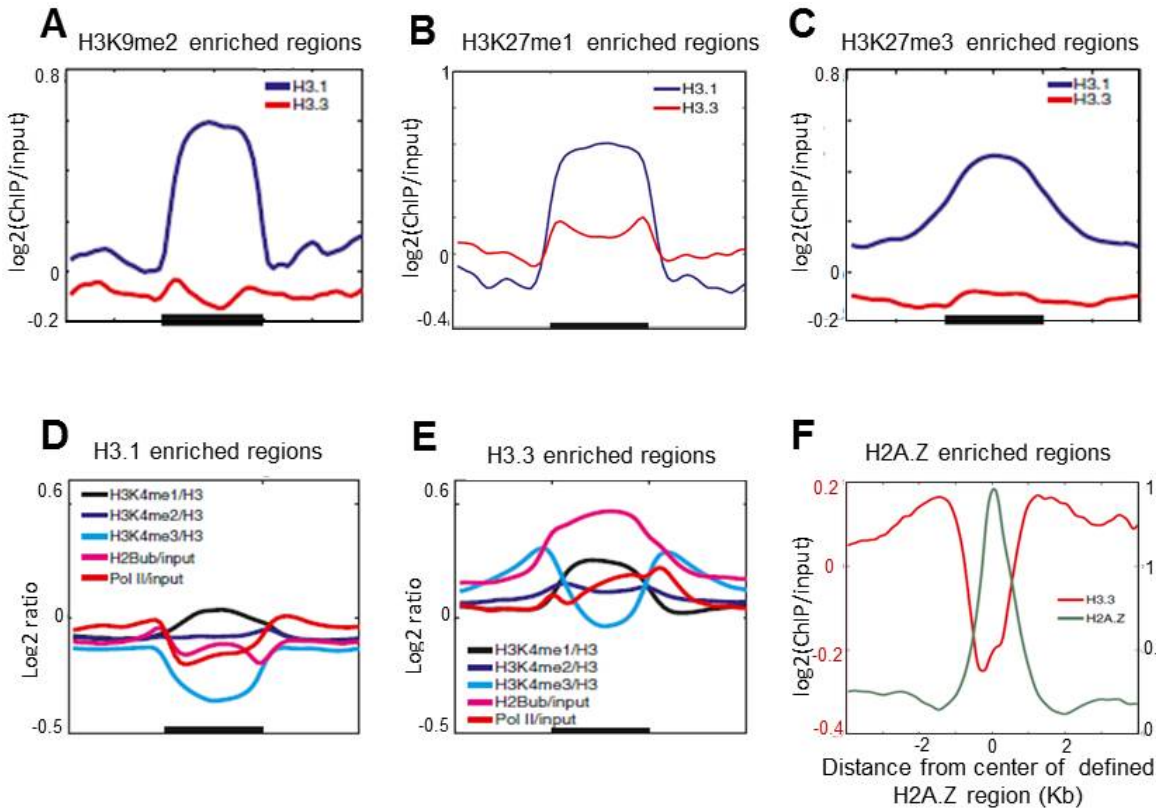

Fig 4.5. Histone H3.1 is enriched in silencing marks and H3.3 is enriched in active marks (A) H3.1 is enriched over H3K9me2 regions located in the arms of chromosomes (B) Positive correlation of H3.1 and H3K27me1 regions in the chromosome arms. Black bar represents H3K27me1 enriched regions (C) H3.1 is associated with H3K27me3. Black bar represents H3K27me3 enriched regions (D) Active chromatin marks distributed over H3.1 enriched regions. (E) H3.3 is enriched in active chromatin marks. Black bar represents H3.3 enriched regions (F) Distribution of H2A.Z and H3.3 over defined H2A.Z regions (black bar) shows anticorrelation between both histones. In all cases flanking regions are the same length as the middle region, that represents in each case an enriched region.

As pericentromeric regions are known to be nucleosome dense (Chodavarapu et al., 2010), we next wondered if regions outside pericentromeric heterochromatin, enriched in H3.1 and repressive marks, would also be tightly packed. To answer this question we plotted the nucleosome content over H3K9me2 and H3K27me3 rich regions. Nucleosome content was evaluated in three different ways: using data from micrococcal nuclease mapping (Nuc-seq), data from ChIP-seq experiments where total H3 was immunoprecipitated (H3 ChIP-seq) (Chodavarapu et al., 2010) and a theoretical nucleosome prediction algorithm (Kaplan et al., 2009). Independently of the method, both sets of regions were nucleosome dense (Fig 4.6B;C), indicating that H3.1 is associated with silent regions that have high nucleosome content. Since H3.1 is associated with densely packed regions, it was not expected to correlate with transcription factor binding sites, which are usually enriched at low nucleosome density regions. The same prediction also applied to H3.3, as transcription factor binding sites are depleted in gene bodies (Zhang et al., 2007), where H3.3 is enriched. Our

data confirmed these two predictions since both H3.1 and H3.3 are depleted at transcription factor binding sites, H3.3 being less depleted than H3.1 (Fig 4.6C) probably because it is sometimes associated with *cis*-regulatory elements (Mito et al., 2007). Nucleosome depletion was validated with all three nucleosome maps (Fig 4.6D).

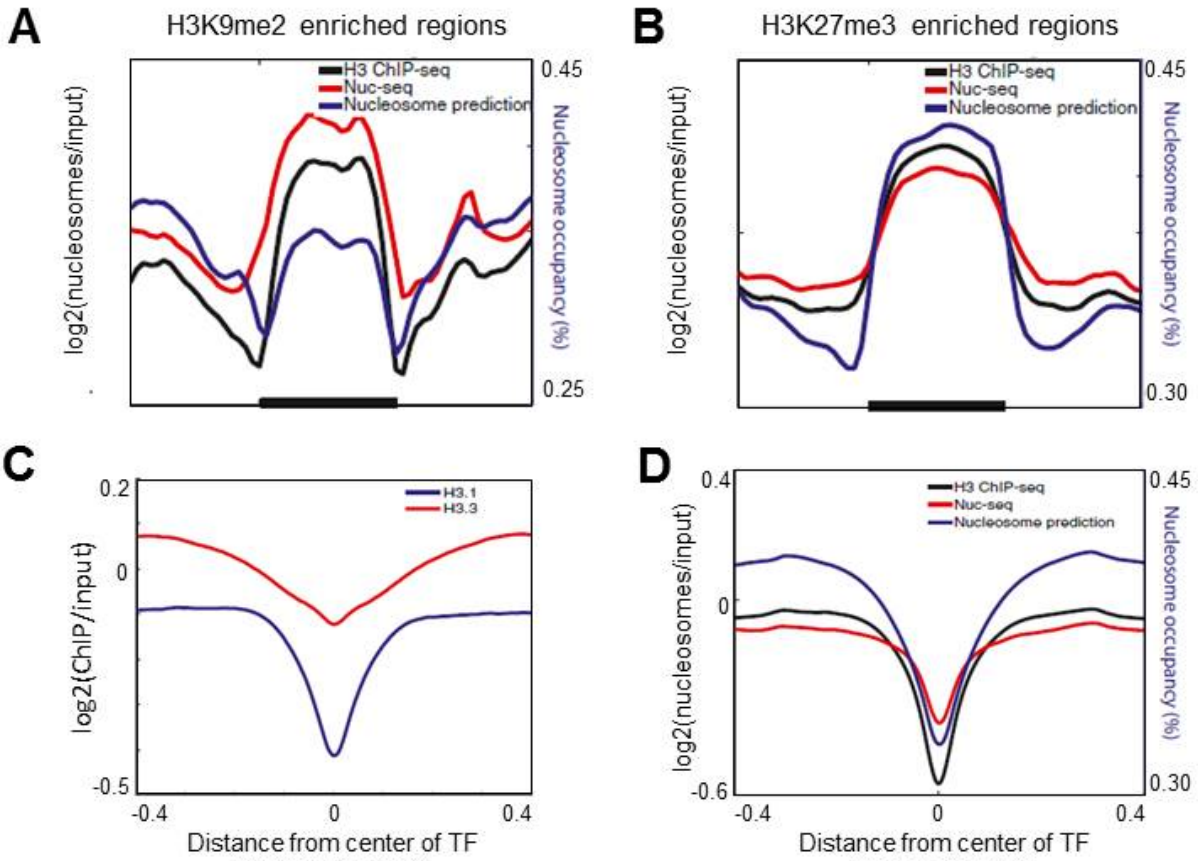

Fig 4.6. H3.1 is enriched over nucleosome dense regions. H3.1 and H3.3 are depleted at transcription factor binding sites H3K9me2 (A) and H3K27me3 (B) enriched regions are nucleosome dense. (C) H3.1 and H3.3 are depleted at transcription factor binding sites. (D) Nucleosome depletion at transcription factor binding sites.

Altogether, these data indicate that H3.1 is clearly associated with silent regions of the genome, areas that tend to be nucleosome dense and enriched in different kinds of silencing chromatin marks. On the contrary, H3.3 is associated with gene expression and active marks, peaking towards the 3' end of the genes.

4.1.4 H3 and replication origins.

We were also interested in knowing if either H3.1 or H3.3 content could be a specific feature of replication origins (Roberts et al., 2002). To answer this question we mapped H3.1 and H3.3 reads over replication origins profiled in cultured cells (Costas et al., 2011). Unexpectedly, we found that both H3.1 and H3.3 were enriched over replication origins (Fig

4.7A), suggesting that Arabidopsis ORIs are preferentially located in nucleosome-dense chromatin regions. Nucleosome content analyzed by the three different methods confirmed nucleosome enrichment in origins of replication (Fig 4.7B).

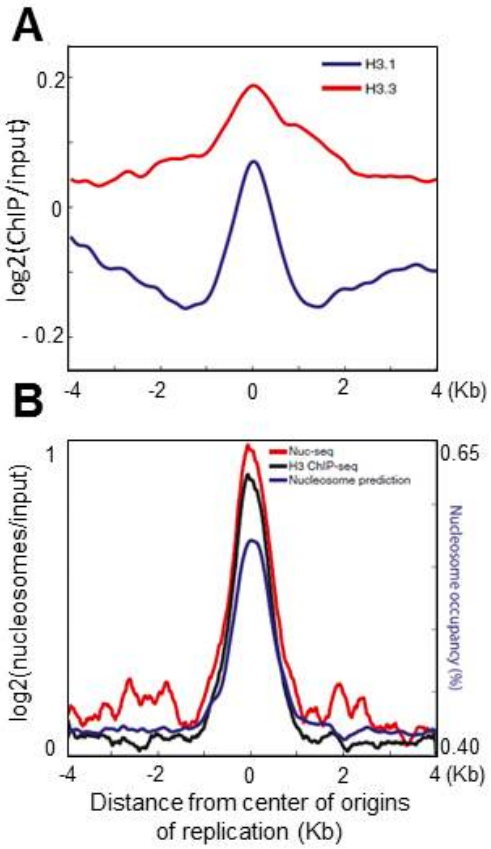

Fig 4.7. H3 reads over replication origins (A) Both H3.1 and H3.3 are enriched over origins of replication mapped in cultured cells. (B) Replication origins are enriched in nucleosome content, independently of the method used to map chromatin density

Taken together, data derived from this analysis show that H3.1 and H3.3 in Arabidopsis follow similar trends as observed in animals, with some plant-specific characteristics, suggesting convergent evolution.

4.2 H3 dynamics in cell cycle uncovers functional domains during Arabidopsis development

4.2.1 The role of the H3.1/H3.3 balance in plant development

The main histone chaperones are essential in vertebrates (Quivy et al., 2001; Roberts et al., 2002; Houlard et al., 2006; Sanematsu et al., 2006). Although these mutants in Arabidopsis are viable, they usually show pleiotropic developmental defects (Exner et al., 2006; Zhu et al., 2011; Nie et al., 2014) (Fig 4.8A), and, consequently, we inferred that a correct balance of H3 histones should be important for development. Therefore, we focused on H3 dynamics during two keystone events in Arabidopsis: embryogenesis (Fig 4.8B) and organogenesis, which in plants is a postembryonic process.

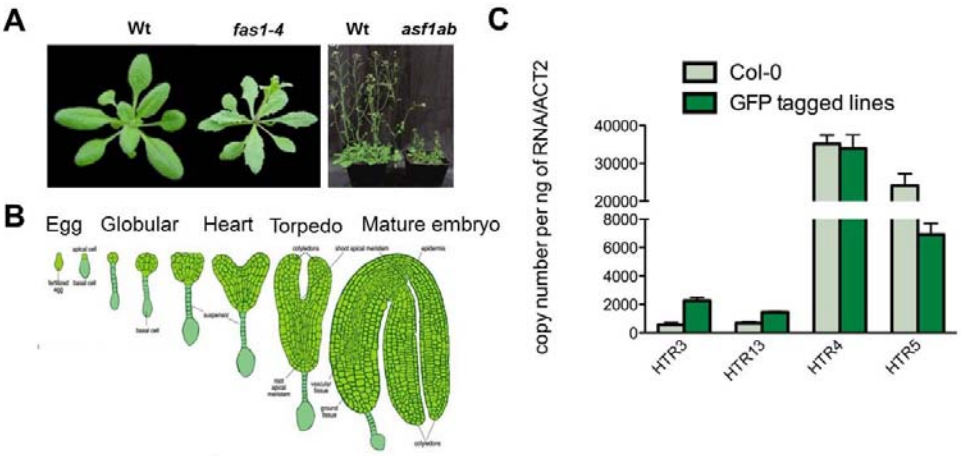

Fig 4.8. Preliminary data that prompted us to initiate these studies (A) Arabidopsis chaperone mutants showing pleiotropic developmental defects: a knockdown of *FAS1* and a double knockout of *ASF1A* and *ASF1B* genes. Adapted from (Exner et al., 2006) and (Zhu et al., 2011) respectively (B) Stages of embryo development in Arabidopsis. Adapted from (Wolpert, 2011) (C) Comparison of the expression of endogenous and GFP-tagged genes in Col-0 and tagged lines.

To monitor H3 proteins, we used the tagging strategy previously described (Fig 4.1A), in this case by fusing the proteins to fluorescent proteins (GFP and mRFP) under the control of their endogenous promoters, the transgene expression paralleling the endogenous one (Fig 4.1C). Even if no difference of expression pattern among histones in the same class had been previously reported (Ingouff et al., 2010), we performed all the studies with two proteins of each class (HTR3 and HTR13 for H3.1; HTR4 and HTR5 for H3.3) to avoid possible gene-specific behaviors. We found that, the two proteins of each category followed the same trends, as expected since proteins within each group are identical.

4.2.2 H3 dynamics during embryo development reveals H3.1 is associated with highly proliferating cells.

We first sought to determine the histone H3.1/H3.3 pattern during embryo development, as it contains a population of highly proliferating cells, where rapid cell cycles and patterning are tightly coordinated (Jenik et al., 2005). Noteworthy, the expected patchy labelling pattern for H3.1, typical of cell-cycle regulated proteins, was vague in the first stages of embryo development for both HTR3 and HTR13 (Fig 4.9A,B,E,F), probably because cell cycle in embryonic cells is much faster than in other organs (around 10 hours in Arabidopsis embryos (Jenik et al., 2005) compared to the average 18.6 hours in cortical cells of the root (Beemster and Baskin, 1998).

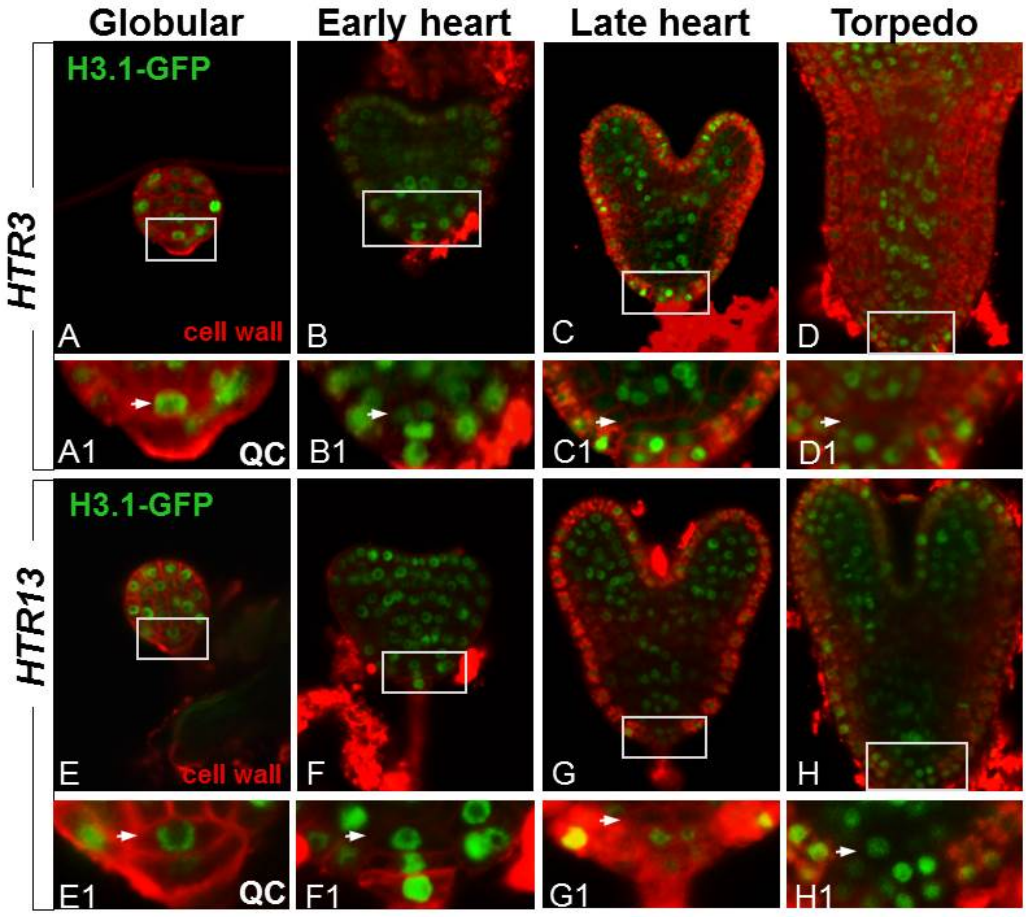

Fig 4.9 H3.1 during embryo development. HTR3-GFP pattern in embryo development. (A-D) Details of the QC region in A1 –D1. Note the reduction in H3.1 content at late heart (C1) and torpedo (D1) stages. HTR13 distribution follows the same trends as HTR3 pattern. Details of the QC region in E1-H1.

However, from heart stage onwards some cells start to acquire fate, repressing cell cycle genes (Spencer et al., 2007), a situation concomitant with the recovery of the typical patchy pattern in H3.1 (Fig 4.9C,D,G,H). In particular, at late heart stage the typical stem

cell niche division pattern of the future root meristem is established (Scheres et al., 2002), including the quiescent center (QC), the organizer of the stem cell niche, with cells that will divide infrequently. Interestingly we observed that during the first stages of embryogenesis, characterized by rapid cell divisions, QC cells are decorated with a high content of H3.1, an amount that decreases from the late heart stage forward, when QC cells become mitotically inactive (Fig 4.9C1;D1). To further corroborate these results we crossed HTR3-GFP (H3.1) with HTR5-mRFP, an H3.3 that is constitutively expressed and that will help us perceive changes in the H3.1/H3.3 balance. Again we observed a reduced amount of H3.1 as embryo development progresses, especially after late heart stage, with QC cells at torpedo preferentially containing H3.3mRFP (Fig 4.10). Overall, these data suggest that H3.1 is enriched in cells with high proliferation capacity.

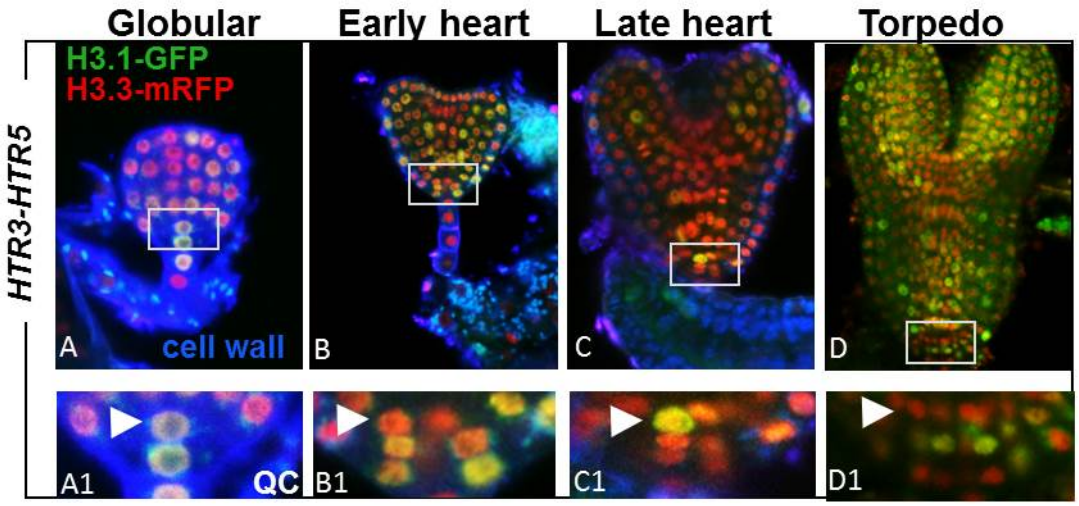

Fig 4.10. H3.1/H3.3 balance in embryo development. HTR3-GFP/HTR5-mRFP from globular to torpedo stage. (A1-D1) Detail of the QC in A –D.

4.2.3 The H3.1/H3.3 balance reveals different cell populations in the developing root.

Based on this result, we wondered if the proliferation/differentiation status of a cell in a developing organ could be assessed by its H3.1/H3.3 balance. We focused on the Arabidopsis root, a cylinder with different concentric cell layers. First, we observed that in the middle plane, the QC of the primary root meristem was enriched in H3.3 (HTR4, HTR5) (Fig 4.11B) and the content of H3.1 (for both HTR3, HTR13) was low or undetectable (Fig 4.11A), as reported in the embryos.

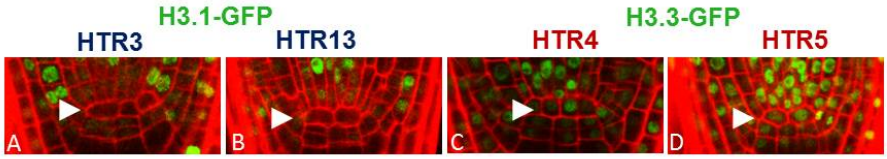

Fig 4.11. Histone H3 in the QC of the primary root. Both H3.1, HTR3 (A) and HTR13 (B) show a reduced content in the QC. HTR4 (C) and HTR5 (D) are enriched in the QC.

In the epidermis, the external cell layer, we confirmed that the two H3.3 are constitutively expressed (Fig 4.12B) while the two H3.1 show the patchy pattern associated with cell-cycle regulated proteins (Fig 4.12A) (Ingouff et al., 2010), with some cells having a very reduced or undetectable amount of H3.1.

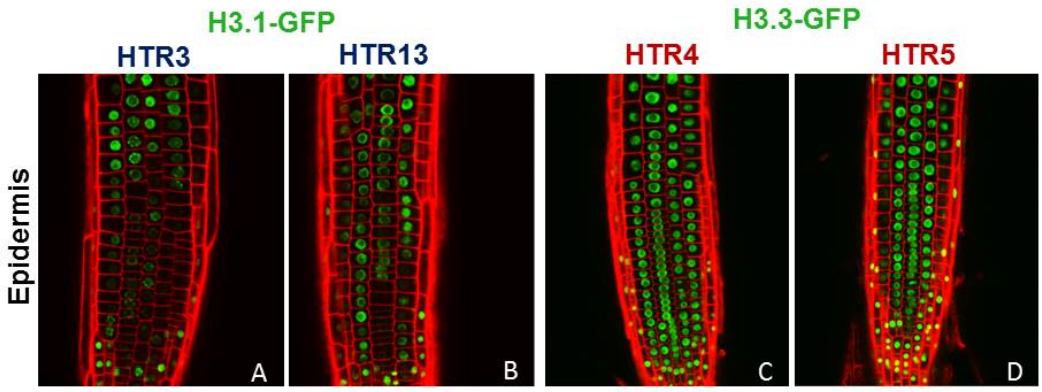

Fig 4.12. H3-GFP pattern in the root epidermis. H3.1 pattern, HTR3 (A) and HTR13 (B). H3.3 pattern, HTR4 (C) and HTR5 (D).

As the content of H3.1 seems to be associated with the proliferation capacity of the cell, we were interested in studying the dynamics of H3.1 during cell cycle. It is known that H3.1 is incorporated during the S phase (Otero et al., 2014) but the phase when it is replaced remains unknown (Fig 4.13A). To address this question we used the cross between H3.1-GFP plants (H3.1) and HTR5-mRFP lines (H3.3). We focused on mitotic figures since the presence of the constitutive histone ensures their visualization, as a clear reference in cell cycle. In the confocal images of the root, two different types of mitosis could be observed: those with a high content of H3.1 and some others with a small amount of this histone (Fig 4.13B), independently of the mitotic phase. These results were confirmed by *in vivo* live imaging (Fig 4.13C), indicating that once H3.1 is incorporated it can be either evicted from chromatin before mitosis, likely in G2, or be kept during the mitosis. Visual inspection of the different roots suggested that the location of mitotic figures along the root was not random, the H3.1-rich mitosis being more abundant near the stem cell niche. This strongly pointed to a possible positional regulation of H3.1 along the root. Indeed, the root tissue is very organized: around the QC, the stem cells provide the different layers with new cells that

rapidly divide (Tsukagoshi et al., 2010). Together, they constitute the root meristem, where two different domains can be distinguished: the proliferation domain, where cells rapidly divide, and the transition domain, where mitosis are rare (Ivanov and Dubrovsky, 2013) as the cell proliferation capacity of the cells decreases at the end of the root meristem.

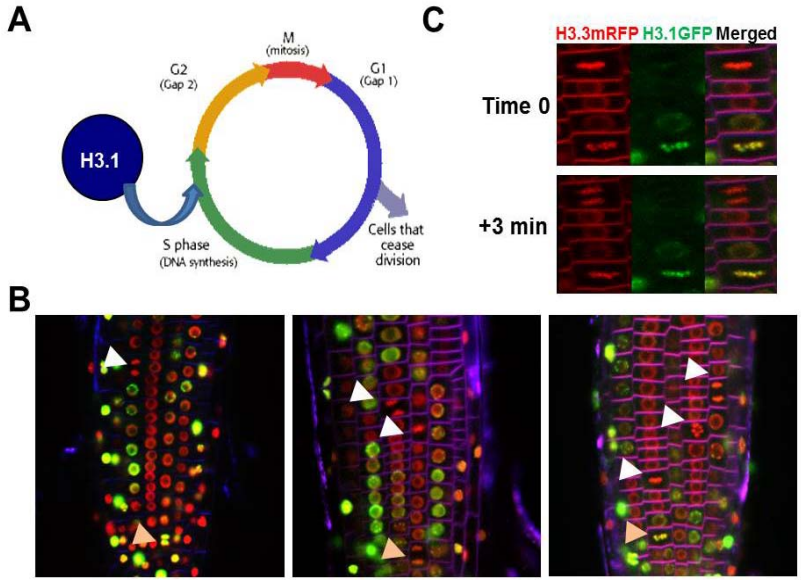

Fig 4.13. H3 dynamics during cell cycle. (A) H3.1 is incorporated during S phase (B) Views of different roots showing mitosis with a high (orange arrow) or low (white arrow) content of H3.1 (C) Live imaging showing two different mitosis.

To confirm our observation of the H3.1 labeled mitosis and fit it in a physiological context, we scored the mitotic figures in relation to their H3.1 content and their position in the root meristem, quantifying the data as indicated in Materials and Methods. With this analysis we verified that most of the mitotic figures are found in the first half of the root and also discovered two different populations within the proliferation domain, solely based on the H3.1 content (Fig 4.14). Importantly, cells that have a lower amount of H3.1 are those in their last cell cycle, as they will not likely divide again. On the contrary H3.1-rich mitoses occur in cells that are proliferating more actively. Together these data define the H3.1/H3.3 balance as a molecular marker suitable to distinguish two populations with different functional characteristics.

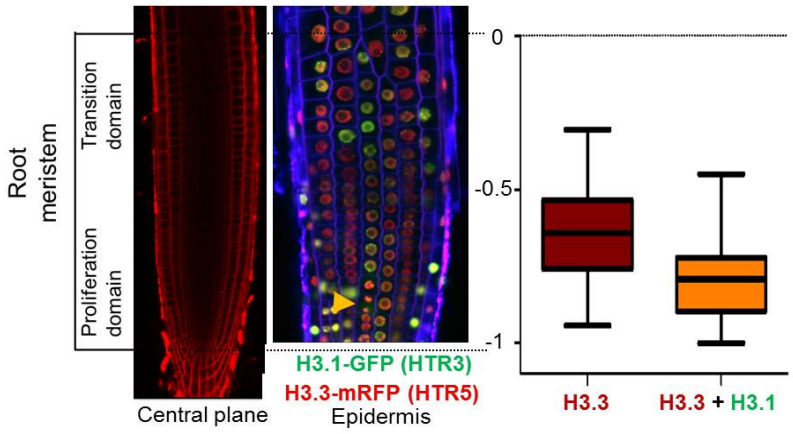

Fig 4.14. Two different populations in the root meristem are identified based on H3.1 content. An example of a root meristem in the middle plane is shown accompanied by a picture of the epidermis of the H3.1-GFP/H3.3-mRFP (HTR3/HTR5) plants used for this study. The graph represents quantification of the different mitoses in relation to their H3.1 content and their position in the meristem. The two populations are statistically different (n=53; α=0.05; t-test).

To validate the results obtained, we crossed H3.1-mRFP (HTR13) with CYCB1;1-GFP (Colon-Carmona et al., 1999), a cell cycle marker present from G2 to anaphase that spots the high-division-rate domain. The population of H3.1-rich mitoses coincides in the root meristem with the CYCB1;1:GFP expression domain, which occupies the more rootward half of the meristem (Fig 4.15). This confirms that the population of H3.1-rich mitoses marks the cells with the highest proliferation capacity, that is, the dividing stem cell derivatives before they enter their last cell cycle.

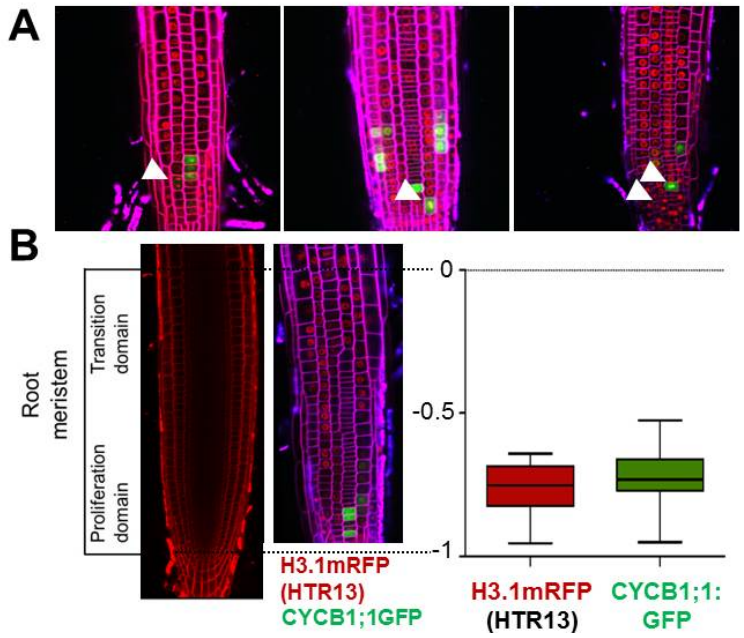

Fig 4.15. The population of H3.1 mitoses matches CYCB1;1 expression domain.
(A) Different examples of HTR13mRFPxCYCB1;1:GFP plants. White arrows point at H3.1 rich mitoses. (B) Quantification of H3.1-rich mitoses and cells expressing CYCB1;1-GFP. The two populations are statistically similar (n=77; α=0.05; t-test).

Overall, our data indicate that the cells undergoing their last cell cycle in the root meristem remodel their chromatin by massively replacing H3.1.

Concomitant with the decrease of H3.1 content, an analysis of the transcriptomic data in the root longitudinal slices of the meristem (1, 2 and 3 compared to slice 4, (Brady et al., 2007), as explained in Materials and Methods) showed a decrease in cell cycle and chromatin genes (Supplementary Tables 9.1.1 and 9.1.2) in this area of the meristem, supporting chromatin changes and a decrease of proliferation activity.

4.2.4 Upstream regulators of the H3 reprogramming.

To identify upstream regulators of the H3 reprogramming, we searched TFBS in the promoters of H3.1, H3.3 and main histone chaperones genes (CAF-1, HIRA, ASF1A, ASF1B) (Fig 4.16A) and to refine our analysis we clustered the genes having these TFBS according to their expression patterns along the root (Brady et al., 2007). Among the five classes found (Fig 4.16B), we focused on the pattern of genes highly expressed in slices 1-2 that then decreased from slice 3 onwards (class A): E2F, YABBY (YAB), LEAFY (LFY),

DNA BINDING WITH ONE FINGER DOMAIN (DOF) and AINTEGUMENTA (ANT) sites. Putative E2F target genes, involved in the G1/S transition are expected in this cluster, reinforcing our analysis. The other four groups are all implicated in developmental transitions. The role of YAB and LFY has not been described in roots and one of the DOF TF has been reported to regulate cell cycle in certain organs but not in the primary root. However, ANT TFs belong to the APETALA2 (AP2) branch of the AP 2/ ethylene-response element binding protein (AP2/EREBP) family (Riechmann and Meyerowitz, 1998; Dietz et al., 2010), a classification also shared by PLETHORA (PLT) transcription factors, members of the AINTEGUMENTA- LIKE subclass of the same AP2 subfamily (Horstman et al., 2014), which possibly share the same binding site as ANT. Recently PLT proteins have been described as master regulators of the longitudinal developmental zones in the root (Mahonen et al., 2014). Noticeably PLT1, PLT2, PLT3 and BABYBOOM are expressed in the root meristem, and the PLT1 domain coincides with the proliferation domain marked by mitosis with a high content in H3.1.

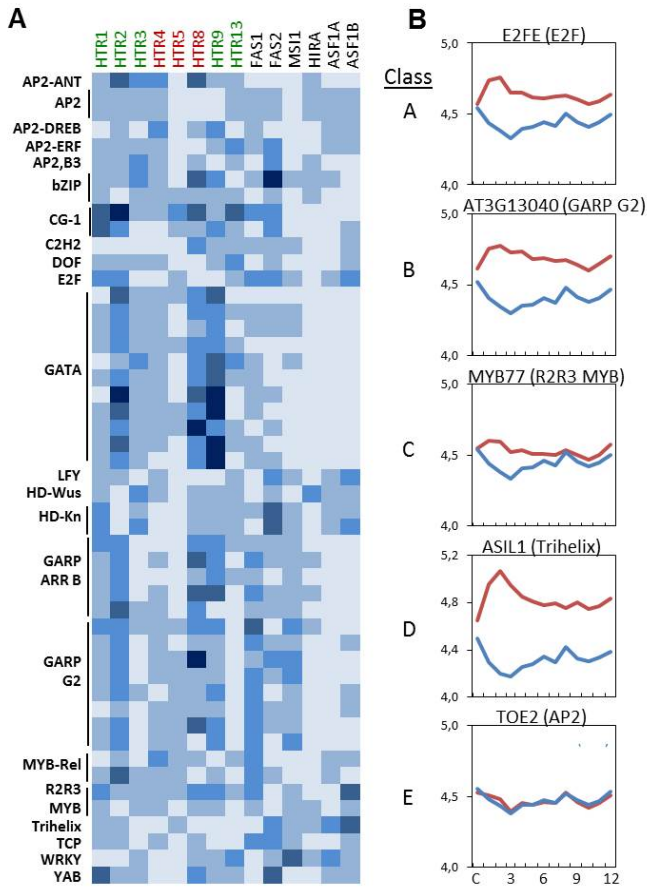

Fig 4.16. Transcription binding sites in the promoters of our target genes (A) A heat map representation of the number of TF-binding sequences in the promoter regions (0.5 kb upstream the TSS) of genes for H3.1, H3.3 and related chaperones is shown. The color code represents the number of sites, ranging from 0 (light blue) to 4 (dark blue). Binding sequences selected were enriched at least 1.70-fold ($p<0.05$, hypergeometric distribution) relative to the representation of these motifs in the complete TAIR10 promoter set. Binding sequences were grouped relative to their TF family or subfamily. (B) Median expression values (Log2 intensity) along root slices of the genes containing (red line) and not containing (blue line) the TF-binding sequences indicated within 0.5 kb upstream regions. Representative examples of the 5 different classes of expression patterns along the root of genes with binding sites for the different TF (A-E) are shown. Columella (C) and slices 1-12 are shown in the x-axis. (Brady et al., 2007)

Together, these data point to a potential regulation of the H3 reprogramming by different transcription factors, among which PLT proteins are interesting candidates.

4.3 The H3.1/H3.3 balance is a marker of cell differentiation

4.3.1 H3 dynamics during endocycle

After cycling in the root meristem, cells enter the endocycle program that precedes rapid cell elongation (Hayashi et al., 2013). As mentioned before, the endocycle is a cell cycle variant that consists of bypassing mitosis after DNA replication, resulting in an increase of DNA content that generates *polyploid* cells (De Veylder et al., 2011; Edgar et al., 2014). Remarkably, it either occurs in cells with high metabolic activity or in cell types that require specialized differentiation (Sugimoto-Shirasu and Roberts, 2003), the latter option being the case for root cells lineages. Since we had been able to detect different functional domains in the cycling population of the root meristem based on the H3 dynamics, we wondered if a similar situation could take place in the elongation zone during the endoreplication process. In addition, since H3.3 content has been observed to vary during cell differentiation in mammalian cells (Goldberg et al., 2010), we thought it would be interesting to monitor the histone balance during endoreplication, a fundamental event in the developmental process of differentiation.

Examining the boundary of the meristematic and the elongation zones *in vivo*, we observed the incorporation of H3.1-GFP into pairs of mostly red (H3.3-mRFP) nuclei, that is, cells that have resulted from mitosis with a low content of H3.1 (Fig 4.17).

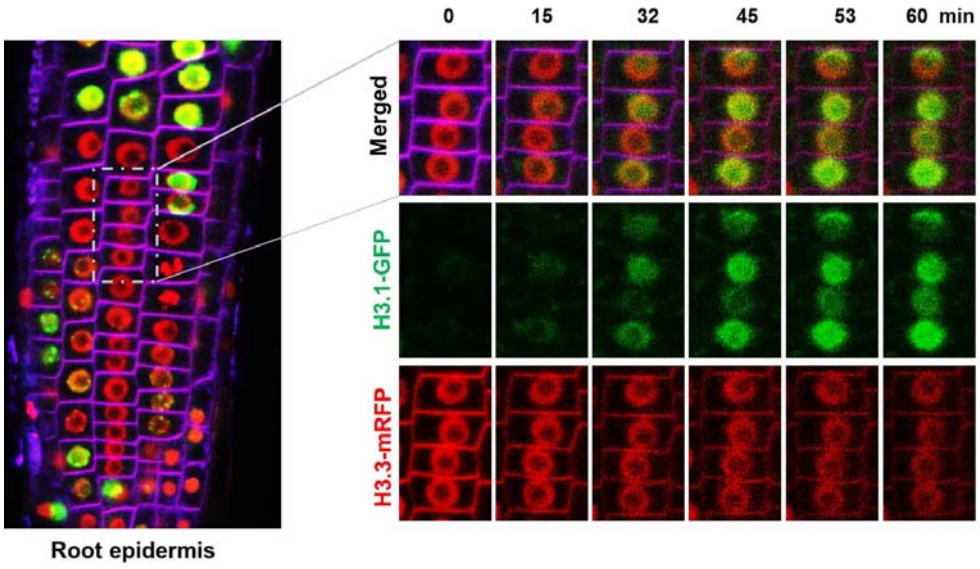

Fig 4.17. H3.1 is incorporated in the S phase of the endocycle. A root was followed for an hour using *in vivo* live imaging, taking pictures every few minutes. Representative shots are shown, bleach was compensated using Fiji. FM4-64 was used to stain the plasma membranes. H3.1=HTR3; H3.3=HTR5.

Adjacent cells are usually coordinated to start the S-phase (Hayashi et al., 2013), and as these cells have already stopped cycling, they must be starting the S-phase of an endocycle program.

However, in the differentiated part of the root, the content of H3.1 is again low (Fig 4.19A). To analyze H3 content during endoreplication in all ploidy levels, we did flow cytometry with the GFP-tagged lines, isolating nuclei and staining them with DAPI as detailed in Materials and Methods. We defined the GFP negative gate with wild type Col-0 roots, whereas H3.3 was used to select the GFP positive nuclei, as it is the constitutive histone present in all cells. Analyzing H3.1-GFP nuclei, we observed that there is a gradient of H3.1 in all ploidy levels (Fig 4.18).

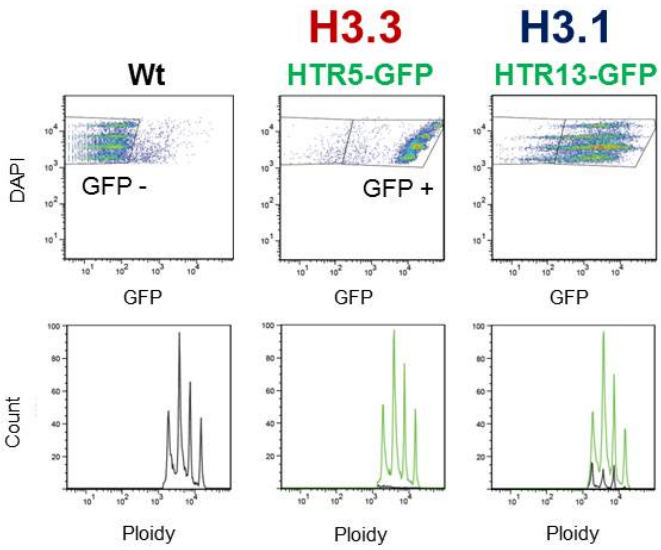

Fig 4.18. Ploidy profiles of root nuclei by flow cytometry. Representative graphs of flow cytometry using nuclei from roots of GFP-tagged histone lines. DAPI is used to stain the nuclei and show the 4 different ploidy populations, ranging from 2C to 16C. Wild type Col-0 nuclei are used to select the GFP negative (GFP-) population. The GFP positive population (GFP+) is selected with the H3.3-GFP nuclei.

As the differentiated part of the root is longer than the apical one, we cut the root tip to enrich in apical tissue and analyzed both materials separately. We observed that the number of GFP positive cells for H3.1, HTR3 (Fig 4.19B) as well as HTR13 (Fig 4.19C), was always higher in the apical part of the root. The percentage of positive cells in the differentiated tissue clearly revealed that the decrease in H3.1-GFP positive cells is larger in the highest ploidy levels. The trend is similar for both H3.1 proteins, suggesting that H3.1 eviction in nuclei of high ploidy may be a general feature of the differentiation process in the root (Fig 4.19D,E).

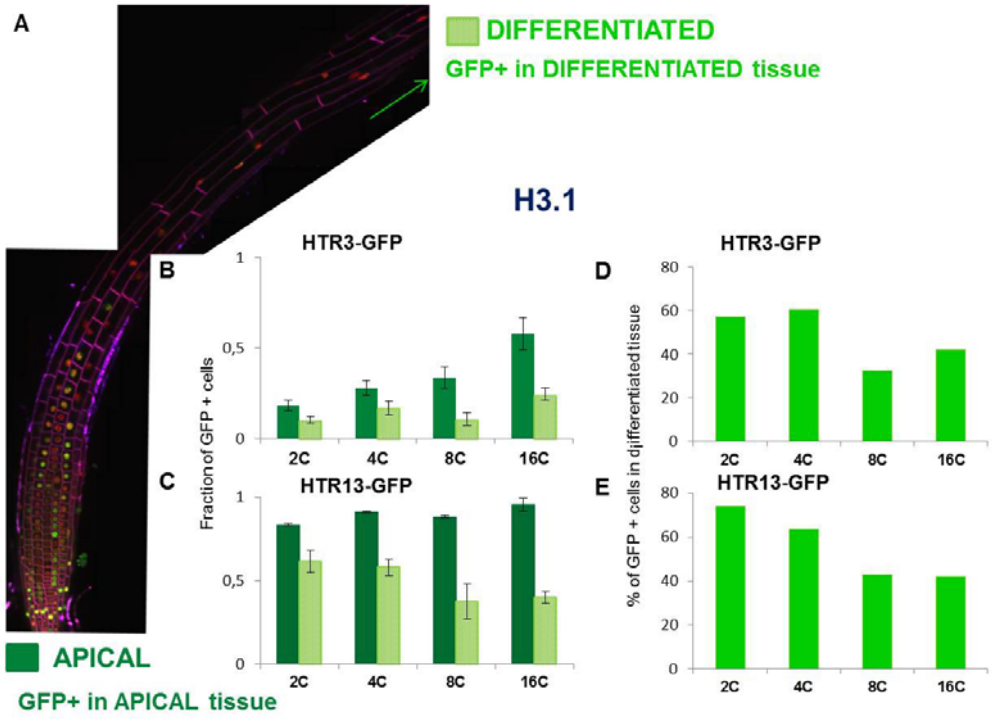

Fig 4.19. H3.1 in the root endocycle. (A) H3.1 content is high in the boundary between meristem and elongation zones but then decays in the differentiated part of the root. (B) Fraction of H3.1 (HTR3) positive nuclei in the apical and differentiated part of the root. (C) Fraction of H3.1 (HTR13) positive nuclei in the apical and differentiated part of the root.(D) Percentage of HTR3-GFP positive cells in the differentiated part of the root. (E) Percentage of HTR13-GFP positive cells in the differentiated part of the root. The decrease in GFP positive cells is always higher in the highest ploidy levels. These percentages were calculated using average values shown in B and C. Each experiment was repeated 3 times.

Root development involves coordination between cell proliferation and endocycle. To observe histone dynamics only in cells undergoing endoreplication, we chose the hypocotyl, an organ built exclusively by cell expansion (no cell division). During skotomorphogenesis or etiolation (seeds germinated in the dark), the length of the hypocotyl epidermal cells can expand 100 times the length of embryonic cells (Gendreau et al., 1997), performing only one extra endocycle (Edgar et al., 2014).

We analyzed the H3.1 distribution in the different ploidy levels by flow cytometry, in this case, isolating nuclei from the aerial part of etiolated seedlings grown in the dark for different periods of time. We observed that the number of positive cells for both H3.1 proteins was higher at the beginning of hypocotyl development (3/4 dps) and, as time goes by and differentiation progresses (7 dps), the number of H3.1-GFP positive cells decreases (Fig 4.20A,B). Differences in the number of positive cells for HTR13 and HTR3 could be due to different expression levels of each histone in the hypocotyl.

As it can be observed, the first 32C cells appear 5 days after sowing (Fig 4.20C). At this time, when H3.1 content (HTR3) is already low or undetectable in all other ploidy levels, most 32C cells are positive for H3.1. As differentiation progresses, the number of H3.1-GFP positive cells also decreases in 32C (Fig 4.20C).

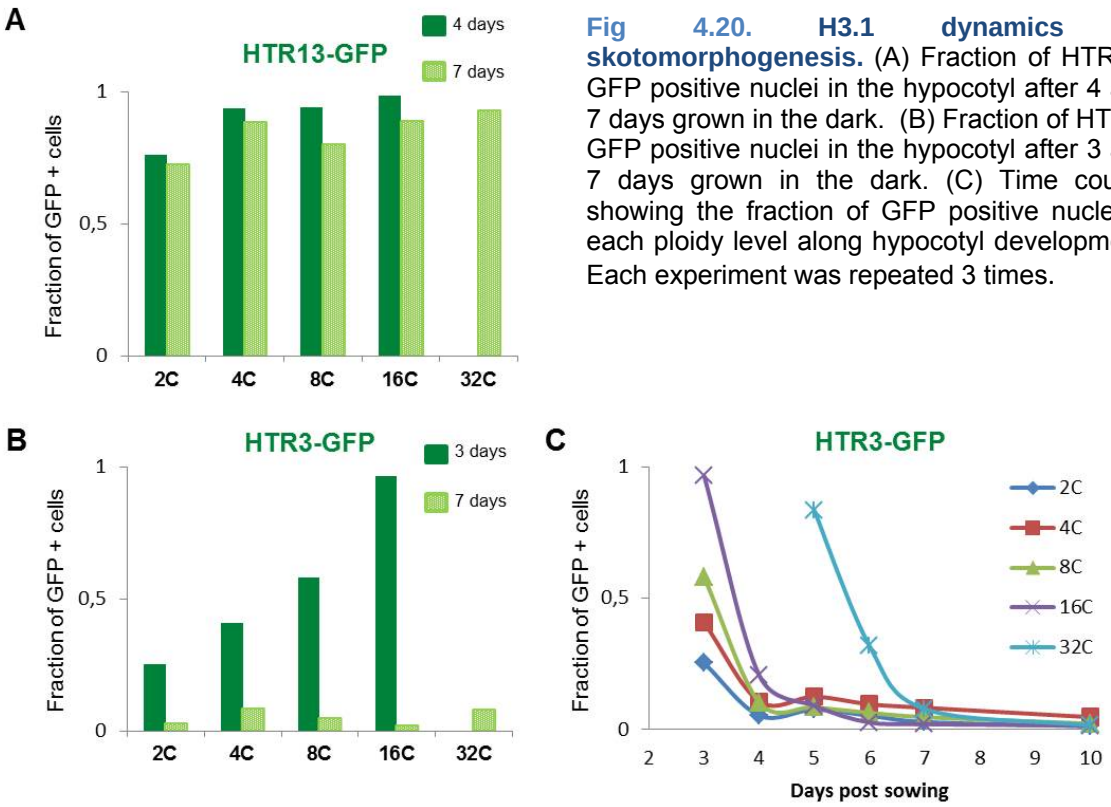

Fig 4.20. H3.1 dynamics in skotomorphogenesis. (A) Fraction of HTR13-GFP positive nuclei in the hypocotyl after 4 and 7 days grown in the dark. (B) Fraction of HTR3-GFP positive nuclei in the hypocotyl after 3 and 7 days grown in the dark. (C) Time course showing the fraction of GFP positive nuclei in each ploidy level along hypocotyl development. Each experiment was repeated 3 times.

Taken together, the data collected in hypocotyl generalize the processes observed in the root.

Interestingly, these results could be explained either because H3.1 is replaced once the cell has reached the final ploidy level or because in each S-phase of the endocycle less and less H3.1 is incorporated. To test these hypotheses we measured the fluorescence intensity of all nuclei in each of the epidermis root cell files, atrichoblasts (Fig 4.21A) and a trichoblasts (Fig 4.21B).

The H3.3-mRFP content was used as a measure for ploidy level. As ploidy rose, H3.1 content increased in a proportional way in each endocycle, H3.1 amount decreasing sometime after every S-phase. Accordingly, we inferred that H3.1 incorporation was related to the genome size and that H3.1 was being replaced at some point in the G phase of the endocycle.

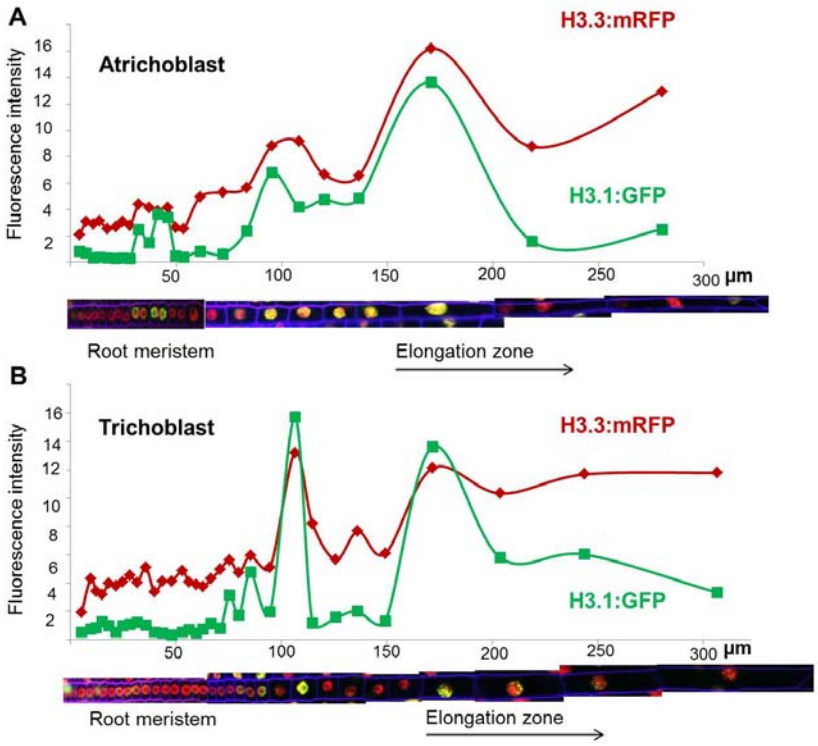

Fig 4.21. H3.1/H3.3 content in the nuclei of a root cell file. The fluorescence intensity of H3.1-GFP (HTR3) and H3.3-mRFP (HTR5) in each nucleus of an epidermis root cell file was plotted against the position of each cell in the root meristem (µm). A reconstruction of each cell file is shown in the bottom, indicating the root meristem and the beginning of the elongation zone. A representative example of an atrichoblast is shown in (A) and a trichoblast is shown in (B).

To identify more precisely the time when H3.1 is replaced, we incubated roots with 5-ethynyl-29-deoxy-uridine (EdU) for 30 or 60 minutes, to label cells in S-phase. We fixed the roots, immunodetected H3.1-GFP and stained with DAPI to highlight all nuclei, as detailed in Materials and Methods. We observed a progressive decrease in H3.1 content in the outer layers of the root, still keeping some H3.1-GFP a long distance away from the last EdU stained cell (Fig 4.22A,B). We deduced that H3.1 is progressively replaced in the G phase of the endocycle.

In the root central cylinder, the presence of the canonical histone is high, probably because some cells in the vascular tissue are still proliferating, as indicated by EdU staining (Fig 4.22B). Indeed, procambium cells remain undifferentiated (Furuta et al., 2014a). Altogether, these data indicate that H3.1 content decreases upon differentiation in endoreplicated tissues.

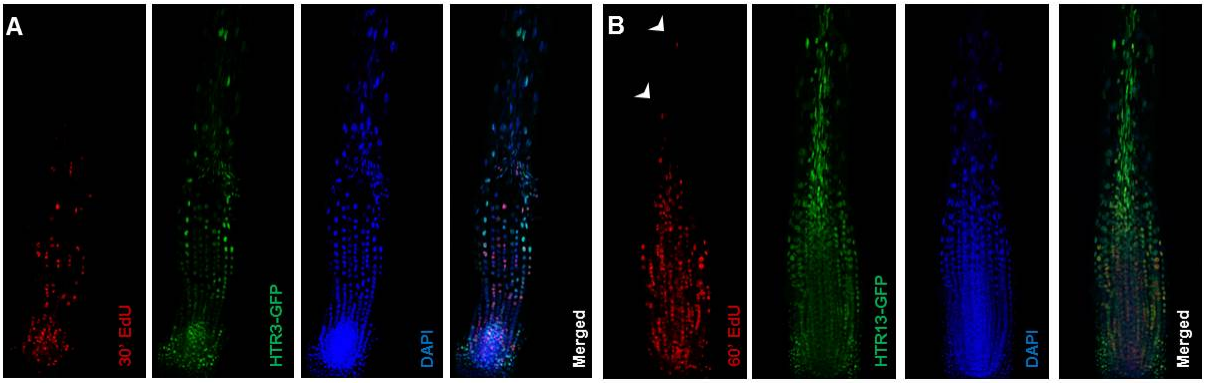

Fig 4.22. H3.1 progressively decreases after each S-phase of the endocycle. (A) HTR3-GFP root incubated for 30 minutes with EdU. (B) HTR13-GFP root incubated for 60 minutes with EdU. Arrowhead indicates nuclei of the stele marked with EdU.

4.3.2 H3.1 decreases upon differentiation in a mitotic cell lineage.

To test if the decrease (eviction) of H3.1 is a characteristic associated with differentiation in cell lineages that do not endoreplicate, we studied H3 dynamics during stomatal development, a well-known process of differentiation (Dow and Bergmann, 2014). We observed that the precursor cells (meristemoids) have a high content of H3.1 while the differentiated cells have a smaller amount of the canonical histone (Fig 4.23).

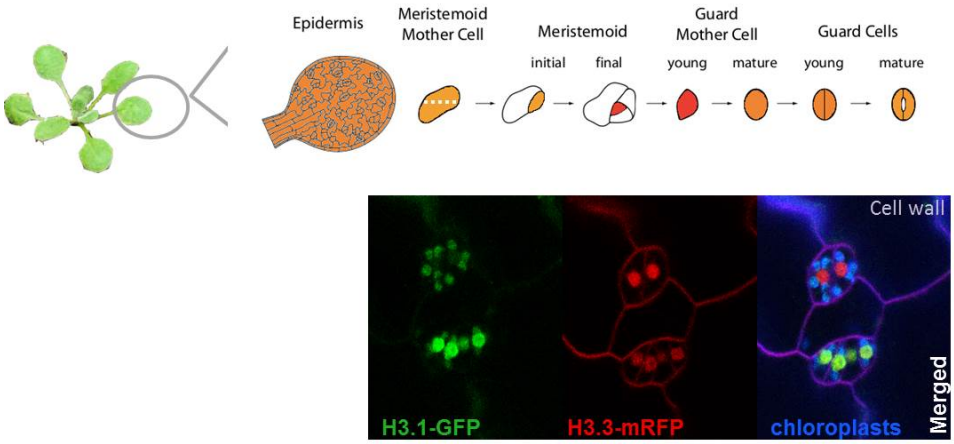

Fig 4.23. H3 dynamics during stomatal differentiation. H3.1 content is high in the meristemoids while it is lower in the differentiated guard cells. Scheme adapted from D. Bergmann. H3.1-GFP=HTR3; H3.3-mRFP=HTR5. Dots around nuclei correspond to the chloroplasts autofluorescence.

Overall, these data suggest that the H3.1/H3.3 balance is a marker of cell differentiation in Arabidopsis.

4.4 Influence of H3.1/H3.3 unbalance in *fas* phenotype.

4.4.1 FAS1, a subunit of CAF-1 causing pleiotropic defects.

Arabidopsis is the only known multicellular organism with viable mutants for all 3 subunits of the CAF-1 chaperone (FASCIATA1, FAS1 a homolog of p150, FASCIATA2, FAS2, a homolog of p60 and MULTICOPY SUPRESSOR OF IRA 1, MSI1, the homolog of p48). MSI1 is part of other protein complexes, like some of the Polycomb group, and as a consequence *msi1* plants exhibit some unique characteristics. However, *fas1* and *fas2* mutants show very similar pleiotropic developmental defects. Macroscopic observation shows that *fas* plants are smaller and display fasciated dark-green leaves (Fig 4.24A,B). Studies with these mutants have highlighted the importance of CAF-1 for multiple developmental processes, such as trichome differentiation and a correct coordination between cell proliferation and endoreplication, the mutants showing fewer cells and usually increased ploidy (Exner et al., 2006). Interestingly, *fas* plants have shorter roots (Fig 4.24C) (Leyser, 1992; Kaya et al., 2001; Ramirez-Parra and Gutierrez, 2007) due to a reduction in the elongation zone, that is positioned in a more rootward location in the mutants (Fig 4.24F,G) (Kaya et al., 2001). Another remarkable fact in the meristem of *fas* mutants is that the organization of QC and stem cell initials is disturbed (Fig 4.24D,E). In addition, the expression of SCARECROW (SCR), a transcription factor that maintains QC identity and is a master regulator of several key pathways in the root meristem (Petricka et al., 2012), is altered in a stochastic way (Fig 4.24H-K).

At the molecular level, *fas* mutants have reduced heterochromatin and show upregulation of some H3 and DNA repair genes (Schonrock et al., 2006; Ramirez-Parra and Gutierrez, 2007). The disruption of the transcriptional gene silencing of some genes and transposable elements in a random way has also been reported, pointing to a role for CAF-1 in the maintenance of silent chromatin states (Ono et al., 2006).

Since we have observed an important decrease in H3.1 every time the cell is approaching a transition, e.g. the last cycle in the meristem or the last endocycle in the elongation zone, we wondered if the defects described for *fas* mutants could be derived from a misbalance of the H3.1/H3.3 content.

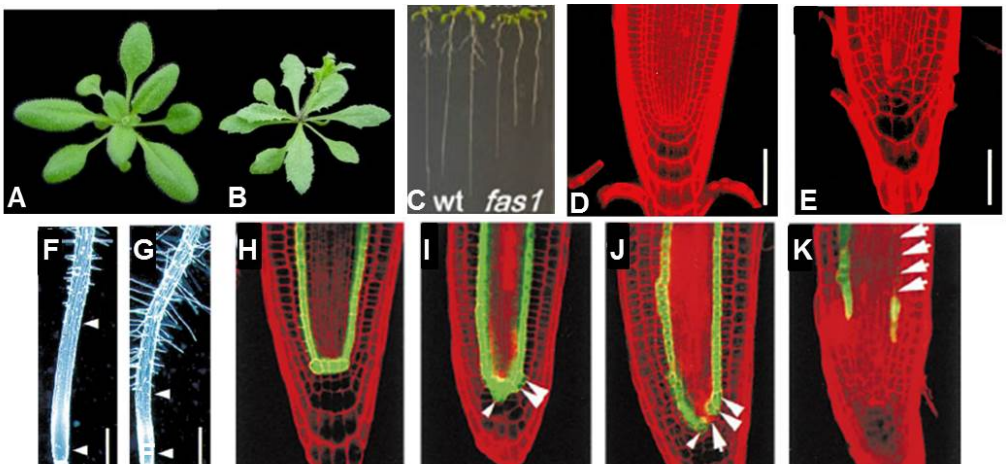

Fig 4.24. *fas* mutants' phenotypes. 3-week-old Wt Col-0 (A) and *fas1-4* mutant plants (B), adapted from (Exner et al., 2006). (C) *fas1* mutants have shorter roots, adapted from Ramírez-Parra and Gutierrez (2007). RAM of 6-day-old seedlings in Wt Enkheim (En) (D) and *fas1-1* (E). Root of 10-day-old seedlings, Wt (En) (F) and *fas1-1* (G) Arrowheads delimit the differentiation zone. SCR::GFP expression in Wt (En) (H) and *fas1-1* mutants (I-K). Arrowheads indicate ectopic expression of SCR (I,J) or lack of expression in the endodermis (K). D-K adapted from (Kaya et al., 2001)

4.4.2 H3.3 replaces H3.1 in *fas* chromocenters.

To gain insight into the dynamics of H3 proteins in *fas* mutants, we crossed the GFP-tagged lines to heterozygous *fas1-4* plants, a knockdown mutant in the Col-0 background (Exner et al., 2006). We crossed heterozygous plants for *fas1-4* to minimize the unfertility problems associated with telomeric and rDNA copy loss (Mozgova et al., 2010). Only some crosses produced viable homozygous plants. Double homozygous lines HTR5-GFP/*fas1-4* displayed seedling lethality and could not be propagated. In some other lines the transgene was silenced. Finally, we obtained HTR3-GFP/*fas1-4* double homozygous lines and HTR4-GFP/*fas1-4* lines, homozygous for *fas1-4* and heterozygous for HTR4-GFP (HTR4-GFP$^{+/-}$/fas1-4$^{-/-}$). As expected, we observed a general decrease of H3.1 in the mutant background and a loss of the nuclear dots observed in the wild type plants corresponding to the chromocenters (Shi et al. 2011) (Fig 4.25A,B). On the contrary, in addition to the uniform nuclear distribution of HTR4-GFP in the *fas1-4* background, H3.3 substituted H3.1 in the chromocenters (Fig 4.25C,D), consistent with the reported decrease in heterochromatin (Schonrock et al., 2006), their more decondensed nature, and the transcriptional activation of TE (Ono et al. 2006). The swap between H3.1 and H3.3 would generate a more open chromatin with increased activation marks (Stroud et al., 2012) and altered chromocenters.

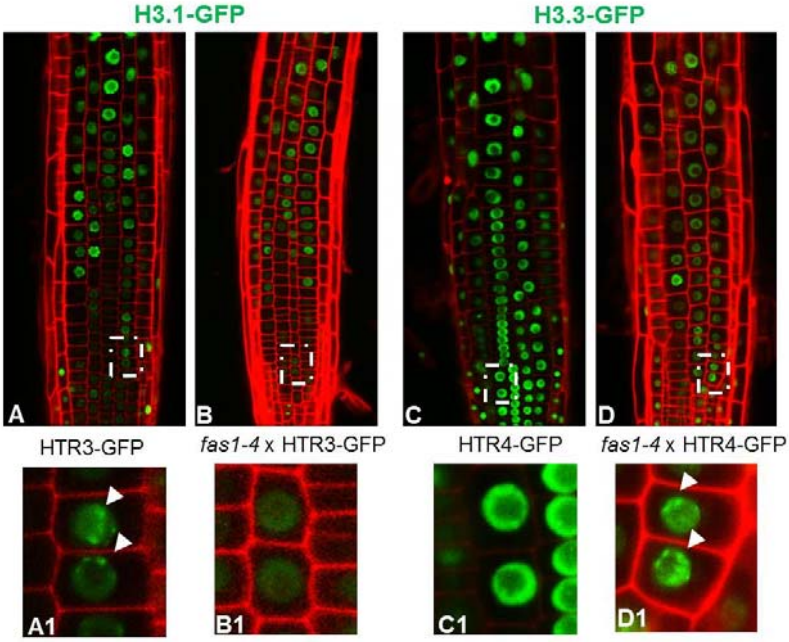

Fig 4.25. GFP-tagged histone lines in *fas1-4* background. Primary root of 9dps (A) HTR3-GFP seedlings (B) HTR3x*fas1-4* (C) HTR4-GFP (D) *fas1-4*x HTR4-GFP. Note this last line is heterozygous for HTR4-GFP. Each Wt line and its mutant were photographed with the same GFP conditions. Squares gate the magnified zones in each picture. Arrowheads point to chromocenters.

4.4.3 H3.1/H3.3 dynamics in *fas* background

To test if the developmental defects in *fas* mutant roots could be attributed to a more opened chromatin, we decided to cross the doubly-labeled HTR3-GFP/HTR5-mRFP plants to *fas1-4* mutants. Plants homozygous for *fas1-4* in combination with both tagged histones displayed seedling lethality, even with tagged histones genes in heterozygosity. To bypass this obstacle, we plated segregating F1 seeds and selected *fas1-4* homozygous seedlings according to root size (Fig 4.26A). The *fas* phenotype observed in these crossed plants was stronger, similar to the one observed in *fas1-4*/H3.3 plants and to the *fas* phenotype in other ecotypes, like Enkheim (Kaya et al., 2001), pointing to a possible higher expression of histone H3.3 genes in other backgrounds. Consistent with the cell cycle arrest and endoreplication phenotype of *fas* (Ramirez-Parra and Gutierrez, 2007), few mitotic figures were observed, many of them showing chromosomal aberrations (Fig 4.26B), a possible cause of the upregulation of the DNA repair machinery.

We then followed the dynamics of H3.1 and H3.3 by monitoring the expression of both histones in all the nuclei of different root epidermal cell files, a representative example shown in Fig 4.26C. We observed that the content of H3.1 was higher in the more rootward cells or in those undergoing endoreplication. Cells in their last cell cycle had a small amount of H3.1, mimicking the wild type situation. However, as previously stated, the root meristem in *fas* mutants is smaller and the elongation zone starts at a more apical position (Kaya et al., 2001). Considering these results we can deduce that early entrance into endoreplication is coincident with an early decrease in H3.1 content.

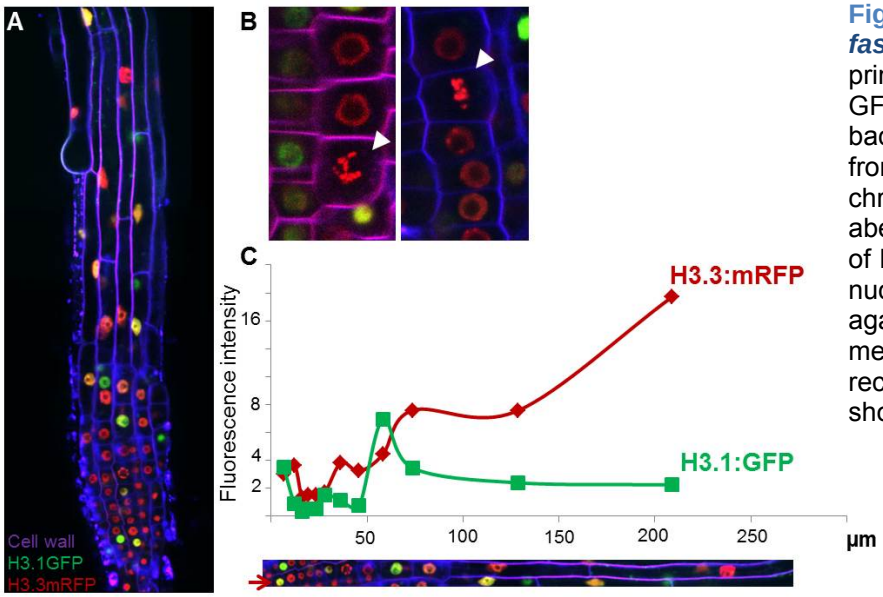

Fig 4.26. H3 dynamics in *fas1-4* background. (A) 7 dps primary root of HTR3-GFP/HTR5-mRFP in *fas1-4* background. (B) Mitotic figures from different roots showing chromosome segregation aberrations. (C) Fluorescence of both histones in the different nuclei of a root cell file plotted against cell position in the root meristem (measured in µm). A reconstruction of the file is shown at the bottom.

Altogether, these data suggest that the atypical balance of H3.1/H3.3 histones could be responsible for some characteristics of the *fas* phenotype, highlighting the importance of histone H3 variants in development.

Moreover, our studies of wild type and *fas* mutants revealed the robustness of the developmentally regulated process of H3.1 eviction associated with cell cycle and endoreplication transition within the root meristem.

4.5. The role of H3.1 and H3.3 in specific cell types.

4.5.1. Mapping H3 proteins in specific cell lineages forming the ground tissue.

H3.3 enrichments have been shown to change at cell type-specific genes and regulatory elements along differentiation in mammalian cells (Goldberg et al., 2010). In Arabidopsis, H3.3 has also been involved in developmental transitions, as H3.3 content changes in genes that are repressed or induced during leaf differentiation (Wollmann et al., 2012). However, H3.1 and H3.3 proteins have never been mapped in plant specific cell types, an important information given that every cell lineage displays specific transcription profiles and unique developmental programs.

The Arabidopsis root is a cylinder formed by concentric cell layers arising from stem cells around the organizing center, the QC cells. The cortex and endodermis layers are derived from the cortex/endodermis initial cell (CEI), through a longitudinal asymmetric cell division (Cui and Benfey, 2009) (Fig 4.27A). This fact presents an ideal scenario to study cell differentiation, as two different cell types come from the same progenitor.

To profile H3 proteins in CEI and ground tissue we crossed our Myc-tagged versions of histone H3.1 (HTR3, HTR13) and H3.3 (HTR4, HTR5) with cell-type specific markers: pCYCD6;1::GFP expressed in cortex/endodermis initial (CEI) cells and CEI daughter cells (Fig 4.27B) (Sozzani et al., 2010), pCo2::YFP_{H2B} expressed in cortex and excluded from the QC, the ground tissue stem cells, and their undivided daughters (Fig 4.27C) (Heidstra et al., 2004) and pEn7::YFP_{H2B}, expressed in the endodermis but excluded from the QC (Fig 4.27D) (Heidstra et al., 2004).

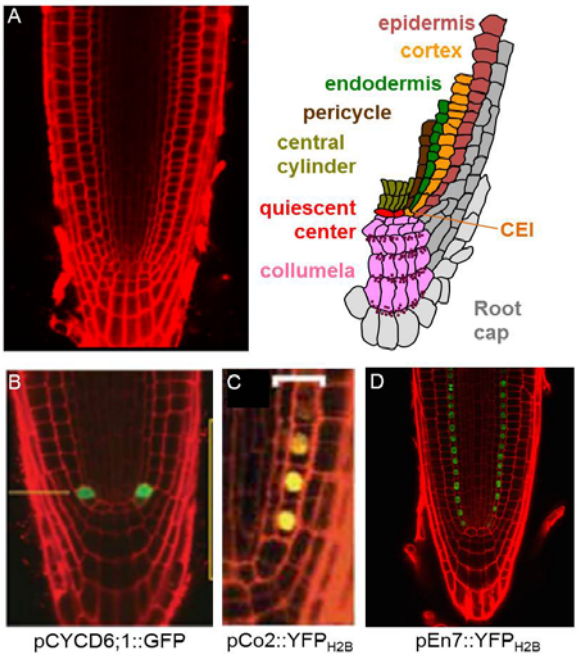

Fig 4.27. Root layers in Arabidopsis. (A) Example of a root meristem with the different cell types indicated in colors (B) pCYCD6;1::GFP expression in CEI cells, source (Sozzani et al., 2010). (C)pCo2::YFP_{H2B} expression in cortex cells, adapted from (Heidstra et al., 2004) (D) pEN7::YFP_{H2B} expression in endodermis, (Heidstra et al., 2004) (kindly provided by María Fernández Marcos).

This project was carried out in collaboration with the Benfey lab (Duke University, USA) to take advantage of their expertise in root protoplasting and cell sorting. After some preliminary tests, endodermal cells were chosen in the first place because they offered the best sorting yields. Cells were sorted based on YFP signal under conditions adapted to the sorter of our institution (Fig 4.28). Cells (protoplasts) scatter light in all directions when they pass through a focused laser beam. Light that scatters in the same direction as the laser beam is called forward scatter and informs about the size of the cells. On the contrary, light that scatters mostly perpendicular to the laser beam is called side scatter and reflects the internal complexity of the particle. Combining both side (SSC-H) and forward scatter (FSC-H) allows discriminating cell populations from background. Cells are excited with blue laser (488 nm) and the emissions in FL1 filter (530/30 nm) and FL2 (585/42 nm) are collected. Cell autofluorescence emits equally at these wavelengths, forming a diagonal while on the contrary the positive cells for YFP signal will emit more intensely in FL1. With Col-0 wild type plants we establish the GFP negative gate (Fig 4.28A) and we select the YFP positive cells (endodermal cells) for sorting (Fig 4.28B,C). An aliquot of sorted cells is passed again through the cytometer to measure the sorting efficiency.

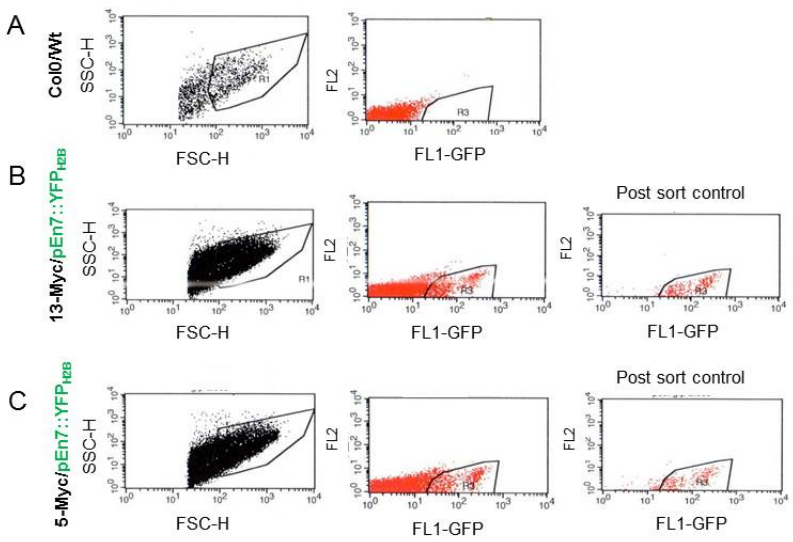

Fig 4.28. Sorting plots using pEN7::YFP$_{H2B.}$ Side scatter and forward scatter are used to discriminate cell populations. Confronting FL2 and FL1, the autofluorescence of the cells forms a diagonal, YFP population detected in FL1. Col-0/Wt protoplasts delimit GFP negative population (A). (B) Example of a sorting experiment with 13Myc (H3.1) x pEN7::YFP$_{H2B.}$ (C) Same sorting experiment with 5Myc (H3.3) x pEN7::YFP$_{H2B.}$ The post sort control checks that the sorted cells appear in the original gate.

Around 200,000 recovered cells of each type were fixed and used for ChIP, immunoprecipitating H3 proteins with anti-Myc as indicated in Materials and Methods. ChIP result was analyzed by qPCR with primer pairs previously tested, selected for their efficiency and differential enrichment between H3.1 and H3.3 in seedlings and roots (Fig 4.29). The amount of immunoprecipitated DNA was estimated using standard curves. We calculated we had immunoprecipitated around 1ng of DNA and planned to accumulate more material before preparing the library for sequencing. Once we will get the sequencing data we will

analyze H3 distribution in this specific cell type and correlate these data with gene expression profiles of endodermal cells (Brady et al., 2007). As previously indicated, cortex cells will be the next to get processed.

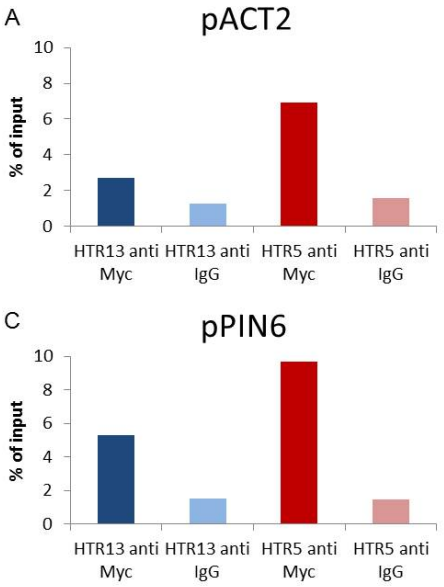

Fig 4.29. ChIP of endodermal cells analyzed through qPCR. (A) Percentage of immunoprecipitated DNA relative to the input in the promoter of ACT2 (At3g18780), IgG representing the negative control. (B) H3 enrichment in the GRP promoter (At4g30450). (C) ChIP result in the PIN6 promoter (At1g77110)

4.5.2 H3.1 and H3.3 dynamics during pollen development.

In somatic tissue, the expression of all usual H3.1 and H3.3 genes is detected. However, in mature pollen and mature egg cells, only a small subset of H3 proteins is present, all H3.1 histones being absent in both cases (Ingouff et al., 2010). Unlike in mammals, in plants germ cells differentiate from haploid spores after meiosis. Interestingly, during male gametogenesis DNA methylation reprogramming takes place. It has been reported that CHH methylation levels decrease in sperm cells compared to microspores, while CG levels remain constant. On the contrary the situation is different in the vegetative cell, where CG methylation decreases with respect to the microspore (Kawashima and Berger, 2014). Intrigued by the chromatin differences between the sperm and vegetative cells during reprogramming and by the absence of H3.1 in mature pollen, we decided to study H3 dynamics along pollen development in collaboration with the group of Pilar Sánchez Testillano (CIB, Madrid).

Using our GFP-tagged H3.1 lines we extracted pollen at different developmental stages and stained it with DAPI. We observed that HTR13-GFP is present in late vacuolated microspores and the generative cell of late bicellular pollen, something expected as it could have been incorporated during the S-phase that precedes first and second mitosis (Fig. 4.30).

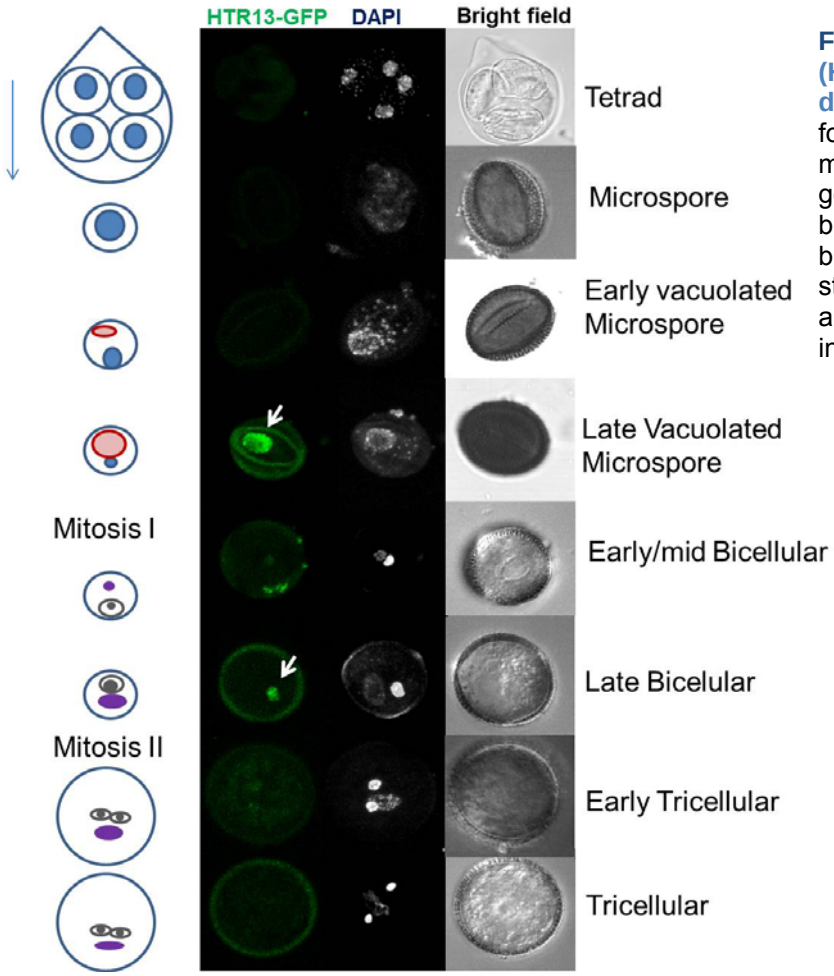

Fig 4.30. HTR13 dynamics (H3.1) during pollen development. HTR13 is found in late vacuolated microspore and in the generative cell of late bicellular pollen. In mid bicellular pollen HTR13 starts to be detected (white arrows). No HTR13 is found in the other stages.

Surprisingly, HTR3-GFP (H3.1) is only present in the vegetative cell of late bicellular pollen, where chromocenters marked by DAPI and HTR3 are observed (Fig 4.31). This result is unexpected, as the companion vegetative cell has been reported as an haploid cell that has arrested cell cycle progression and will not undergo S-phase (Borges et al., 2012), the cell cycle phase where canonical histones H3.1 are incorporated.

In view of these results, we can conclude that, while both H3.1 proteins have similar expression patterns in somatic tissues, during pollen development each H3.1 is expressed in different cells and at different stages. Whereas HTR13 dynamics is expected and can be attributed to S-phase incorporation, the exclusive presence of HTR3 in the vegetative nucleus of bicellular pollen is more baffling. It could be attributed to the S-phase of a possible endocycle or simply an S-phase from 1C to 2C, although none of these processes has been reported. One interesting point is that, as HTR3 is present in the chromocenters of the vegetative cell, we can infer that HTR3 incorporation in the companion cell precedes the chromatin decondensation event described in these cells (Slotkin et al., 2009). In addition, the

incorporation of HTR3 in the chromatin of the vegetative nucleus could be a product of the DNA repair machinery after DNA damage.

In general, we conclude that, even if none of the H3.1 histones is detected in the mature pollen grain, the chromatin of the gametic and nongametic lineages undergoes different reprogramming processes that involve distinct histone H3.1 proteins.

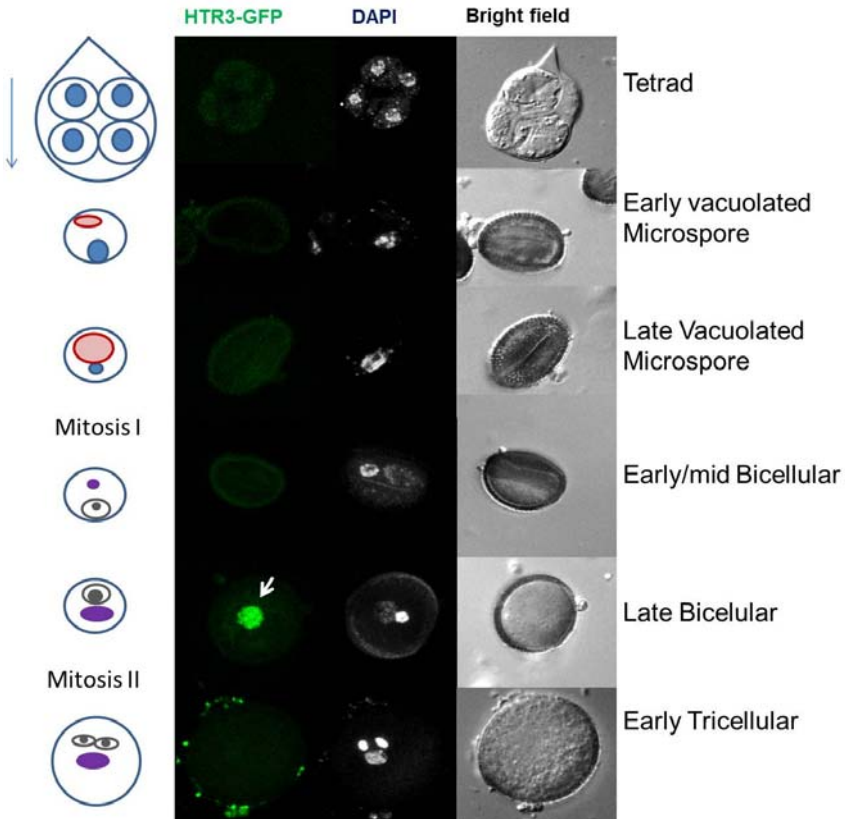

Fig 4.31. HTR3 dynamics (H3.1) during pollen development. HTR3-GFP was only detected in the vegetative cell of late bicellular pollen (white arrow).

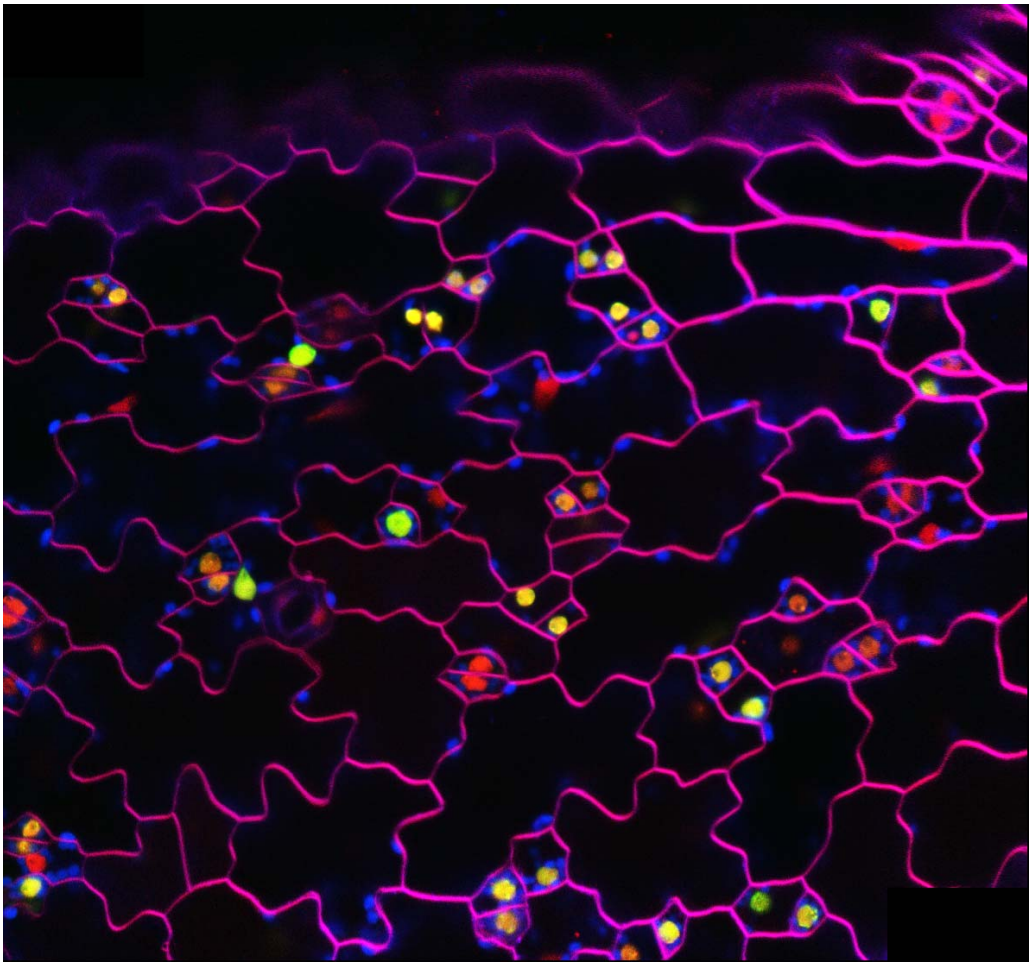

5. Discussion

5.1 Histone H3.1 and H3.3 help create different chromatin states.

The genome-wide maps generated have shown that H3.1 is enriched at transcriptionally silent regions of the genome and repressive marks while the variant H3.3 correlates with gene expression and is associated with active chromatin and active marks. These results show that in general both histones follow similar trends as observed in animals but with some specific characteristics. Similar results were obtained in another study (Wollmann et al., 2012).

The relative values of H3.1 in Arabidopsis preferentially position the canonical histone in pericentromeric and dispersed heterochromatin. In animals however the canonical histone is evenly distributed along the genome (Wirbelauer et al., 2005), with gene-rich regions more enriched in H3.3 than in H3.2 (Goldberg et al., 2010). Also H3.3 is enriched at pericentric heterochromatin in mouse embryonic fibroblasts (Drane et al., 2010). We have also shown that the repressive marks that strongly correlate with the canonical histone are H3K27me1, H3K27me3 and H3K9me2 (Fig 5.1).

It has been shown that H3K27me1 is responsible for preventing heterochromatin overreplication and more importantly, that it is exclusive of H3.1 (Fig 5.1), as the enzymes monomethylating K27 (ATXR5 and ATXR6) have a catalytic domain where the A_{31} of H3.1 (and not T_{31} of H3.3) specifically fits, discriminating the canonical from the variant (Jacob et al., 2014). This fact highlights that the SET domain that many enzymes contain varies from protein to protein, diversifying the function of methyl transferases. In addition, this demonstrates that some modifications are not allowed in H3.3, probably protecting the variant from repressive states.

On the contrary, H3K27me3 is the mark established by the Polycomb group (PcG) proteins to maintain developmental regulators in a repressed state. The PcG system is conserved in plants and animals (even if some proteins vary), with PRC2 and Plant Homeodomain (PHD) proteins in charge of establishing H3K27me3 (Hennig and Derkacheva, 2009). In mammals this mark strongly correlates with H3.2 and H3.1, with a weaker association with H3.3 (Fig 5.1) (Hake et al., 2006). Recently, it was discovered that H3.3 is necessary to enrich H3K27me3 in the bivalent promoters (which contain both active H3K4me3 and repressive H3K27me3 and are poised for activation) of developmental genes in mouse ESC (Banaszynski et al., 2013). Direct evidence of the existence of bivalent promoters in plants has been recently obtained (Sequeira-Mendes et al., 2014). Interestingly, bivalent chromatin occurs in somatic plant cells, suggesting evolutionary differences with animals where bivalent chromatin has been identified in embryonic cells. It would be interesting to determine which H3 protein is enriched in

H3K27me3 in these specific promoters and test if in plants, like in animals, H3.3 can also be sometimes associated with silent states.

Contrary to H3K27me3, present in gene rich regions, H3K9me2 is the silencing mark pre-dominant in heterochromatin, specially enriched in pericentromeric heterochromatin but also in patches of silent chromatin in euchromatin (Feng and Jacobsen, 2011). The corresponding mark in animals, H3K9me3, is more enriched in the replication dependent histones than in the variant, confirming that in general, in eukaryotes, H3.1 tends to be enriched in silencing marks. The role of the CAF-1 subunit p150 in heterochromatin maturation, which is essential in mouse embryo development, also validates the association of H3.1 and silent chromatin (Houlard et al., 2006).

Another feature confirming the strong relationship between H3.1 and silent chromatin is the association of the canonical H3 with all kinds of DNA methylation. This mark, found in all eukaryotes is thought to be associated with transcriptional repression in all organisms when found in the promoters. However, in animals and plants methylation of gene bodies (usually mCG), is not related to gene silencing (Zemach et al., 2010). Indeed this mark is enriched within H3.3 rich regions.

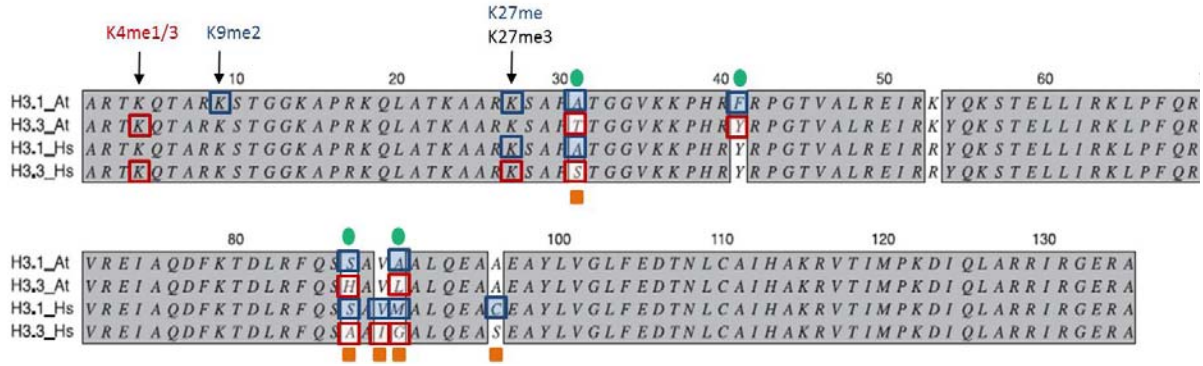

Fig 5.1. Marks associated with H3.1 or H3.3 either in Arabidopsis or humans. While H3K4me1/3 is associated with H3.3 both in plants and mammals, H3K9me2 correlates with H3.1 in plants. H3K27me1 is exclusive of H3.1 in Arabidopsis. In turn, H3K27me3 is usually associated with H3.1 in both species. H3K27me3 has been found in the promoters of bivalent genes in mammals. Green circles mark aa specific of H3.1 or H3.3 in plants. Specific aa of both histones in humans are marked by orange squares. Adapted from (Jacob et al., 2014)

Contrary to H3.1, both in humans and plants, H3.3 correlates with gene expression and various markers of transcription (RNA Polymerase II, H3K4me3 and H3K4me1 in both organisms and H2Bub in plants) (Goldberg et al., 2010; Stroud et al., 2012), reinforcing the conserved association of H3.3 and active euchromatin. Nevertheless, H3.3 mapping in mammals presents several differences with respect to H3.3 mapping in plants. While in both organisms the presence of H3.3 in gene bodies correlates with gene expression, H3.3 in mouse cells is enriched

around the TSS (Goldberg et al., 2010) while in plants H3.3 peaks towards the 3' end of the genes (Stroud et al., 2012; Wollmann et al., 2012). The correlation with RNA Pol II could help explain the abundance of H3.3 towards the transcriptional termination site, as H3.3 is probably introduced in gene regions disturbed by RNA Pol II elongation. The presence of H3.3 at TSS in mammals and not in plants could point to the need of nucleosome remodeling to allow the binding of the transcriptional machinery in plants while mammals would have more unstable nucleosomes, also formed by H2A.Z (Jin et al., 2009). Remarkably, in plants the variant H2A.Z is enriched in the 5' end of the genes (Zilberman et al., 2008). It has been shown that nucleosome core particles containing both H3.3 and H2A.Z are unusually unstable and are only mapped when the nucleosomes are isolated under low salt conditions (150mM considered high salt conditions, (Jin et al. 2009). Strikingly, H2A.Z and H3.3 distributions anticorrelate in our study. A possibility to be tested in the future is that H3.3 is actually paired with H2A.Z at the TSS thus becoming undetectable under our ChIP conditions (150mM NaCl in the ChIP dilution buffer).

It has been shown that H2A.Z also negatively correlates with DNA methylation (Zilberman et al., 2008), in agreement with H3.3 being enriched within body methylated genes. The presence of H2A.Z in gene bodies of highly expressed genes leads to a decrease in their transcription. As a consequence, DNA methylation is thought to prevent H2A.Z incorporation into highly or constitutively expressed genes (Coleman-Derr and Zilberman, 2012). In this context, H3.3, gene body methylation and lack of H2A.Z would favor gene expression. In turn, genes enriched in H2A.Z are those responding to environmental and developmental stimuli (Coleman-Derr and Zilberman, 2012). The relationship between variants H2A.Z and H3.3 still needs to be studied. A clue pointing to possible cooperative roles is that responsive genes downregulated in *hira* mutant plants are upregulated in *h2a.z* mutants (Nie et al., 2014).

Following with the comparison between H3 distribution in plants and animals, H3.3 is enriched at TFBS in mammals (Goldberg et al., 2010). However, we discovered that these sites are depleted of both H3.1 and H3.3 in Arabidopsis, in agreement with the enrichment of TFBS in low nucleosome dense regions (Zhang et al., 2007). Although we did not observe enrichment of any of the histones in intergenic regions, a posterior study detected H3.3 downstream of the TTS in genes with high expression (also observed in mouse ESCs, (Goldberg et al., 2010)) and in promoters containing GA motifs (Shu et al., 2014). The discrepancy probably obeys to the different promoters used in both studies: while we and Wollmann and collaborators used endogenous promoters, Shu and colleagues generated overexpressor lines fusing H3.3 to the 35S promoter, a strategy that could cause ectopic incorporation of the variant.

In addition, the telomeres are extragenic regions of enormous functional relevance. Telomeres are enriched in H3.3 in mouse ESCs, underscoring another situation where the variant is associated with gene silencing. Using our data and those from Wollmann and collaborators, the same trend has been confirmed in Arabidopsis telomeres (Vaquero-Sedas and Vega-Palas, 2013), illustrating that in plants H3.3 can be associated to silent chromatin with specific characteristics.

Interestingly, H3.3 deposition in gene bodies is HIRA dependent while ATRX/Daxx is in charge of chaperoning H3.3 to telomeres (Goldberg et al., 2010; Lewis et al., 2010). Thus, it would be interesting to map H3.3 in *hira* mutant backgrounds to identify chaperone-specific H3.3 enrichment sites. Also, a homolog of Daxx is apparently lacking from the Arabidopsis genome, but it contains a gene coding a homolog of ATRX and four genes coding DEK proteins (Pendle et al., 2005; Otero et al., 2014). Mapping H3.3 in these mutant backgrounds could help unveil the roles of these chaperones in Arabidopsis. In addition, analyzing the correlation between an H3.3 misbalance and possible phenotypic abnormalities (is telomere integrity maintained?) would provide key information about the roles of H3.3 and the different chaperones along development. The same experiments would be relevant in CAF-1 mutant backgrounds. The characteristics detailed in this study are summarized in Fig 5.2.

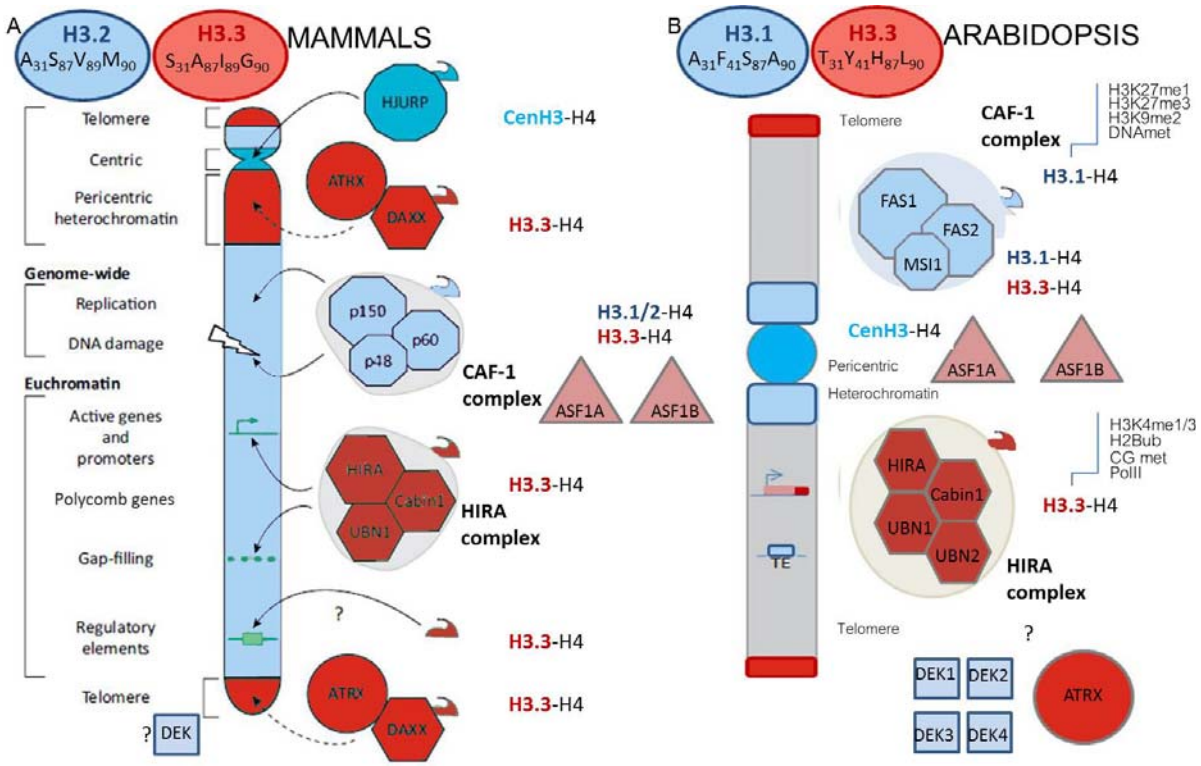

Fig 5.2. State of the art of H3 distribution in mammals (A) and Arabidopsis (B). After this study, H3.1 was shown to be enriched in pericentromeric and dispersed heterochromatin in the model plant. H3.3 is enriched in active chromatin and it peaks towards the 3'end of the genes.

Another similarity with animals is that the profile of H3.3 changes along differentiation. Indeed, the content of the variant parallels changes in gene expression, indicating a possible role of H3.3 in developmental transitions (Goldberg et al., 2010; Wollmann et al., 2012).

One of the most surprising results obtained in our study was finding that DNA replication origins (Roberts et al., 2002) in plants are enriched in both H3.1 and H3.3, and predicted to be nucleosome dense (Stroud et al., 2012). Consistent with this, ORIs are preferentially located in GC-rich regions, known to favor nucleosome assembly (Costas et al., 2011). In many eukaryotes, like Drosophila and *Saccharomyces cerevisiae*, ORIs have been reported over nucleosome depleted regions (NDR) (Eaton et al., 2010; MacAlpine et al., 2010), although they also tend to be located at GC-rich regions (Cayrou et al., 2011). In *Schizosaccharomyces pombe*, the origin recognition complex (ORC) binding and ORIs are not enriched over NDR (de Castro et al., 2012). Besides, it was shown that ORC prefers binding nucleosomes with silencing marks in mammals (Bartke et al., 2010) and also that replication start sites occur at positions of high nucleosome occupancy, even if ORC was detected to bind unstable nucleosomes within the ORI region (Lombrana et al., 2013). Taken together these results suggest that in each genome the nucleosome content at ORIs could vary. In Arabidopsis, the possibility that ORC binds nucleosomes or even that it binds the less stable nucleosomes at ORIs needs to be addressed in the future.

Nevertheless, it should also be taken into account that we are comparing data with different origins: while the H3.1/H3.3 maps were obtained from 10-day-old seedlings, ORIs were mapped in cultured cells (Costas et al., 2011). This could be important because seedlings are a mixture of asynchronously dividing cell types with only a small percentage undergoing S phase, and the high nucleosome content could correspond to the same genomic areas in cells that are not replicating DNA. To confirm the association between replication origins and high nucleosome content in Arabidopsis it should be important to compare the data to ORI mapping in seedlings, a study which is under way in our laboratory. Even so, nucleosome occupancy algorithms also predict high nucleosome content at ORIs in cultured cells.

In conclusion, regarding histone H3, most of the trends observed in our study are conserved in animals, pointing out that the evolutionary constraints affecting histones are important and lead to a similar final result despite independent evolution of plant and animal lineages.

What is the significance behind the differential histone distribution? Some years ago Hake and Allis presented the barcode hypothesis (Hake and Allis, 2006). They suggested

histones index the genome, being deposited in a non-random way, creating chromatin territories that can then adapt to environmental changes by different posttranslational modification (immediate response) while long-term memory of epigenetic stages would be maintained by the histone choice (Fig 5.3). They already proposed that H3.3 was associated with active chromatin and assigned the canonical H3 proteins to heterochromatin. Interestingly they proposed that the chromatin domains changed along differentiation and that each cell lineage would have a different histone bar code depending on their specific gene expression patterns. We now know that H3.3 can also be associated with silent states (e.g at telomeres) and that the enrichment of a histone in a certain region or the association of a mark with a variant doesn't mean exclusiveness, but a preferential combination and a more probable outcome regarding gene expression or silencing. Indeed, in Arabidopsis, 9 chromatin states have been defined taking into account the GC content, GC methylation, H3.1, H3.3, H2A.Z and several histone marks (Sequeira-Mendes et al., 2014). H3.1 is enriched in several chromatin states, all of them associated with gene silencing (constitutive or facultative heterochromatin, the polycomb state and other states marking genes with low expression) whereas on the contrary H3.3 content is high in states of active transcription. Even if the barcode hypothesis may be too simple for the chromatin complexity, it provides a very useful framework where histone variants have a fundamental role in the generation of chromatin states that are heritable along cell generations.

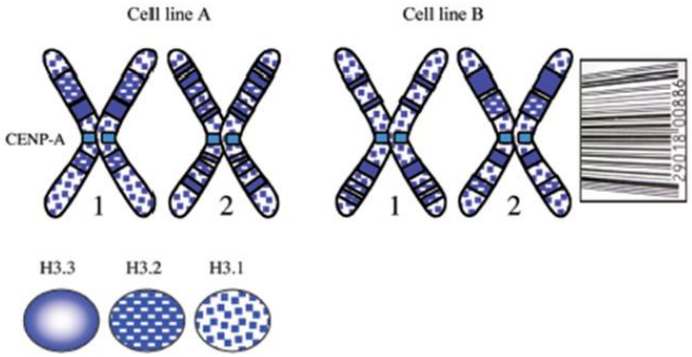

Fig 5.3. The barcode hypothesis. Each cell line would have a different non-random H3 distribution. Adapted from (Hake and Allis, 2006).

5.2 H3 dynamics reveals chromatin reprogramming upon differentiation

In this study we have followed H3 dynamics along Arabidopsis development by tagging H3 proteins to fluorescent epitopes. The use of two different genes for each H3 protein allowed us to confirm that similar data were obtained for identical proteins in somatic tissue, although double checking was necessary to discard possible discrepancies based on specificities of regulatory regions, as promoters and UTRs vary among genes of the same group.

Despite that CAF1 and ASF1 mutants show pleiotropic developmental defects in Arabidopsis, and since chaperone mutants are embryonic lethal in mammals, the H3 dynamics along development has been a mostly unexplored topic. It was first addressed in mature and bicellular pollen, where the presence or disappearance of some of the H3 histones was followed, revealing a differential behavior of H3.1 and H3.3 in the mature male gametes of Arabidopsis (Ingouff et al., 2007; Ingouff and Berger, 2010), as discussed below.

Another interesting study managed to distinguish the old and newly synthesized histones using a dual-color system. Interestingly, they showed the asymmetric delivery of H3.1 in the asymmetric division of the male germline stem cells of Drosophila: old H3.1 was observed to be retained in the stem cell while the new H3.1 histones were distributed to the differentiating daughter cell (Tran et al., 2012). The authors suggested that retaining old H3.1 was a way to preserve the unique properties of the stem cells, but the asymmetric distribution still needs to be confirmed in other stem cells and organisms.

In turn, in a very recent work, the mRNA of core histones H2A, H3.1 and H3.2 fused to GFP was injected in mouse embryos. Using a FRAP strategy (Fluorescence Recovery After Photobleaching), it was found that these canonical histones are more mobile in the chromatin of 2-cell mouse embryos than at the 8-cell stage: in the first case H3.1 signal recovers quickly and strongly after photobleaching while in the latter situation the H3.1 signal did not reach a high recovery (Boskovic et al., 2014). This is in agreement with earlier observations regarding the different gene expression potential of nuclei during early mouse development (Martinez-Salas et al., 1989). However, since the mRNA of these canonical histones is injected, the expression is cell-cycle independent and the fluorescence recovery in the bleached regions could be a result of both mobility of other histones to the zone (chromatin remodeling) and incorporation of new histones. In any case, H3.3 is not recovered with the same strength in 2-cell or 8-cell embryos so the turnover of this histone is longer in embryo development. On the contrary, the canonical histones seem to have a more crucial role in the first stages of embryogenesis and the importance is higher at younger totipotent stages. Indeed, the authors also suggest a possible association between the mobility of canonical histones and cellular plasticity. Along the same lines, applying FRAP to H2B in the Arabidopsis root has reported that histone mobility is higher in meristematic cells than in differentiated cells, and that these transitions are partly controlled by histone acetylation (Rosa et al., 2014), a modification that curiously affects histone H3 and H4.

Our interest in H3 dynamics during embryogenesis and organogenesis led us to follow the H3.1/H3.3 balance at different moments of Arabidopsis development and unveil the clear

association of H3.1 and proliferation capacity of the cells. Altogether these data point to functional differences between the chromatin of highly proliferating cells and those undergoing differentiation, as also noticed by the changes in H2B mobility (Rosa et al., 2014). As in animals, Arabidopsis chromatin could be a reflection of cellular plasticity.

The H3.1/H3.3 balance has also uncovered different functional domains within the Arabidopsis root (Fig 5.4). In the RAM, cells that are actively proliferating retain H3.1 till mitosis while those undergoing the last cell cycle massively evict H3.1 in G2, a result confirmed by the overlap between the domain of high proliferation (mitosis rich in H3.1) and that of cells expressing CYCB1;1. Interestingly, the two domains are clear and statistically significant when all the mitotic figures found in epidermis are taken into account or in atrichoblasts. However, in trichoblasts the two populations get mixed, probably because trichoblasts have a higher division rate than atrichoblasts (Berger et al., 1998), generating more cells per file and increasing the chances to have H3.1 containing mitosis in a more shootward part of the root. Overall, our data on H3.1 massive replacement points to a chromatin reprogramming before cell elongation and differentiation.

With H3.1 replacement, H3.1 associated marks are also diluted till the next S-phase. This could be important for the genes involved in differentiation and repressed by the PcG proteins. Indeed, hundreds of genes gain or lose H3K27me3 upon differentiation (Deal and Henikoff, 2010; Lafos et al., 2011). In particular, the cell type-specific genes whose expression changes most in comparison to other tissues have been shown to have low levels of H3K27me3 and a high content of H3K4me3 in hair and non-hair cells of the root (Deal and Henikoff, 2010). As H3.1 is preferentially associated with H3K27me3 and H3.3 with H3K4me3, the reprogramming observed could help change the balance between these two marks. However, not all cell type-specific genes show this signature in their chromatin (Deal and Henikoff, 2010), and some other mechanisms must be associated with gene activation in different cell lineages, for instance a more opened chromatin facilitated by H3.3. In addition, H3.3 has proved to be a key factor to maintain epigenetic memory (Ng and Gurdon, 2008), a memory that could be established after reprogramming occurs.

A question of primary relevance is how the H3.1/H3.3 balance is controlled along the RAM. In view of our results, a possible interpretation would be that H3.1 is simply passively diluted: it is incorporated in the S-phase and the content of H3.1 decreases by H3.3 replacement until the next replication round. However, the retention of H3.1 in mitosis in the highly proliferative domain and its eviction in G2 in the cells undergoing the last cell cycle would imply a different length of cell cycles along the RAM, which is not consistent with

measurements of the division rates, approximately constant throughout the meristem (Beemster and Baskin, 1998).

In addition, we have also studied the RAM domains in *fas* mutants. *fas1-4* mutants are knockdowns and incorporate a small amount of H3.1. In roots of these mutants the chromocenters are not marked by H3.1 but by H3.3, showing that the H3 misbalance is responsible for the decrease in heterochromatin of these plants. As previously detailed, *fas* mutants have shorter roots and meristems. Even in this condition, the functional domains uncovered by H3 dynamics are conserved, indicating that the longitudinal zonation pattern is not disturbed by the H3 disequilibrium. Therefore, H3 histones are reporters of the root domains and the reprogramming events but are not the causing agents. Accordingly, we wondered if any of the root patterning genes could be in charge of controlling chromatin reprogramming along the RAM.

The promoter analysis revealed the presence of several binding sites for different transcription factors, a list that was further processed according to the expression pattern of genes containing these TFBS along the root. (Brady et al., 2007). Class A was the most attractive, as it matched the H3 dynamics along the RAM. As previously described, E2F transcription factors regulate the G1/S transition and are expected to be present in cell-cycle regulated genes implicated in S-phase, validating our analysis. YABBY genes control leaf morphogenesis (Ha et al., 2010; Bonaccorso et al., 2012) and a role in roots has not been described yet. The same applies to LEAFY, implicated in the meristem identity transition in seedlings and in floral patterning, with no described function in roots (Winter et al., 2011). In turn, a member of the DOF transcription family not expressed in the primary root regulates cell cycle in response to developmental signaling (Skirycz et al., 2008) and some other members regulate early phloem development in roots (Furuta et al., 2014a). It could be interesting to check if any member of the family could alter H3 developmental domains. However, ANT sites specially caught our attention, since PLT proteins belong to this subclass of transcription factors, proteins that control the longitudinal zonation pattern of the root, PLT1 expression domain coinciding in the root meristem with the high proliferation domain we described (Galinha et al., 2007; Mahonen et al., 2014). In addition, our analysis also shows that the ANT motif is enriched in the promoters of genes expressed mostly in the proliferation domain of the RAM, underscoring the importance of PLT genes in regulating meristematic processes.

Altogether, these data point to a possible role of PLT, and possibly other transcription factors, in controlling the longitudinal cell cycle potential in the RAM, including chromatin reprogramming for the last cell cycle. We tried to test the *in silico* results experimentally in *plt*

mutants. We found that the expression of cell cycle genes was not altered in single mutants, likely due to redundancy of *PLT* gene family members. However, *plt1/plt2* mutants have downregulated levels of many of our target genes containing ANT sites in their promoters. Despite this, some cell cycle genes that do not contain ANT sites were also downregulated, probably because these mutants have very short roots and a reduced meristem (Aida et al., 2004), hindering the distinction between a specific effect derived from the lack of PLT proteins and a global cell cycle arrest. Under this situation, future experiments should aim at identifying the binding site of PLT and whether they are present in genes relevant for H3 dynamics and other possible genes in the network.

In line with the reprogramming observed in the RAM, we have become aware of another reprogramming event that takes place when the cell reaches the last endoreplication cycle (Fig 5.4). As shown with the flow cytometry experiments, we have observed a decrease in the number of H3.1-GFP positive cells in root differentiated tissue, more pronounced in the highest ploidy levels. Interestingly, during hypocotyl development, an organ built exclusively by cell expansion, the same reprogramming is observed, indicating that it is not a root exclusive process. During skotomorphogenesis, the maximum ploidy level reached is 32C. When cells reach this nuclear DNA content at day 5, most 32C nuclei were positive for H3.1-GFP. The following days the percentage of cells positive for H3.1 also decreases. This way we have tracked the evolution of H3.1 content in a concrete ploidy level since its appearance, indicating that H3.1 is incorporated in each replication round and decays as time goes by.

To distinguish if H3.1 decay was a consequence of H3.1 eviction or of a subsequent decrease of incorporation, we measured the H3.1 and H3.3 content in each nucleus along root cell files, using H3.3-RFP as a measure of the ploidy level. In some nuclei we detected roughly maximum incorporation of H3.1 in each ploidy level, demonstrating that loss of H3.1 is a consequence of H3.1 eviction and not a lack of H3.1 incorporation.

The EdU staining and immunofluorescence of H3.1 experiments show that the decay of H3.1 is not abrupt but gradual, as revealed in cells with a certain content of H3.1 but negative for EdU. Conspicuously, the stele nuclei have a high amount of H3.1, something expectable, as the procambial tissue remains undifferentiated (Furuta et al., 2014a) and therefore does not have to be reprogrammed.

With our data we have confirmed that the reprogramming occurs at the end of the endocycle and also in proliferating cells of the RAM that are about to exit cell cycle and enter the endocycle program.

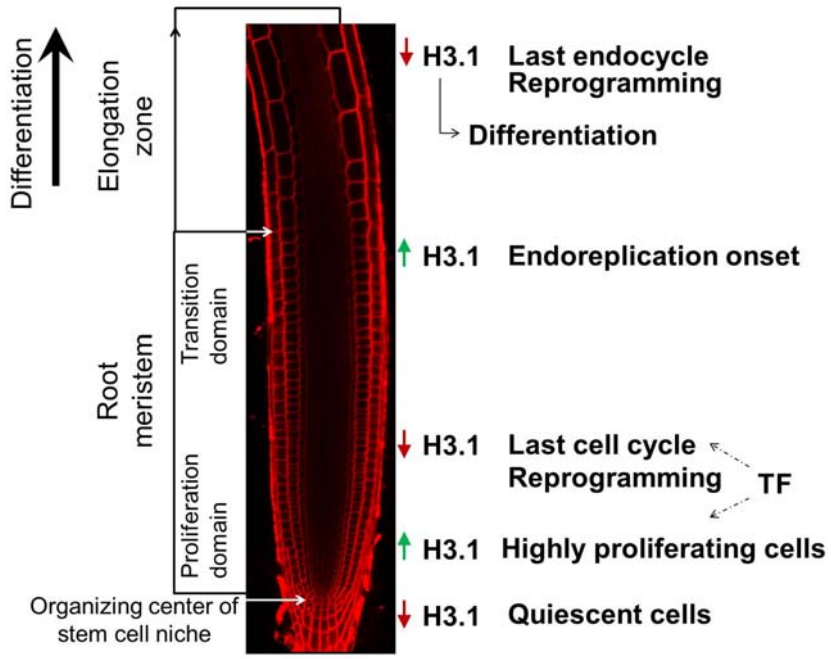

Fig 5.4. H3 dynamics model in the RAM. The H3.1 decrease in the cells undergoing the last cell cycle, possibly controlled by a network of TF (E2F, ANT, KNAT etc), reprograms the chromatin before starting elongation and endoreplication. The reprogramming is also observed in the last endocycle. H3.1 decrease is associated with differentiation in the root and other organs.

The observations in the stomatal lineage confirm that the reprogramming also takes place in cells that are not undergoing endoreplication but that differentiate immediately after cell cycle exit, associating H3.1 and differentiation independently of the developmental process that lead to cell maturation. It would be interesting to follow H3.1 dynamics in dedifferentiation processes and check if the content of H3.1 increases. Also it would be informative to test if cells can dedifferentiate just by changing their chromatin states, for instance by overexpressing CAF-1 and histone H3.1.

5.3. Different dynamics of H3.1 proteins in the male gamete.

Studies of the distribution of H3.1 and H3.3 in specific cell types have been addressed only in mammalian cells, showing the association of H3.3 and differentiation (Goldberg et al., 2010). Our ongoing studies with Arabidopsis sorted cell types would help to follow the results of histone reprogramming in specific genes and also to distinguish which genomic elements suffer higher histone remodeling. A complementary approach is focusing on the gametes. In Arabidopsis, histone dynamics in the gametes and zygote have been extensively studied.

In the female gamete, no H3.1 fluorescent signal is detected in the egg cell and the H3.3 histones come from the expression of two different genes (*HTR5* and *HTR8*) (Ingouff et al., 2010) In addition, no CENH3 signal is observed, although clear chromocenters can be

appreciated (Ingouff et al., 2010). In the central cell, the cell that will produce the endosperm and will nourish the embryo after fertilization, H3.1 proteins can be found together with the already mentioned H3.3 histones and the unusual HTR14.

In mature pollen, the 2 identical sperm cells that will carry out the double fertilization process are characterized by the presence of CENH3, the unusual pollen-specific histone H3 (HTR10) and HTR5, a paradigmatic H3.3. In turn, the large vegetative cell, in charge of producing the pollen tube that will guide the sperm cells to the female gamete, features the expression of 2 H3.3 genes *(HTR5* and *HTR8)* and *HTR14*. The different histone content between the sperm and vegetative cell evidences a distinct chromatin composition in gametic and nongametic lineages. Interestingly, no H3.1 expression has been detected in the male germline (Ingouff et al., 2010).

Overall, the data available point to a major absence of H3.1 in the gametes. Within hours after fertilization, histone variants from both male and female gametes are eliminated from the zygote in a replication-independent process, a mechanism that may contribute to the reprogramming necessary to acquire totipotency maybe by incorporating H3.1, that, as mentioned before is associated with cellular plasticity (Boskovic et al., 2014). On the contrary, in the endosperm the elimination of the parental histones seems to be passive and associated to the S phase of cell cycle (Ingouff et al., 2007). Soon after fertilization, *de novo* synthesis of the different histones starts and the somatic balance is already restored at the 2-cell embryo (Ingouff et al., 2010). These studies are an example of histone reprogramming and open several questions, such as why and when during germline development H3.1 proteins stop being necessary or what histones are incorporated during the S phase of the gametes that precedes fertilization.

To address these questions we followed H3.1 dynamics along pollen development and found out surprising results. While HTR13 behaves like a typical H3.1, being incorporated in each S-phase preceding the two mitotic divisions, HTR3 has been only observed in the vegetative cell of bicellular pollen, a cell that will not divide again and that is arrested in G0 (Berger and Twell, 2011) (Fig 5.5). How is HTR3 incorporated if it is a canonical H3.1, loaded into chromatin in a replication dependent manner?

In bicellular pollen the presence of HTR10, the pollen specific histone, and CENH3 had been previously followed, and they are present only in the generative cell (Ingouff et al., 2007). The absence of CENH3 highlights presumable chromatin changes in the centromeric region. Lack of HTR13 and the detected presence of H3.3 histones in this cell may also contribute to chromatin decondensation. Curiously, in the vegetative cell *DDM1* expression is downregulated

and *Athila* retrotransposons are activated to target silencing in the gametes (Slotkin et al., 2009). In addition, CG methylation is lost in a hundred transposons and retrotransposons (Calarco et al., 2012), transposons that according to our ChIP-seq data are enriched in H3.1, maybe pointing to a simultaneous loss of H3.1 in these regions. Altogether these data underscore a deep and poorly understood chromatin reprogramming in the vegetative cell, as histone composition and DNA methylation change, causing the activation of different TEs in several ways. Could all these rearrangements be causing DNA damage and the activation of the repair machinery? Since H3.1 is incorporated by CAF-1 also during DNA repair (Adam et al., 2013) we speculate that a massive chromatin repair could lie behind the presence of HTR3 in the vegetative cell. Future experiments such as detection of H2A.X, the use of G1 cell cycle markers, or the study of *htr3* mutants would help determine the relevance of HTR3 in the vegetative cell. In any case, what this result shows is that in the male germline, H3.1 proteins have different dynamics, something never observed in somatic tissue. This again highlights the specific features of the gametophytic phase of Arabidopsis, reflected even at the deep level of chromatin.

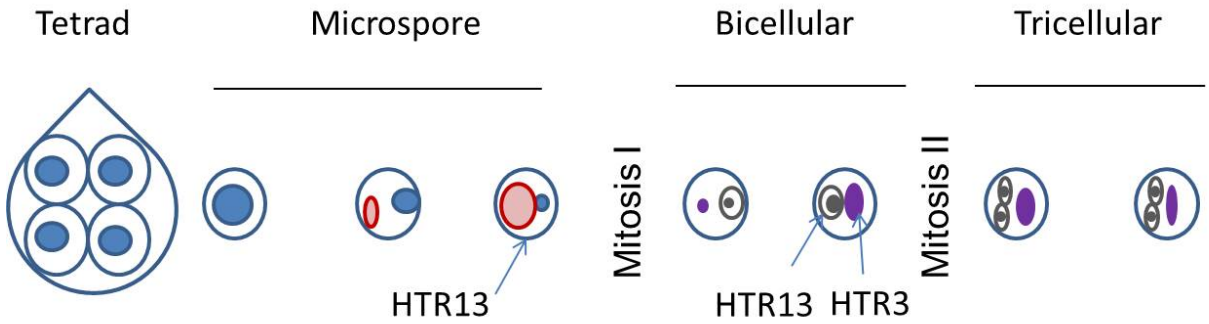

Fig 5.5. HTR13 and HTR3 are incorporated at different points of pollen development. Red: vacuole. Purple: vegetative cell. Grey: Generative/Sperm cells.

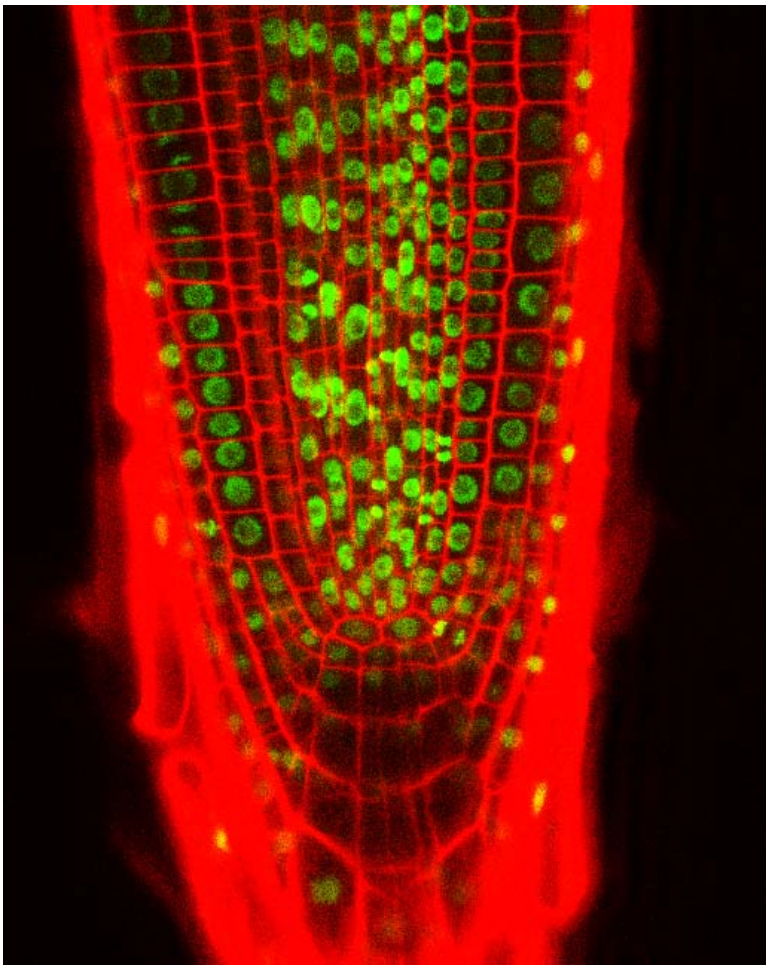

6. Conclusions

Conclusions

1. Histone H3.1 is enriched in pericentromeric and dispersed heterochromatin and colocalizes with silent chromatin marks. On the contrary, histone H3.3 correlates with active chromatin marks and is associated with active chromatin, peaking towards the 3' end of the genes.
2. Both histone H3.1 and H3.3 are enriched in genomic sites used as replication origins.
3. In spite of independent evolution, plant histones H3.1 and H3.3 exhibit characteristics similar to those of animals, although with plant specific features, suggesting that similar constraints led the evolution of H3 proteins in plants and animals.
4. Cells with high proliferation potential have a high content of histone H3.1.
5. Cells undergoing the last cell cycle in the RAM before exit the proliferation domain suffer a massive histone H3 reprogramming in G2, showing a low H3.1/H3.3 ratio in mitosis.
6. The promoters of genes involved in histone H3 reprogramming contain putative binding sites for PLT (AINTEGUMENTA-LIKE) and other transcription factors, e.g. E2F, strongly suggesting a link between H3 reprogramming, root patterning genes and cell division potential.
7. When cell initiate the endocycle after cell cycle arrest they incorporate histone H3.1 during the S-phase and during the last endocycle large amounts of H3.1 are evicted, in a process similar to that occurring during the last cell cycle.
8. The histone H3 reprogramming event takes place when cell faces differentiation, independently of whether it belongs to endoreplicating, e.g., root cells, or proliferating cell lineages, e.g. stomata.
9. The H3.1/H3.3 misbalance contributes to the decreased heterochromatin phenotype of *fas* mutants but does not affect the developmental domains of the root and its associated histone H3.1 reprogramming pattern.
10. Histone H3.1 proteins show different expression patterns along pollen development.

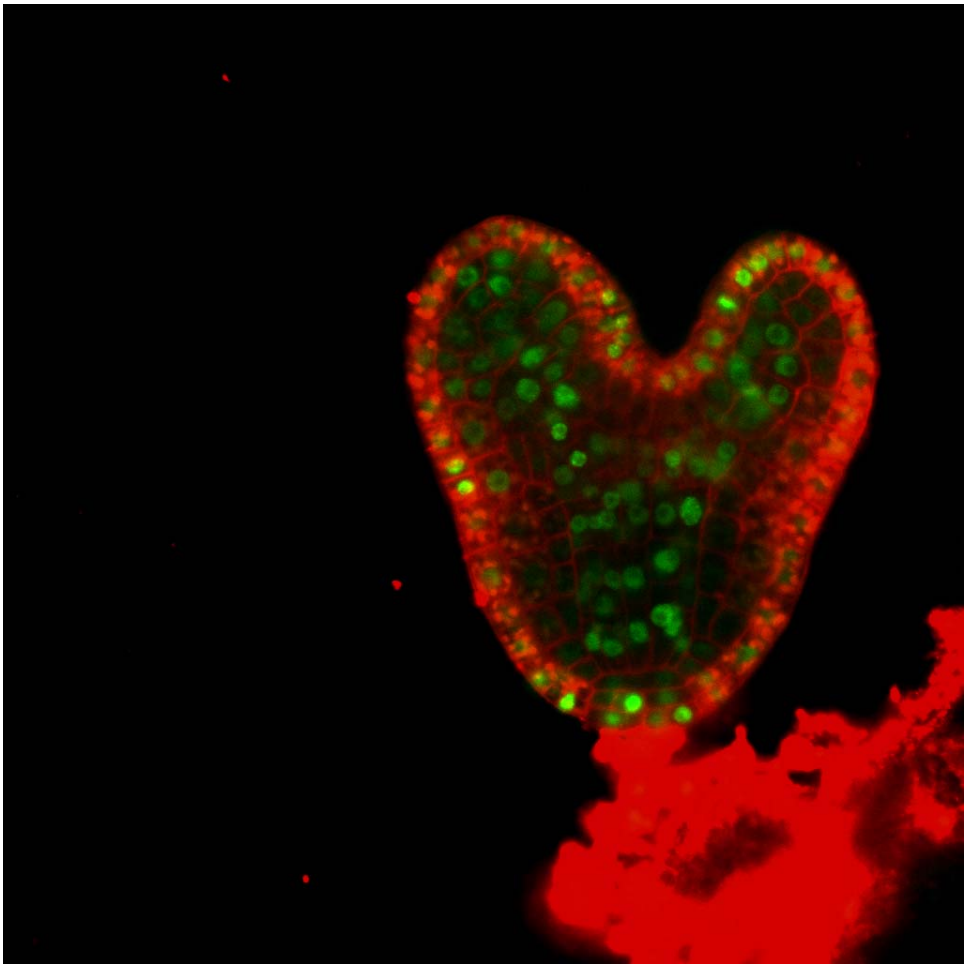

7. Conclusiones

Conclusiones

1. La heterocromatina pericentromérica y dispersa está enriquecida en la histona H3.1, que colocaliza con marcas de silenciamiento. Por el contrario, la histona H3.3 correlaciona con marcas de activación y está asociada con cromatina activa, alcanzando un máximo en el extremo 3' de los genes.
2. Los sitios genómicos usados como orígenes de replicación están enriquecidos tanto en histona H3.1 como en H3.3.
3. A pesar de haber evolucionado de manera independiente, las histonas H3.1 y H3.3 de plantas tienen características similares a las de animales, aunque con algunas cualidades específicas, lo que sugiere que la evolución de las histonas H3 en plantas y animales tuvo restricciones semejantes.
4. Las células con un elevado potencial de proliferación tienen un alto contenido en H3.1.
5. Antes de abandonar el dominio de proliferación, las células que atraviesan su último ciclo en el meristemo apical de la raíz sufren una reprogramación masiva de su contenido en H3 durante G2, mostrando un bajo ratio de H3.1/H3.3 en mitosis.
6. Los promotores de genes implicados en la reprogramación de H3 contienen sitios putativos de unión a PLETHORA (tipo AINTEGUMENTA) y otros factores de transcripción como E2F, señalando un vínculo entre la reprogramación de H3 y los genes que controlan el potencial de división celular y el desarrollo y patrón anatómico de la raíz.
7. Cuando las células inician el endociclo tras el final del programa de ciclo celular, incorporan H3.1 durante la fase S y, en un proceso similar al ocurrido en el último ciclo celular, grandes cantidades de H3.1 son sustituidas por H3.3 en el último endociclo.
8. El evento de reprogramación de la histona H3 tiene lugar cuando la célula se prepara para la diferenciación, independientemente de si pertenece a linajes donde se produce endoreplicación, como las células de la raíz, o a linajes proliferantes, como en el caso de los estomas.
9. El desequilibrio en el ratio H3.1/H3.3 en los mutantes *fas* contribuye al fenotipo de disminución de la heterocromatina pero no afecta a los dominios de desarrollo de la raíz ni a la reprogramación de H3.1 asociada.
10. Las histonas H3.1 exhiben distintos patrones de expresión a lo largo del desarrollo del polen.

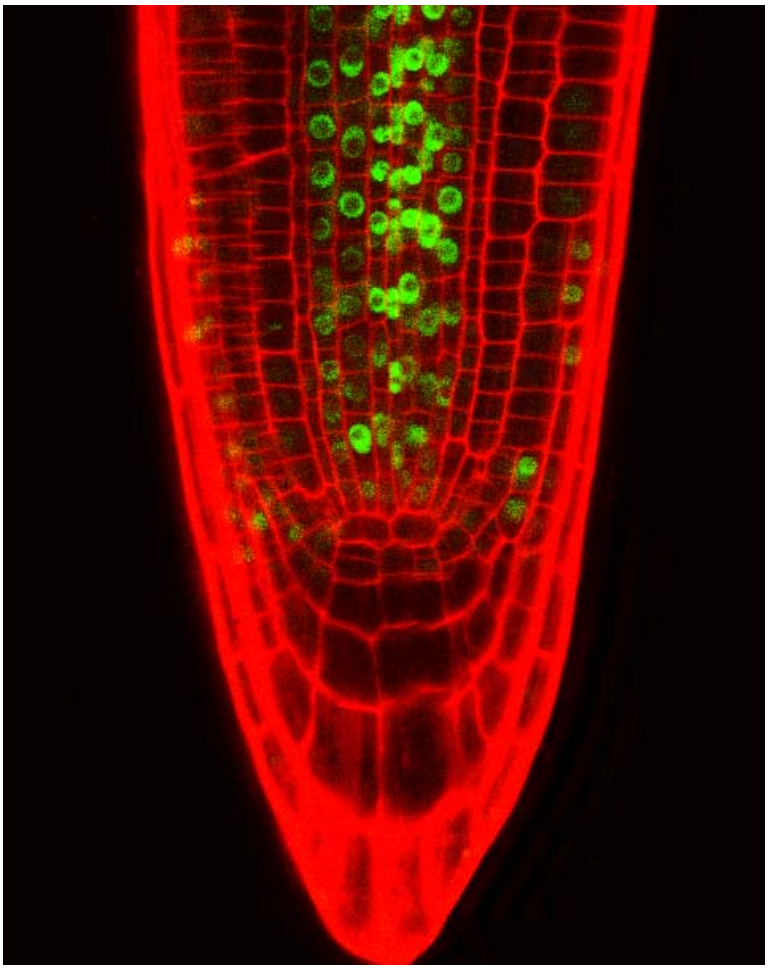

8. Bibliography

References

Ach, R.A., Durfee, T., Miller, A.B., Taranto, P., Hanley-Bowdoin, L., Zambryski, P.C., Gruissem, W. (1997). RRB1 and RRB2 encode maize retinoblastoma-related proteins that interact with a plant D-type cyclin and geminivirus replication protein. Mol Cell Biol **17,** 5077-5086.

Adam, S., Polo, S.E., and Almouzni, G. (2013). Transcription recovery after DNA damage requires chromatin priming by the H3.3 histone chaperone HIRA. Cell **155,** 94-106.

Ahmad, K., and Henikoff, S. (2002). The histone variant H3.3 marks active chromatin by replication-independent nucleosome assembly. Mol Cell **9,** 1191-1200.

Aida, M., Beis, D., Heidstra, R., Willemsen, V., Blilou, I., Galinha, C., Nussaume, L., Noh, Y.S., Amasino, R., and Scheres, B. (2004). The PLETHORA genes mediate patterning of the Arabidopsis root stem cell niche. Cell **119,** 109-120.

Arabidopsis Genome, I. (2000). Analysis of the genome sequence of the flowering plant Arabidopsis thaliana. Nature **408,** 796-815.

Ausin, I., Alonso-Blanco, C., Jarillo, J.A., Ruiz-Garcia, L., and Martinez-Zapater, J.M. (2004). Regulation of flowering time by FVE, a retinoblastoma-associated protein. Nat Genet **36,** 162-166.

Balaji, S., Iyer, L.M., and Aravind, L. (2009). HPC2 and ubinuclein define a novel family of histone chaperones conserved throughout eukaryotes. Mol Biosyst **5,** 269-275.

Banaszynski, L.A., Wen, D., Dewell, S., Whitcomb, S.J., Lin, M., Diaz, N., Elsasser, S.J., Chapgier, A., Goldberg, A.D., Canaani, E., Rafii, S., Zheng, D., and Allis, C.D. (2013). Hira-dependent histone H3.3 deposition facilitates PRC2 recruitment at developmental loci in ES cells. Cell **155,** 107-120.

Bannister, A.J., and Kouzarides, T. (2011). Regulation of chromatin by histone modifications. Cell Res **21,** 381-395.

Bartke, T., Vermeulen, M., Xhemalce, B., Robson, S.C., Mann, M., and Kouzarides, T. (2010). Nucleosome-interacting proteins regulated by DNA and histone methylation. Cell **143,** 470-484.

Beemster, G.T., and Baskin, T.I. (1998). Analysis of cell division and elongation underlying the developmental acceleration of root growth in Arabidopsis thaliana. Plant Physiol **116,** 1515-1526.

Berger, F., and Twell, D. (2011). Germline specification and function in plants. Annu Rev Plant Biol **62,** 461-484.

Berger, F., Hung, C.Y., Dolan, L., and Schiefelbein, J. (1998). Control of cell division in the root epidermis of Arabidopsis thaliana. Dev Biol **194,** 235-245.

Bernatavichute, Y.V., Zhang, X., Cokus, S., Pellegrini, M., and Jacobsen, S.E. (2008). Genome-wide association of histone H3 lysine nine methylation with CHG DNA methylation in Arabidopsis thaliana. PLoS One **3,** e3156.

Bonaccorso, O., Lee, J.E., Puah, L., Scutt, C.P., and Golz, J.F. (2012). FILAMENTOUS FLOWER controls lateral organ development by acting as both an activator and a repressor. BMC Plant Biol **12,** 176.

Bonnefoy, E., Orsi, GA., Couble, P., Loppin, B. (2007) The essential role of Drosophila HIRA for de novo assembly of paternal chromatin at fertilization. PLoS Genet 10, 1991-2006.

Borges, F., Calarco, J.P., and Martienssen, R.A. (2012). Reprogramming the epigenome in Arabidopsis pollen. Cold Spring Harb Symp Quant Biol **77,** 1-5.

Boskovic, A., Eid, A., Pontabry, J., Ishiuchi, T., Spiegelhalter, C., Raghu Ram, E.V., Meshorer, E., and Torres-Padilla, M.E. (2014). Higher chromatin mobility supports totipotency and precedes pluripotency in vivo. Genes Dev **28,** 1042-1047.

Bouveret, R., Schonrock, N., Gruissem, W., and Hennig, L. (2006). Regulation of flowering time by Arabidopsis MSI1. Development **133,** 1693-1702.

Brady, S.M., Orlando, D.A., Lee, J.Y., Wang, J.Y., Koch, J., Dinneny, J.R., Mace, D., Ohler, U., and Benfey, P.N. (2007). A high-resolution root spatiotemporal map reveals dominant expression patterns. Science **318,** 801-806.

Brown, R. (1833). Observations on the organs and mode of fecundation in Orchidae and Asclepiadeae. Trans. Linn. Soc **16,** 685-743.

Burgess, R.J., and Zhang, Z. (2013). Histone chaperones in nucleosome assembly and human disease. Nat Struct Mol Biol **20,** 14-22.

Calarco, J.P., Borges, F., Donoghue, M.T., Van Ex, F., Jullien, P.E., Lopes, T., Gardner, R., Berger, F., Feijo, J.A., Becker, J.D., and Martienssen, R.A. (2012). Reprogramming of DNA methylation in pollen guides epigenetic inheritance via small RNA. Cell **151,** 194-205.

Campos, E.I., and Reinberg, D. (2009). Histones: annotating chromatin. Annu Rev Genet **43,** 559-599.

Carlsbecker, A., Lee, J.Y., Roberts, C.J., Dettmer, J., Lehesranta, S., Zhou, J., Lindgren, O., Moreno-Risueno, M.A., Vaten, A., Thitamadee, S., Campilho, A., Sebastian, J., Bowman, J.L., Helariutta, Y., and Benfey, P.N. (2010). Cell signalling by microRNA165/6 directs gene dose-dependent root cell fate. Nature **465,** 316-321.

Casamitjana-Martinez, E., Hofhuis, H.F., Xu, J., Liu, C.M., Heidstra, R., and Scheres, B. (2003). Root-specific CLE19 overexpression and the sol1/2 suppressors implicate a CLV-like pathway in the control of Arabidopsis root meristem maintenance. Curr Biol **13,** 1435-1441.

Cayrou, C., Coulombe, P., Vigneron, A., Stanojcic, S., Ganier, O., Peiffer, I., Rivals, E., Puy, A., Laurent-Chabalier, S., Desprat, R., and Mechali, M. (2011). Genome-scale analysis of metazoan replication origins reveals their organization in specific but flexible sites defined by conserved features. Genome Res **21,** 1438-1449.

Chodavarapu, R.K., Feng, S., Bernatavichute, Y.V., Chen, P.Y., Stroud, H., Yu, Y., Hetzel, J.A., Kuo, F., Kim, J., Cokus, S.J., Casero, D., Bernal, M., Huijser, P., Clark, A.T., Kramer, U., Merchant, S.S., Zhang, X., Jacobsen, S.E., and Pellegrini, M. (2010). Relationship between nucleosome positioning and DNA methylation. Nature **466,** 388-392.

Coleman-Derr, D., and Zilberman, D. (2012). Deposition of histone variant H2A.Z within gene bodies regulates responsive genes. PLoS Genet **8,** e1002988.

Colon-Carmona, A., You, R., Haimovitch-Gal, T., and Doerner, P. (1999). Technical advance: spatio-temporal analysis of mitotic activity with a labile cyclin-GUS fusion protein. Plant J **20,** 503-508.

Cook, A.J., Gurard-Levin, Z.A., Vassias, I., and Almouzni, G. (2011). A specific function for the histone chaperone NASP to fine-tune a reservoir of soluble H3-H4 in the histone supply chain. Mol Cell **44,** 918-927.

Corpet, A., De Koning, L., Toedling, J., Savignoni, A., Berger, F., Lemaitre, C., O'Sullivan, R.J., Karlseder, J., Barillot, E., Asselain, B., Sastre-Garau, X., and Almouzni, G. (2011). Asf1b, the necessary Asf1 isoform for proliferation, is predictive of outcome in breast cancer. EMBO J **30,** 480-493.

Costas, C., de la Paz Sanchez, M., Stroud, H., Yu, Y., Oliveros, J.C., Feng, S., Benguria, A., Lopez-Vidriero, I., Zhang, X., Solano, R., Jacobsen, S.E., and Gutierrez, C. (2011). Genome-wide mapping of Arabidopsis thaliana origins of DNA replication and their associated epigenetic marks. Nat Struct Mol Biol **18,** 395-400.

Couldrey, C., Carlton, M.B., Nolan, P.M., Colledge, W.H., and Evans, M.J. (1999). A retroviral gene trap insertion into the histone 3.3A gene causes partial neonatal lethality, stunted growth, neuromuscular deficits and male sub-fertility in transgenic mice. Hum Mol Genet **8,** 2489-2495.

Cubas, P., Vincent, C., and Coen, E. (1999). An epigenetic mutation responsible for natural variation in floral symmetry. Nature **401,** 157-161.

Cui, H., and Benfey, P.N. (2009). Cortex proliferation: simple phenotype, complex regulatory mechanisms. Plant Signal Behav **4,** 551-553.

Das, C., Tyler, J.K., and Churchill, M.E. (2010). The histone shuffle: histone chaperones in an energetic dance. Trends Biochem Sci **35,** 476-489.

de Castro, E., Soriano, I., Marin, L., Serrano, R., Quintales, L., and Antequera, F. (2012). Nucleosomal organization of replication origins and meiotic recombination hotspots in fission yeast. EMBO J **31,** 124-137.

De Veylder, L., Larkin, J.C., and Schnittger, A. (2011). Molecular control and function of endoreplication in development and physiology. Trends Plant Sci **16,** 624-634.

De Veylder, L., Beeckman, T., Beemster, G.T., de Almeida Engler, J., Ormenese, S., Maes, S., Naudts, M., Van Der Schueren, E., Jacqmard, A., Engler, G., and Inze, D. (2002). Control of proliferation, endoreduplication and differentiation by the Arabidopsis E2Fa-DPa transcription factor. EMBO J **21,** 1360-1368.

Deal, R.B., and Henikoff, S. (2010). A simple method for gene expression and chromatin profiling of individual cell types within a tissue. Dev Cell **18,** 1030-1040.

del Pozo, J.C., Diaz-Trivino, S., Cisneros, N., and Gutierrez, C. (2006). The balance between cell division and endoreplication depends on E2FC-DPB, transcription factors regulated by the ubiquitin-SCFSKP2A pathway in Arabidopsis. Plant Cell **18,** 2224-2235.

Desvoyes, B., Fernandez-Marcos, M., Sequeira-Mendes, J., Otero, S., Vergara, Z., and Gutierrez, C. (2014). Looking at plant cell cycle from the chromatin window. Front Plant Sci **5,** 369.

Dietz, K.J., Vogel, M.O., and Viehhauser, A. (2010). AP2/EREBP transcription factors are part of gene regulatory networks and integrate metabolic, hormonal and environmental signals in stress acclimation and retrograde signalling. Protoplasma **245,** 3-14.

Doerner, P. (1995). Arabidopsis embryogenesis. Radicle development(s). Curr Biol **5,** 110-112.

Dow, G.J., and Bergmann, D.C. (2014). Patterning and processes: how stomatal development defines physiological potential. Curr Opin Plant Biol **21,** 67-74.

Drane, P., Ouararhni, K., Depaux, A., Shuaib, M., and Hamiche, A. (2010). The death-associated protein DAXX is a novel histone chaperone involved in the replication-independent deposition of H3.3. Genes Dev **24,** 1253-1265.

Drews, G.N., and Koltunow, A.M. (2011). The female gametophyte. Arabidopsis Book **9,** e0155.

Du, J., Zhong, X., Bernatavichute, Y.V., Stroud, H., Feng, S., Caro, E., Vashisht, A.A., Terragni, J., Chin, H.G., Tu, A., Hetzel, J., Wohlschlegel, J.A., Pradhan, S., Patel, D.J., and Jacobsen, S.E. (2012). Dual binding of chromomethylase domains to H3K9me2-containing nucleosomes directs DNA methylation in plants. Cell **151,** 167-180.

Dunleavy, E.M., Almouzni, G., and Karpen, G.H. (2011). H3.3 is deposited at centromeres in S phase as a placeholder for newly assembled CENP-A in G(1) phase. Nucleus **2,** 146-157.

Eaton, M.L., Galani, K., Kang, S., Bell, S.P., and MacAlpine, D.M. (2010). Conserved nucleosome positioning defines replication origins. Genes Dev **24,** 748-753.

Edgar, B.A., Zielke, N., and Gutierrez, C. (2014). Endocycles: a recurrent evolutionary innovation for post-mitotic cell growth. Nat Rev Mol Cell Biol **15,** 197-210.

Exner, V., Taranto, P., Schonrock, N., Gruissem, W., and Hennig, L. (2006). Chromatin assembly factor CAF-1 is required for cellular differentiation during plant development. Development **133,** 4163-4172.

Feng, S., and Jacobsen, S.E. (2011). Epigenetic modifications in plants: an evolutionary perspective. Curr Opin Plant Biol **14,** 179-186.

Feng, S., Jacobsen, S.E., and Reik, W. (2010). Epigenetic reprogramming in plant and animal development. Science **330,** 622-627.

Filipescu, D., Szenker, E., and Almouzni, G. (2013). Developmental roles of histone H3 variants and their chaperones. Trends Genet **29,** 630-640.

Flemming, W. (1882). Zellsubstanz, Kern und Zelltheilung F. C. W. Vogel.

Forzani, C., Aichinger, E., Sornay, E., Willemsen, V., Laux, T., Dewitte, W., and Murray, J.A. (2014). WOX5 suppresses CYCLIN D activity to establish quiescence at the center of the root stem cell niche. Curr Biol **24,** 1939-1944.

Franco-Zorrilla, J.M., Lopez-Vidriero, I., Carrasco, J.L., Godoy, M., Vera, P., and Solano, R. (2014). DNA-binding specificities of plant transcription factors and their potential to define target genes. Proc Natl Acad Sci U S A **111,** 2367-2372.

Furuta, K.M., Hellmann, E., and Helariutta, Y. (2014a). Molecular control of cell specification and cell differentiation during procambial development. Annu Rev Plant Biol **65,** 607-638.

Furuta, K.M., Yadav, S.R., Lehesranta, S., Belevich, I., Miyashima, S., Heo, J.O., Vaten, A., Lindgren, O., De Rybel, B., Van Isterdael, G., Somervuo, P., Lichtenberger, R., Rocha, R., Thitamadee, S., Tahtiharju, S., Auvinen, P., Beeckman, T., Jokitalo, E., and Helariutta, Y. (2014b). Plant development. Arabidopsis NAC45/86 direct sieve element morphogenesis culminating in enucleation. Science **345,** 933-937.

Galinha, C., Hofhuis, H., Luijten, M., Willemsen, V., Blilou, I., Heidstra, R., and Scheres, B. (2007). PLETHORA proteins as dose-dependent master regulators of Arabidopsis root development. Nature **449,** 1053-1057.

Geldner, N., and Salt, D.E. (2014). Focus on roots. Plant Physiol **166,** 453-454.

Gendreau, E., Traas, J., Desnos, T., Grandjean, O., Caboche, M., and Hofte, H. (1997). Cellular basis of hypocotyl growth in Arabidopsis thaliana. Plant Physiol **114,** 295-305.

Goldberg, A.D., Banaszynski, L.A., Noh, K.M., Lewis, P.W., Elsaesser, S.J., Stadler, S., Dewell, S., Law, M., Guo, X., Li, X., Wen, D., Chapgier, A., DeKelver, R.C., Miller, J.C., Lee, Y.L., Boydston, E.A., Holmes, M.C., Gregory, P.D., Greally, J.M., Rafii, S., Yang, C., Scambler, P.J., Garrick, D., Gibbons, R.J., Higgs, D.R., Cristea, I.M., Urnov, F.D., Zheng, D., and Allis, C.D. (2010). Distinct factors control histone variant H3.3 localization at specific genomic regions. Cell **140,** 678-691.

Gornik, S.G., Ford, K.L., Mulhern, T.D., Bacic, A., McFadden, G.I., and Waller, R.F. (2012). Loss of nucleosomal DNA condensation coincides with appearance of a novel nuclear protein in dinoflagellates. Curr Biol **22,** 2303-2312.

Groth, A., Ray-Gallet, D., Quivy, J.P., Lukas, J., Bartek, J., and Almouzni, G. (2005). Human Asf1 regulates the flow of S phase histones during replicational stress. Mol Cell **17,** 301-311.

Groth, A., Corpet, A., Cook, A.J., Roche, D., Bartek, J., Lukas, J., and Almouzni, G. (2007). Regulation of replication fork progression through histone supply and demand. Science **318,** 1928-1931.

Guitton, A.E., Page, D.R., Chambrier, P., Lionnet, C., Faure, J.E., Grossniklaus, U., and Berger, F. (2004). Identification of new members of Fertilisation Independent Seed Polycomb Group pathway involved in the control of seed development in Arabidopsis thaliana. Development **131,** 2971-2981.

Gurard-Levin, Z.A., and Almouzni, G. (2014). Histone modifications and a choice of variant: a language that helps the genome express itself. F1000Prime Rep **6,** 76.

Gutierrez, C. (2009). The Arabidopsis cell division cycle. Arabidopsis Book **7,** e0120.

Ha, C.M., Jun, J.H., and Fletcher, J.C. (2010). Control of Arabidopsis leaf morphogenesis through regulation of the YABBY and KNOX families of transcription factors. Genetics **186,** 197-206.

Hake, S.B., and Allis, C.D. (2006). Histone H3 variants and their potential role in indexing mammalian genomes: the "H3 barcode hypothesis". Proc Natl Acad Sci U S A **103,** 6428-6435.

Hake, S.B., Garcia, B.A., Kauer, M., Baker, S.P., Shabanowitz, J., Hunt, D.F., and Allis, C.D. (2005). Serine 31 phosphorylation of histone variant H3.3 is specific to regions bordering centromeres in metaphase chromosomes. Proc Natl Acad Sci U S A **102,** 6344-6349.

Hake, S.B., Garcia, B.A., Duncan, E.M., Kauer, M., Dellaire, G., Shabanowitz, J., Bazett-Jones, D.P., Allis, C.D., and Hunt, D.F. (2006). Expression patterns and post-translational modifications associated with mammalian histone H3 variants. J Biol Chem **281,** 559-568.

Hayashi, K., Hasegawa, J., and Matsunaga, S. (2013). The boundary of the meristematic and elongation zones in roots: endoreduplication precedes rapid cell expansion. Sci Rep **3,** 2723.

Heidstra, R., Welch, D., and Scheres, B. (2004). Mosaic analyses using marked activation and deletion clones dissect Arabidopsis SCARECROW action in asymmetric cell division. Genes Dev **18,** 1964-1969.

Helariutta, Y., Fukaki, H., Wysocka-Diller, J., Nakajima, K., Jung, J., Sena, G., Hauser, M.T., and Benfey, P.N. (2000). The SHORT-ROOT gene controls radial patterning of the Arabidopsis root through radial signaling. Cell **101,** 555-567.

Henikoff, S., Henikoff, J.G., Sakai, A., Loeb, G.B., and Ahmad, K. (2009). Genome-wide profiling of salt fractions maps physical properties of chromatin. Genome Res **19,** 460-469.

Hennig, L., and Derkacheva, M. (2009). Diversity of Polycomb group complexes in plants: same rules, different players? Trends Genet **25,** 414-423.

Hennig, L., Taranto, P., Walser, M., Schonrock, N., and Gruissem, W. (2003). Arabidopsis MSI1 is required for epigenetic maintenance of reproductive development. Development **130,** 2555-2565.

Heyman, J., Cools, T., Vandenbussche, F., Heyndrickx, K.S., Van Leene, J., Vercauteren, I., Vanderauwera, S., Vandepoele, K., De Jaeger, G., Van Der Straeten, D., and De Veylder, L. (2013). ERF115 controls root quiescent center cell division and stem cell replenishment. Science **342,** 860-863.

Horstman, A., Willemsen, V., Boutilier, K., and Heidstra, R. (2014). AINTEGUMENTA-LIKE proteins: hubs in a plethora of networks. Trends Plant Sci **19,** 146-157.

Houben, A., Demidov, D., Caperta, A.D., Karimi, R., Agueci, F., and Vlasenko, L. (2007). Phosphorylation of histone H3 in plants--a dynamic affair. Biochim Biophys Acta **1769,** 308-315.

Houlard, M., Berlivet, S., Probst, A.V., Quivy, J.P., Hery, P., Almouzni, G., and Gerard, M. (2006). CAF-1 is essential for heterochromatin organization in pluripotent embryonic cells. PLoS Genet **2,** e181.

Huijser, P., and Schmid, M. (2011). The control of developmental phase transitions in plants. Development **138,** 4117-4129.

Ingouff, M., and Berger, F. (2010). Histone3 variants in plants. Chromosoma **119,** 27-33.

Ingouff, M., Hamamura, Y., Gourgues, M., Higashiyama, T., and Berger, F. (2007). Distinct dynamics of HISTONE3 variants between the two fertilization products in plants. Curr Biol **17,** 1032-1037.

Ingouff, M., Rademacher, S., Holec, S., Soljic, L., Xin, N., Readshaw, A., Foo, S.H., Lahouze, B., Sprunck, S., and Berger, F. (2010). Zygotic resetting of the HISTONE 3 variant repertoire participates in epigenetic reprogramming in Arabidopsis. Curr Biol **20,** 2137-2143.

Ivanov, V.B., and Dubrovsky, J.G. (2013). Longitudinal zonation pattern in plant roots: conflicts and solutions. Trends Plant Sci **18,** 237-243.

Jacob, Y., Feng, S., LeBlanc, C.A., Bernatavichute, Y.V., Stroud, H., Cokus, S., Johnson, L.M., Pellegrini, M., Jacobsen, S.E., and Michaels, S.D. (2009). ATXR5 and ATXR6 are H3K27 monomethyltransferases required for chromatin structure and gene silencing. Nat Struct Mol Biol **16,** 763-768.

Jacob, Y., Stroud, H., Leblanc, C., Feng, S., Zhuo, L., Caro, E., Hassel, C., Gutierrez, C., Michaels, S.D., and Jacobsen, S.E. (2010). Regulation of heterochromatic DNA replication by histone H3 lysine 27 methyltransferases. Nature **466,** 987-991.

Jacob, Y., Bergamin, E., Donoghue, M.T., Mongeon, V., LeBlanc, C., Voigt, P., Underwood, C.J., Brunzelle, J.S., Michaels, S.D., Reinberg, D., Couture, J.F., and Martienssen, R.A. (2014). Selective methylation of histone H3 variant H3.1 regulates heterochromatin replication. Science **343,** 1249-1253.

Jarillo, J.A., and Pineiro, M. (2011). Timing is everything in plant development. The central role of floral repressors. Plant Sci **181,** 364-378.

Jenik, P.D., Jurkuta, R.E., and Barton, M.K. (2005). Interactions between the cell cycle and embryonic patterning in Arabidopsis uncovered by a mutation in DNA polymerase epsilon. Plant Cell **17,** 3362-3377.

Jin, C., Zang, C., Wei, G., Cui, K., Peng, W., Zhao, K., and Felsenfeld, G. (2009). H3.3/H2A.Z double variant-containing nucleosomes mark 'nucleosome-free regions' of active promoters and other regulatory regions. Nat Genet **41,** 941-945.

Johnson, L., Mollah, S., Garcia, B.A., Muratore, T.L., Shabanowitz, J., Hunt, D.F., and Jacobsen, S.E. (2004). Mass spectrometry analysis of Arabidopsis histone H3 reveals distinct combinations of post-translational modifications. Nucleic Acids Res **32,** 6511-6518.

Josse, E.M., and Halliday, K.J. (2008). Skotomorphogenesis: the dark side of light signalling. Curr Biol **18,** R1144-1146.

Kaplan, N., Moore, I.K., Fondufe-Mittendorf, Y., Gossett, A.J., Tillo, D., Field, Y., LeProust, E.M., Hughes, T.R., Lieb, J.D., Widom, J., and Segal, E. (2009). The DNA-encoded nucleosome organization of a eukaryotic genome. Nature **458,** 362-366.

Kawashima, T., and Berger, F. (2014). Epigenetic reprogramming in plant sexual reproduction. Nat Rev Genet **15,** 613-624.

Kaya, H., Shibahara, K.I., Taoka, K.I., Iwabuchi, M., Stillman, B., and Araki, T. (2001). FASCIATA genes for chromatin assembly factor-1 in arabidopsis maintain the cellular organization of apical meristems. Cell **104,** 131-142.

Kohler, C., Hennig, L., Bouveret, R., Gheyselinck, J., Grossniklaus, U., and Gruissem, W. (2003). Arabidopsis MSI1 is a component of the MEA/FIE Polycomb group complex and required for seed development. EMBO J **22,** 4804-4814.

Kotogany, E., Dudits, D., Horvath, G.V., and Ayaydin, F. (2010). A rapid and robust assay for detection of S-phase cell cycle progression in plant cells and tissues by using ethynyl deoxyuridine. Plant Methods **6,** 5.

Kuzmichev, A., Nishioka, K., Erdjument-Bromage, H., Tempst, P., and Reinberg, D. (2002). Histone methyltransferase activity associated with a human multiprotein complex containing the Enhancer of Zeste protein. Genes Dev **16,** 2893-2905.

Lafos, M., Kroll, P., Hohenstatt, M.L., Thorpe, F.L., Clarenz, O., and Schubert, D. (2011). Dynamic regulation of H3K27 trimethylation during Arabidopsis differentiation. PLoS Genet **7,** e1002040.

Lario, L.D., Ramirez-Parra, E., Gutierrez, C., Spampinato, C.P., and Casati, P. (2013). ANTI-SILENCING FUNCTION1 proteins are involved in ultraviolet-induced DNA damage repair and are cell cycle regulated by E2F transcription factors in Arabidopsis. Plant Physiol **162,** 1164-1177.

Lermontova, I., Schubert, V., Fuchs, J., Klatte, S., Macas, J., and Schubert, I. (2006). Loading of Arabidopsis centromeric histone CENH3 occurs mainly during G2 and requires the presence of the histone fold domain. Plant Cell **18,** 2443-2451.

Levesque, M.P., Vernoux, T., Busch, W., Cui, H., Wang, J.Y., Blilou, I., Hassan, H., Nakajima, K., Matsumoto, N., Lohmann, J.U., Scheres, B., and Benfey, P.N. (2006). Whole-genome analysis of the SHORT-ROOT developmental pathway in Arabidopsis. PLoS Biol **4,** e143.

Lewis, P.W., Elsaesser, S.J., Noh, K.M., Stadler, S.C., and Allis, C.D. (2010). Daxx is an H3.3-specific histone chaperone and cooperates with ATRX in replication-independent chromatin assembly at telomeres. Proc Natl Acad Sci U S A **107,** 14075-14080.

Leyser, H.M.O., Furner, I. J. (1992). Characterisation of three shoot apical meristem mutants of Arabidopsis thaliana. Development **116,** 397-403.

Li, L., and Clevers, H. (2010). Coexistence of quiescent and active adult stem cells in mammals. Science **327,** 542-545.

Lin, C.J., Koh, F.M., Wong, P., Conti, M., and Ramalho-Santos, M. (2014). Hira-mediated H3.3 incorporation is required for DNA replication and ribosomal RNA transcription in the mouse zygote. Dev Cell **30,** 268-279.

Lombrana, R., Almeida, R., Revuelta, I., Madeira, S., Herranz, G., Saiz, N., Bastolla, U., and Gomez, M. (2013). High-resolution analysis of DNA synthesis start sites and nucleosome architecture at efficient mammalian replication origins. EMBO J **32,** 2631-2644.

Loppin, B., Bonnefoy, E., Anselme, C., Laurencon, A., Karr, T.L., and Couble, P. (2005). The histone H3.3 chaperone HIRA is essential for chromatin assembly in the male pronucleus. Nature **437,** 1386-1390.

Loyola, A., and Almouzni, G. (2004). Histone chaperones, a supporting role in the limelight. Biochim Biophys Acta **1677,** 3-11.

MacAlpine, H.K., Gordan, R., Powell, S.K., Hartemink, A.J., and MacAlpine, D.M. (2010). Drosophila ORC localizes to open chromatin and marks sites of cohesin complex loading. Genome Res **20,** 201-211.

Mahonen, A.P., Bishopp, A., Higuchi, M., Nieminen, K.M., Kinoshita, K., Tormakangas, K., Ikeda, Y., Oka, A., Kakimoto, T., and Helariutta, Y. (2006). Cytokinin signaling and its inhibitor AHP6 regulate cell fate during vascular development. Science **311,** 94-98.

Mahonen, A.P., ten Tusscher, K., Siligato, R., Smetana, O., Diaz-Trivino, S., Salojarvi, J., Wachsman, G., Prasad, K., Heidstra, R., and Scheres, B. (2014). PLETHORA gradient formation mechanism separates auxin responses. Nature **515,** 125-129.

Malik, H.S., and Henikoff, S. (2003). Phylogenomics of the nucleosome. Nat Struct Biol **10,** 882-891.

March-Diaz, R., and Reyes, J.C. (2009). The beauty of being a variant: H2A.Z and the SWR1 complex in plants. Mol Plant **2,** 565-577.

Martinez-Salas, E., Linney, E., Hassell, J., and DePamphilis, M.L. (1989). The need for enhancers in gene expression first appears during mouse development with formation of the zygotic nucleus. Genes Dev **3,** 1493-1506.

Mathelier, A., Zhao, X., Zhang, A.W., Parcy, F., Worsley-Hunt, R., Arenillas, D.J., Buchman, S., Chen, C.Y., Chou, A., Ienasescu, H., Lim, J., Shyr, C., Tan, G., Zhou, M., Lenhard, B., Sandelin, A., and Wasserman, W.W. (2014). JASPAR 2014: an extensively expanded and updated open-access database of transcription factor binding profiles. Nucleic Acids Res **42,** D142-147.

Maze, I., Noh, K.M., Soshnev, A.A., and Allis, C.D. (2014). Every amino acid matters: essential contributions of histone variants to mammalian development and disease. Nat Rev Genet **15,** 259-271.

McCormick, S. (2004). Control of male gametophyte development. Plant Cell **16,** 142-153.

Melaragno, J.E., Mehrotra, B., and Coleman, A.W. (1993). Relationship between Endopolyploidy and Cell Size in Epidermal Tissue of Arabidopsis. Plant Cell **5,** 1661-1668.

Michaelson, J.S., Bader, D., Kuo, F., Kozak, C., and Leder, P. (1999). Loss of Daxx, a promiscuously interacting protein, results in extensive apoptosis in early mouse development. Genes Dev **13,** 1918-1923.

Mito, Y., Henikoff, J.G., and Henikoff, S. (2005). Genome-scale profiling of histone H3.3 replacement patterns. Nat Genet **37,** 1090-1097.

Mito, Y., Henikoff, J.G., and Henikoff, S. (2007). Histone replacement marks the boundaries of cis-regulatory domains. Science **315,** 1408-1411.

Miyashima, S., Koi, S., Hashimoto, T., and Nakajima, K. (2011). Non-cell-autonomous microRNA165 acts in a dose-dependent manner to regulate multiple differentiation status in the Arabidopsis root. Development **138,** 2303-2313.

Mozgova, I., Mokros, P., and Fajkus, J. (2010). Dysfunction of chromatin assembly factor 1 induces shortening of telomeres and loss of 45S rDNA in Arabidopsis thaliana. Plant Cell **22,** 2768-2780.

Nakagawa, T., Kurose, T., Hino, T., Tanaka, K., Kawamukai, M., Niwa, Y., Toyooka, K., Matsuoka, K., Jinbo, T., and Kimura, T. (2007a). Development of series of gateway binary vectors, pGWBs, for realizing efficient construction of fusion genes for plant transformation. J Biosci Bioeng **104,** 34-41.

Nakagawa, T., Suzuki, T., Murata, S., Nakamura, S., Hino, T., Maeo, K., Tabata, R., Kawai, T., Tanaka, K., Niwa, Y., Watanabe, Y., Nakamura, K., Kimura, T., and Ishiguro, S. (2007b). Improved Gateway binary vectors: high-performance vectors for creation of fusion constructs in transgenic analysis of plants. Biosci Biotechnol Biochem **71,** 2095-2100.

Nakajima, K., Sena, G., Nawy, T., and Benfey, P.N. (2001). Intercellular movement of the putative transcription factor SHR in root patterning. Nature **413,** 307-311.

Ng, R.K., and Gurdon, J.B. (2008). Epigenetic memory of an active gene state depends on histone H3.3 incorporation into chromatin in the absence of transcription. Nat Cell Biol **10,** 102-109.

Nie, X., Wang, H., Li, J., Holec, S., and Berger, F. (2014). The HIRA complex that deposits the histone H3.3 is conserved in Arabidopsis and facilitates transcriptional dynamics. Biol Open **3,** 794-802.

Okada, T., Endo, M., Singh, M.B., and Bhalla, P.L. (2005). Analysis of the histone H3 gene family in Arabidopsis and identification of the male-gamete-specific variant AtMGH3. Plant J **44,** 557-568.

Ono, T., Kaya, H., Takeda, S., Abe, M., Ogawa, Y., Kato, M., Kakutani, T., Mittelsten Scheid, O., Araki, T., and Shibahara, K. (2006). Chromatin assembly factor 1 ensures the stable maintenance of silent chromatin states in Arabidopsis. Genes Cells **11,** 153-162.

Ooi, S.L., Henikoff, J.G., and Henikoff, S. (2010). A native chromatin purification system for epigenomic profiling in Caenorhabditis elegans. Nucleic Acids Res **38,** e26.

Otero, S., Desvoyes, B., and Gutierrez, C. (2014). Histone H3 dynamics in plant cell cycle and development. Cytogenet Genome Res **143,** 114-124.

Pendle, A.F., Clark, G.P., Boon, R., Lewandowska, D., Lam, Y.W., Andersen, J., Mann, M., Lamond, A.I., Brown, J.W., and Shaw, P.J. (2005). Proteomic analysis of the Arabidopsis nucleolus suggests novel nucleolar functions. Mol Biol Cell **16,** 260-269.

Perianez-Rodriguez, J., Manzano, C., and Moreno-Risueno, M.A. (2014). Post-embryonic organogenesis and plant regeneration from tissues: two sides of the same coin? Front Plant Sci **5,** 219.

Petricka, J.J., Winter, C.M., and Benfey, P.N. (2012). Control of Arabidopsis root development. Annu Rev Plant Biol **63,** 563-590.

Polyn, S., Willems, A., and De Veylder, L. (2014). Cell cycle entry, maintenance, and exit during plant development. Curr Opin Plant Biol **23C,** 1-7.

Probst, A.V., Dunleavy, E., and Almouzni, G. (2009). Epigenetic inheritance during the cell cycle. Nat Rev Mol Cell Biol **10,** 192-206.

Quivy, J.P., Grandi, P., and Almouzni, G. (2001). Dimerization of the largest subunit of chromatin assembly factor 1: importance in vitro and during Xenopus early development. EMBO J **20,** 2015-2027.

Ramirez-Parra, E., and Gutierrez, C. (2007). E2F regulates FASCIATA1, a chromatin assembly gene whose loss switches on the endocycle and activates gene expression by changing the epigenetic status. Plant Physiol **144,** 105-120.

Ramirez-Parra, E., Lopez-Matas, M.A., Frundt, C., and Gutierrez, C. (2004). Role of an atypical E2F transcription factor in the control of Arabidopsis cell growth and differentiation. Plant Cell **16,** 2350-2363.

Ray-Gallet, D., Woolfe, A., Vassias, I., Pellentz, C., Lacoste, N., Puri, A., Schultz, D.C., Pchelintsev, N.A., Adams, P.D., Jansen, L.E., and Almouzni, G. (2011). Dynamics of histone H3 deposition in vivo reveal a nucleosome gap-filling mechanism for H3.3 to maintain chromatin integrity. Mol Cell **44,** 928-941.

Reinholz, E. (1966). Radiation induced mutants showing change inflorescence characteristics. Arab. Inf. Serv. **3,** 19-20.

Riechmann, J.L., and Meyerowitz, E.M. (1998). The AP2/EREBP family of plant transcription factors. Biol Chem **379,** 633-646.

Roberts, C., Sutherland, H.F., Farmer, H., Kimber, W., Halford, S., Carey, A., Brickman, J.M., Wynshaw-Boris, A., and Scambler, P.J. (2002). Targeted mutagenesis of the Hira gene results in gastrulation defects and patterning abnormalities of mesoendodermal derivatives prior to early embryonic lethality. Mol Cell Biol **22,** 2318-2328.

Roeder, A.H., Chickarmane, V., Cunha, A., Obara, B., Manjunath, B.S., and Meyerowitz, E.M. (2010). Variability in the control of cell division underlies sepal epidermal patterning in Arabidopsis thaliana. PLoS Biol **8,** e1000367.

Roppolo, D., De Rybel, B., Denervaud Tendon, V., Pfister, A., Alassimone, J., Vermeer, J.E., Yamazaki, M., Stierhof, Y.D., Beeckman, T., and Geldner, N. (2011). A novel protein family mediates Casparian strip formation in the endodermis. Nature **473,** 380-383.

Rosa, S., Ntoukakis, V., Ohmido, N., Pendle, A., Abranches, R., and Shaw, P. (2014). Cell differentiation and development in Arabidopsis are associated with changes in histone dynamics at the single-cell level. Plant Cell **26,** 4821-4833.

Roudier, F., Ahmed, I., Berard, C., Sarazin, A., Mary-Huard, T., Cortijo, S., Bouyer, D., Caillieux, E., Duvernois-Berthet, E., Al-Shikhley, L., Giraut, L., Despres, B., Drevensek, S., Barneche, F., Derozier, S., Brunaud, V., Aubourg, S., Schnittger, A., Bowler, C., Martin-Magniette, M.L., Robin, S., Caboche, M., and Colot, V. (2011). Integrative epigenomic mapping defines four main chromatin states in Arabidopsis. EMBO J **30,** 1928-1938.

Sabatini, S., Heidstra, R., Wildwater, M., and Scheres, B. (2003). SCARECROW is involved in positioning the stem cell niche in the Arabidopsis root meristem. Genes Dev **17,** 354-358.

Sakai, A., Schwartz, B.E., Goldstein, S., and Ahmad, K. (2009). Transcriptional and developmental functions of the H3.3 histone variant in Drosophila. Curr Biol **19,** 1816-1820.

Sanematsu, F., Takami, Y., Barman, H.K., Fukagawa, T., Ono, T., Shibahara, K., and Nakayama, T. (2006). Asf1 is required for viability and chromatin assembly during DNA replication in vertebrate cells. J Biol Chem **281,** 13817-13827.

Sarkar, A.K., Luijten, M., Miyashima, S., Lenhard, M., Hashimoto, T., Nakajima, K., Scheres, B., Heidstra, R., and Laux, T. (2007). Conserved factors regulate signalling in Arabidopsis thaliana shoot and root stem cell organizers. Nature **446,** 811-814.

Sawatsubashi, S., Murata, T., Lim, J., Fujiki, R., Ito, S., Suzuki, E., Tanabe, M., Zhao, Y., Kimura, S., Fujiyama, S., Ueda, T., Umetsu, D., Ito, T., Takeyama, K., and Kato, S. (2010). A histone chaperone, DEK, transcriptionally coactivates a nuclear receptor. Genes Dev **24,** 159-170.

Schenk, R., Jenke, A., Zilbauer, M., Wirth, S., and Postberg, J. (2011). H3.5 is a novel hominid-specific histone H3 variant that is specifically expressed in the seminiferous tubules of human testes. Chromosoma **120,** 275-285.

Scheres, B., Benfey, P., and Dolan, L. (2002). Root development. Arabidopsis Book **1,** e0101.

Scheres, B.W., H.; Willemsen, M.; Terlou, W.; Lawson, E.; Dean, C.; Weisbeek, P. (1994). Embryonic origin of the Arabidopsis primary root and root meristem initials. Development **120,** 2475-2487.

Schoft, V.K., Chumak, N., Choi, Y., Hannon, M., Garcia-Aguilar, M., Machlicova, A., Slusarz, L., Mosiolek, M., Park, J.S., Park, G.T., Fischer, R.L., and Tamaru, H. (2011). Function of the DEMETER DNA glycosylase in the Arabidopsis thaliana male gametophyte. Proc Natl Acad Sci U S A **108,** 8042-8047.

Schonrock, N., Exner, V., Probst, A., Gruissem, W., and Hennig, L. (2006). Functional genomic analysis of CAF-1 mutants in Arabidopsis thaliana. J Biol Chem **281,** 9560-9568.

Sequeira-Mendes, J., Araguez, I., Peiro, R., Mendez-Giraldez, R., Zhang, X., Jacobsen, S.E., Bastolla, U., and Gutierrez, C. (2014). The Functional Topography of the Arabidopsis Genome Is Organized in a Reduced Number of Linear Motifs of Chromatin States. Plant Cell **26,** 2351-2366.

Sherwood, P.W., Tsang, S.V., and Osley, M.A. (1993). Characterization of HIR1 and HIR2, two genes required for regulation of histone gene transcription in Saccharomyces cerevisiae. Mol Cell Biol **13,** 28-38.

Shi, L., Wang, J., Hong, F., Spector, D.L., and Fang, Y. (2011). Four amino acids guide the assembly or disassembly of Arabidopsis histone H3.3-containing nucleosomes. Proc Natl Acad Sci U S A **108,** 10574-10578.

Shibahara, K., and Stillman, B. (1999). Replication-dependent marking of DNA by PCNA facilitates CAF-1-coupled inheritance of chromatin. Cell **96,** 575-585.

Shu, H., Nakamura, M., Siretskiy, A., Borghi, L., Moraes, I., Wildhaber, T., Gruissem, W., and Hennig, L. (2014). Arabidopsis replacement histone variant H3.3 occupies promoters of regulated genes. Genome Biol **15,** R62.

Sillje, H.H., and Nigg, E.A. (2001). Identification of human Asf1 chromatin assembly factors as substrates of Tousled-like kinases. Curr Biol **11,** 1068-1073.

Skirycz, A., Radziejwoski, A., Busch, W., Hannah, M.A., Czeszejko, J., Kwasniewski, M., Zanor, M.I., Lohmann, J.U., De Veylder, L., Witt, I., and Mueller-Roeber, B. (2008). The DOF transcription factor OBP1 is involved in cell cycle regulation in Arabidopsis thaliana. Plant J **56,** 779-792.

Slotkin, R.K., Vaughn, M., Borges, F., Tanurdzic, M., Becker, J.D., Feijo, J.A., and Martienssen, R.A. (2009). Epigenetic reprogramming and small RNA silencing of transposable elements in pollen. Cell **136,** 461-472.

Sozzani, R., Cui, H., Moreno-Risueno, M.A., Busch, W., Van Norman, J.M., Vernoux, T., Brady, S.M., Dewitte, W., Murray, J.A., and Benfey, P.N. (2010). Spatiotemporal regulation of cell-cycle genes by SHORTROOT links patterning and growth. Nature **466,** 128-132.

Spencer, M.W., Casson, S.A., and Lindsey, K. (2007). Transcriptional profiling of the Arabidopsis embryo. Plant Physiol **143,** 924-940.

Stedman E., S., E. (1947). The chemical nature and functions of the components of the cell nuclei. Cold Spring Harb Symp Quant Biol **12,** 224-236.

Stroud, H., Greenberg, M.V., Feng, S., Bernatavichute, Y.V., and Jacobsen, S.E. (2013). Comprehensive analysis of silencing mutants reveals complex regulation of the Arabidopsis methylome. Cell **152,** 352-364.

Stroud, H., Otero, S., Desvoyes, B., Ramirez-Parra, E., Jacobsen, S.E., and Gutierrez, C. (2012). Genome-wide analysis of histone H3.1 and H3.3 variants in Arabidopsis thaliana. Proc Natl Acad Sci U S A **109,** 5370-5375.

Sugimoto-Shirasu, K., and Roberts, K. (2003). "Big it up": endoreduplication and cell-size control in plants. Curr Opin Plant Biol **6,** 544-553.

Szenker, E., Lacoste, N., and Almouzni, G. (2012). A developmental requirement for HIRA-dependent H3.3 deposition revealed at gastrulation in Xenopus. Cell Rep **1,** 730-740.

Tagami, H., Ray-Gallet, D., Almouzni, G., and Nakatani, Y. (2004). Histone H3.1 and H3.3 complexes mediate nucleosome assembly pathways dependent or independent of DNA synthesis. Cell **116,** 51-61.

Talbert, P.B., and Henikoff, S. (2014). Environmental responses mediated by histone variants. Trends Cell Biol **24,** 642-650.

Talbert, P.B., Ahmad, K., Almouzni, G., Ausio, J., Berger, F., Bhalla, P.L., Bonner, W.M., Cande, W.Z., Chadwick, B.P., Chan, S.W., Cross, G.A., Cui, L., Dimitrov, S.I., Doenecke, D., Eirin-Lopez, J.M., Gorovsky, M.A., Hake, S.B., Hamkalo, B.A., Holec, S., Jacobsen, S.E.,

Kamieniarz, K., Khochbin, S., Ladurner, A.G., Landsman, D., Latham, J.A., Loppin, B., Malik, H.S., Marzluff, W.F., Pehrson, J.R., Postberg, J., Schneider, R., Singh, M.B., Smith, M.M., Thompson, E., Torres-Padilla, M.E., Tremethick, D.J., Turner, B.M., Waterborg, J.H., Wollmann, H., Yelagandula, R., Zhu, B., and Henikoff, S. (2012). A unified phylogeny-based nomenclature for histone variants. Epigenetics Chromatin **5,** 7.

Tominaga-Wada, R., Ishida, T., and Wada, T. (2011). New insights into the mechanism of development of Arabidopsis root hairs and trichomes. Int Rev Cell Mol Biol **286,** 67-106.

Tran, V., Lim, C., Xie, J., and Chen, X. (2012). Asymmetric division of Drosophila male germline stem cell shows asymmetric histone distribution. Science **338,** 679-682.

Tsukagoshi, H., Busch, W., and Benfey, P.N. (2010). Transcriptional regulation of ROS controls transition from proliferation to differentiation in the root. Cell **143,** 606-616.

Turatsinze, J.V., Thomas-Chollier, M., Defrance, M., and van Helden, J. (2008). Using RSAT to scan genome sequences for transcription factor binding sites and cis-regulatory modules. Nat Protoc **3,** 1578-1588.

Tyler, J.K. (2002). Chromatin assembly. Cooperation between histone chaperones and ATP-dependent nucleosome remodeling machines. Eur. J. Biochem **269,** 2268-2274.

Tyler, J.K., Collins, K.A., Prasad-Sinha, J., Amiott, E., Bulger, M., Harte, P.J., Kobayashi, R., and Kadonaga, J.T. (2001). Interaction between the Drosophila CAF-1 and ASF1 chromatin assembly factors. Mol Cell Biol **21,** 6574-6584.

van den Berg, C., Willemsen, V., Hendriks, G., Weisbeek, P., and Scheres, B. (1997). Short-range control of cell differentiation in the Arabidopsis root meristem. Nature **390,** 287-289.

Vaquero-Sedas, M.I., and Vega-Palas, M.A. (2013). Differential association of Arabidopsis telomeres and centromeres with histone H3 variants. Sci Rep **3,** 1202.

Villar, C.B., and Kohler, C. (2010). Plant chromatin immunoprecipitation. Methods Mol Biol **655,** 401-411.

Waidmann, S., Kusenda, B., Mayerhofer, J., Mechtler, K., and Jonak, C. (2014). A DEK Domain-Containing Protein Modulates Chromatin Structure and Function in Arabidopsis. Plant Cell **26,** 4328-4344.

Weirauch, M.T., Yang, A., Albu, M., Cote, A.G., Montenegro-Montero, A., Drewe, P., Najafabadi, H.S., Lambert, S.A., Mann, I., Cook, K., Zheng, H., Goity, A., van Bakel, H., Lozano, J.C., Galli, M., Lewsey, M.G., Huang, E., Mukherjee, T., Chen, X., Reece-Hoyes, J.S., Govindarajan, S., Shaulsky, G., Walhout, A.J., Bouget, F.Y., Ratsch, G., Larrondo, L.F., Ecker, J.R., and Hughes, T.R. (2014). Determination and inference of eukaryotic transcription factor sequence specificity. Cell **158,** 1431-1443.

Wiedemann, S.M., Mildner, S.N., Bonisch, C., Israel, L., Maiser, A., Matheisl, S., Straub, T., Merkl, R., Leonhardt, H., Kremmer, E., Schermelleh, L., and Hake, S.B. (2010). Identification and characterization of two novel primate-specific histone H3 variants, H3.X and H3.Y. J Cell Biol **190,** 777-791.

Winkler, D.D., Zhou, H., Dar, M.A., Zhang, Z., and Luger, K. (2012). Yeast CAF-1 assembles histone (H3-H4)2 tetramers prior to DNA deposition. Nucleic Acids Res **40,** 10139-10149.

Winter, C.M., Austin, R.S., Blanvillain-Baufume, S., Reback, M.A., Monniaux, M., Wu, M.F., Sang, Y., Yamaguchi, A., Yamaguchi, N., Parker, J.E., Parcy, F., Jensen, S.T., Li, H., and Wagner, D. (2011). LEAFY target genes reveal floral regulatory logic, cis motifs, and a link to biotic stimulus response. Dev Cell **20,** 430-443.

Wirbelauer, C., Bell, O., and Schubeler, D. (2005). Variant histone H3.3 is deposited at sites of nucleosomal displacement throughout transcribed genes while active histone modifications show a promoter-proximal bias. Genes Dev **19,** 1761-1766.

Wise-Draper, T.M., Allen, H.V., Thobe, M.N., Jones, E.E., Habash, K.B., Munger, K., and Wells, S.I. (2005). The human DEK proto-oncogene is a senescence inhibitor and an upregulated target of high-risk human papillomavirus E7. J Virol **79,** 14309-14317.

Wollmann, H., Holec, S., Alden, K., Clarke, N.D., Jacques, P.E., and Berger, F. (2012). Dynamic deposition of histone variant H3.3 accompanies developmental remodeling of the Arabidopsis transcriptome. PLoS Genet **8,** e1002658.

Wolpert, L., Tickle, C.,. (2011). Principles of Development. Oxford University Press.

Zemach, A., McDaniel, I.E., Silva, P., and Zilberman, D. (2010). Genome-wide evolutionary analysis of eukaryotic DNA methylation. Science **328,** 916-919.

Zhang, X., Bernatavichute, Y.V., Cokus, S., Pellegrini, M., and Jacobsen, S.E. (2009). Genome-wide analysis of mono-, di- and trimethylation of histone H3 lysine 4 in Arabidopsis thaliana. Genome Biol **10,** R62.

Zhang, X., Clarenz, O., Cokus, S., Bernatavichute, Y.V., Pellegrini, M., Goodrich, J., and Jacobsen, S.E. (2007). Whole-genome analysis of histone H3 lysine 27 trimethylation in Arabidopsis. PLoS Biol **5,** e129.

Zhang, X., Yazaki, J., Sundaresan, A., Cokus, S., Chan, S.W., Chen, H., Henderson, I.R., Shinn, P., Pellegrini, M., Jacobsen, S.E., and Ecker, J.R. (2006). Genome-wide high-resolution mapping and functional analysis of DNA methylation in arabidopsis. Cell **126,** 1189-1201.

Zhu, Y., Weng, M., Yang, Y., Zhang, C., Li, Z., Shen, W.H., and Dong, A. (2011). Arabidopsis homologues of the histone chaperone ASF1 are crucial for chromatin replication and cell proliferation in plant development. Plant J **66,** 443-455.

Zilberman, D., Coleman-Derr, D., Ballinger, T., and Henikoff, S. (2008). Histone H2A.Z and DNA methylation are mutually antagonistic chromatin marks. Nature **456,** 125-129.

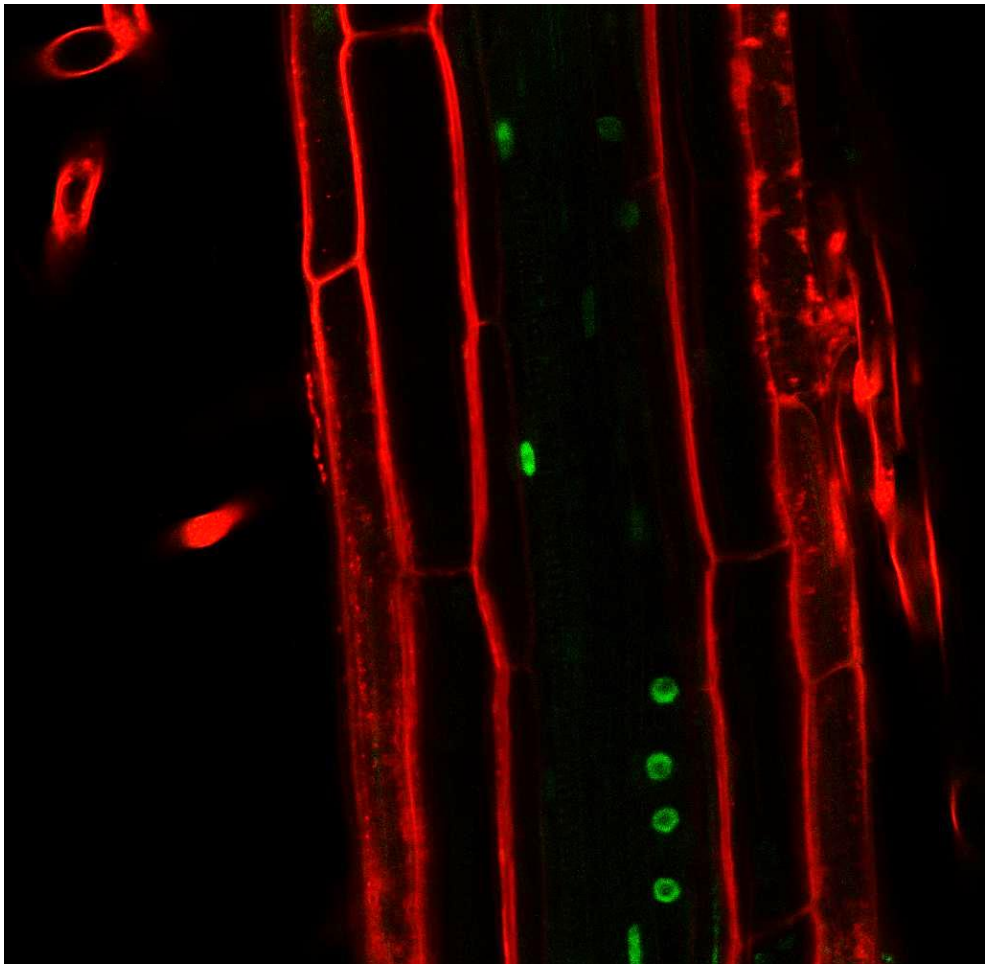

9. Supplementary Tables

9.1 Supplementary tables

9.1.1 Selected genes downregulated from slice 1 and 2 to slice 4, fold change fc > 1.5

Gene ID	Gene name
At4g02020	SWINGER
At5g13960	SUVH4
At4g30860	SDG4
At3g22680	RDM1
AT3G12280	RBR
AT1G77470	RFC3
AT1G63160	RFC2
AT4G02060	MCM7
AT2G01120	ORC4
AT2G37560	ORC2
AT4G29910	ORC5
AT5G58230	MSI1
AT2G16780	MSI2
AT3G25980	MAD2
AT2G16440	MCM4
AT5G49160	MET1
AT1G16970	KU70
AT5G48820	ICK6
AT2G31270	CDT1A
AT2G20000	HOBBIT
AT2G44950	HUB1
AT4G27230	HTA2
AT1G08460	HDA08
AT5G63110	HDA6
AT5G03740	HD2C
AT3G18520	HDA15
AT4G38130	HD1
AT3G15150	HPY2
AT2G45160	HAM1
AT1G54690	GAMMA-H2AX
AT5G13840	FZR3
AT2G40550	ETG1
AT3G01330	DEL3/E2FF
AT5G14620	DRM2
AT5G25480	DNMT2
AT5G16780	DOT2/MDF
AT1G18040	CDKD1;3
AT1G20930	CDKB2;2
AT1G76540	CDKB2;1
AT5G64960	CDKC2
AT3G50070	CYCD3;3
AT5G67260	CYCD3;2
AT1G16330	CYCB3;1
AT1G76310	CYCB2;4
AT4G35620	CYCB2;2
AT2G17620	CYCB2;1
AT1G34460	CYCB1;5
AT2G26760	CYCB1;4
AT3G11520	CYCB1;3
AT1G80370	CYCA2;4
AT1G44110	CYCA1;1
AT1G69770	CMT3
AT3G24340	CHR40
AT5G19310	CHR23
AT1G15660	CENP-C
AT3G01610	CDC48C
AT2G03670	CDC48B
AT1G66750	CAK4
AT5G09790	ATXR5
AT3G48150	APC8
AT1G78770	APC6
AT2G18290	APC10
AT3G33520	ARP6
AT5G43990	SUVR2
AT1G49620	ICK5
AT3G24810	ICK3
AT1G01370	HTR12
AT1G07790	HTB1
AT2G19520	MSI4
AT5G50930	HISTONE SUPERFAMILY
AT1G44780	HISTONE CHAPERONE DOMAIN
AT4G08310	HISTONE CHAPERONE DOMAIN
AT4G08590	VIM6
AT1G57820	VIM1
AT5G39550	VIM3

9.1.2 Selected genes downregulated from slice 2 and 3 to slice 4, fold change fc > 1.5

Gene ID	Gene name
AT5G39550	VIM3
AT4G28190	ULT1
AT5G04940	SUVH1
AT5G15920	SMC5
AT4G30860	SDG4
AT3G12280	RBR
AT5G54640	HTA1
AT2G24490	RPA2
AT1G63160	RFC2
AT4G02060	MCM7
AT2G01120	ORC4
AT2G37560	ORC2
AT1G26840	ORC6
AT4G29910	ORC5
AT5G58230	MSI1
AT4G35050	MSI3
AT5G49160	MET1
AT1G16970	KU70
AT2G31270	CDT1A
AT4G27230	HTA2
AT1G51060	HTA10
AT3G18520	HDA15
AT5G22880	HTB2
AT5G56740	HAG2
AT1G79840	GL2
AT1G54690	GAMMA H2AX
AT3G01330	DEL3/E2FF
AT5G16780	DOT2/MDF
AT5G64960	CDKC2
AT4G37630	CYCD5;1
AT5G43080	CYCA3;1
AT3G25100	CDC45
AT5G24330	ATXR6
AT2G18290	APC10
AT1G01370	HTR12
AT1G07790	HTB1
AT1G08880	HTA5
AT5G50930	HISTONE SUPERFAMILY
AT4G40030	HISTONE SUPERFAMILY
AT5G10400	HISTONE SUPERFAMILY
AT5G10390	HISTONE SUPERFAMILY
AT2G37470	HISTONE SUPERFAMILY
AT3G45930	HISTONE SUPERFAMILY
AT3G27360	HISTONE SUPERFAMILY

9.1.3 Primers used in this project

HTR cloning

Primers used to clone the different HTR genes fused to C-terminal tags under the control of their endogenous promoters:

Amplicon name	Oligo name	Sequence
HTR3	HTR3-GW-F	GGGGACAAGTTTGTACAAAAAAGCAGGCTGGATCCATCTCTTACTTTCCGTAG
	HTR3-GW-R	GGGGACCACTTTGTACAAGAAAGCTGGGTCAGCCCTCTCACCTCTAATCC
HTR4	HTR4-GW-F	GGGGACAAGTTTGTACAAAAAAGCAGGCTAGGAAGCTCCCTTTCCAGAG
	HTR4-GW-R	GGGGACCACTTTGTACAAGAAAGCTGGGTCAGCGCGTTCACCTCTGATAC
HTR5	HTR5-GW-F	GGGGACAAGTTTGTACAAAAAAGCAGGCTCATTTGAGCTCAAGAACGAAGTA
	HTR5-GW-R	GGGGACCACTTTGTACAAGAAAGCTGGGTCAGCACGTTCTCCTCTGATCCT
HTR13	HTR13-GW-F	GGGGACAAGTTTGTACAAAAAAGCAGGCTATTCGTTCTGTCGATCTCCAT
	HTR13-GW-R	GGGGACCACTTTGTACAAGAAAGCTGGGTCAGCTCTTTCTCCTCTGATTCTCC

Primer in linker region to check frame in all HTR genes cloned in pGWB vectors:

Name	Oligo name	Sequence
Frame	H3.3MycR1b	TTTGTACAAGAAAGCTGGGTCAG

qPCR

Primers used to monitor the endogenous expression of HTR genes in Col-0 plants:

Amplicon name	Oligo name	Sequence
Endogenous HTR3	H3.1 8F	TCAAACACGACAGTCTCAACAA
	H3.1 210R	CTACTGTTCCTGGACGGAATCT
Endogenous HTR4	H3.3 F3	CGCTTAAGCCAACCAAGAAT
	H3.3 R2	GAGTTAAAAAGAGTTCGCAACACAC
Endogenous HTR5	HTR5qPCRendoF	GCTTAATTGTGATTGGGAAG
	HTR5 qPCRendoR	CACCATTGTTTCCAAGTCTCC
Endogenous HTR13	HTR13-F-endo2	GCGAGGAGAATCAGAGGAGA
	HTR13-R-endo2	CGCAAATCAAAATCCAGAAA

Primers used to monitor the expression of tagged HTR genes in GFP-tagged lines:

Amplicon name	Oligo name	Sequence
HTR3-GFP	H3.1mycF1b	TAGTGCAGTCGCAGCTCTTC
	H3.3mycR1b	TTTGTACAAGAAAGCTGGGTCAG
HTR4-GFP	H3.3mycF2b	CGTGAGATTGCTCAAGATTTCA
	H3.3mycR1b	TTTGTACAAGAAAGCTGGGTCAG
HTR5-GFP	FredHTRGFP-F	ACAAGCAAAAGAACGGCATC
	FredHTRGFP-R	AAAGGGCAGATTGTGTGGAC
HTR13-GFP	FredHTRGFP-F	ACAAGCAAAAGAACGGCATC

	FredHTRGFP-R	AAAGGGCAGATTGTGTGGAC

Primers used to normalize qPCR data:

Amplicon name	Oligo name	Sequence
ACT2	DIR ACT2 para AB	CCGCTCTTTCTTTCCAAGC
	ACT2 R	CCGGTACCATTGTCACACAC

Mutant genotyping

Primers used to genotype fas1-4 mutants:

Amplicon name	Oligo name	Sequence
Wt plant	FAS1-4F1-genot	TAACATGGAGAAGCAAGGGG
	FAS1-4R1-genot	GATCCTTTTGCAGAGGACGA
fas1-4 mutant	FAS1-4R1-genot	GATCCTTTTGCAGAGGACGA
	FAS1-4LBF-genot	TTAAAAACGTCCGCAATGTG

Primers used in ChIP on sorted cells.

Amplicon name	Oligo name	Sequence
pACT2	pACT2-F1	CCGCTTTGAATTGTCTCGTT
	pACT2-R1	TGGAAAGAAAGAGCGGAAGA
pGRP	pGRP-F2	ATACACGTAGCGGCTCACAC
	pGRP-R2	CGTGTGTTAAGACTTGCCGATA
pPIN6	pPIN6-F2	GAGGTCCAGAAAAAGAAAGTGC
	pPIN6-R2	GAGACTTGTTGACGAGATTACCC

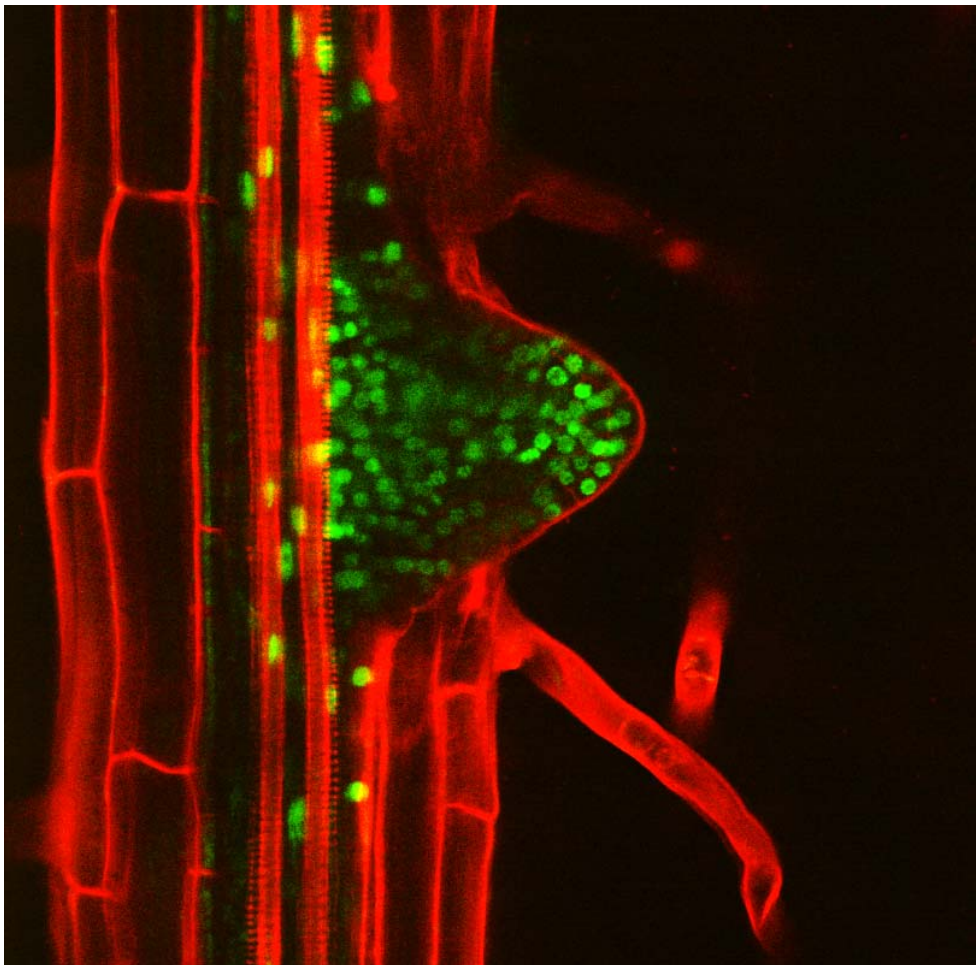

10. Appendix

Publications derived from this report:

Stroud, H.*, Otero, S.*, Desvoyes, B., Ramirez-Parra, E., Jacobsen, S.E., and Gutierrez, C. (2012). Genome-wide analysis of histone H3.1 and H3.3 variants in Arabidopsis thaliana. Proc Natl Acad Sci U S A **109,** 5370-5375. * First co-authors.

Otero, S., Desvoyes, B., Franco-Zorrilla, J.M., Gutierrez, C. (2015) Cell proliferation and histone H3 reprogramming are linked in Arabidopsis organogenesis. (In preparation).

These two papers contain most of the results presented in this Thesis.

Other publications during PhD:

Manzano, C., Ramírez-Parra, E., Casimiro, I., Otero, S., Desvoyes, B., De Rybel, B., Beeckman, T., Casero, P., Gutierrez, C., del Pozo, J.C. (2012) Auxin and epigenetic regulation of *SKP2B*, an F-Box that represses lateral root formation. Plant Physiol. 160, 749-762.

In this paper we collaborated with the group of J.C del Pozo by evaluating the presence of H3.1 and H3.3 in the promoter of *SKP2B* and several other genes.

Otero, S., Desvoyes, B., and Gutierrez, C. (2014). Histone H3 dynamics in plant cell cycle and development. Cytogenet Genome Res **143,** 114-124.

A review on the H3 function and dynamics in plants.

Desvoyes, B., Fernandez-Marcos, M., Sequeira-Mendes, J., Otero, S., Vergara, Z., and Gutierrez, C. (2014). Looking at plant cell cycle from the chromatin window. Front Plant Sci **5,** 369.

A review on the epigenetic changes during cell cycle.